The Pennsylvania State University

The Graduate School

RIBOSOME BIOGENESIS AND TRANSLATIONAL CONTROL IN SKELETAL MUSCLE: INSIGHTS INTO ANABOLIC DEFICITS AND ATROPHY IN CANCER CACHEXIA

A Dissertation in

Integrative and Biomedical Physiology

by

Daniel J. Belcher

Submitted in Partial Fulfillment

of the Requirements

for the Degree of

Doctor of Philosophy

December 2024

The dissertation of Daniel J. Belcher was reviewed and approved by the following:

Gustavo A. Nader
Professor of Kinesiology and Physiology
Dissertation Advisor
Chair of Committee

William B. Staniar
Associate Professor of Equine Science and Physiology

Robert F. Paulson
Professor of Veterinary, Biomedical Sciences, and Physiology

Scot R. Kimball
Professor of Cellular & Molecular Physiology

Gregory C. Shearer
Professor of Nutritional Sciences and Physiology
Chair of the Integrative and Biomedical Physiology Graduate Program

ABSTRACT

Skeletal muscle is a highly plastic and dynamic connective tissue that is predominantly responsible for force generation, bodily movement, basal energy metabolism, and general quality of life. Muscle mass is determined by a balance between protein synthesis and breakdown. This balance can shift towards hypertrophy or atrophy in response to factors such as nutrition, physical activity, hormonal changes, injury, or disease. Ribosomes play a crucial role in facilitating protein synthesis by translating genetic information into functional proteins. The production of ribosomes involves all three RNA polymerases, with the initial and rate-limiting step being the transcription of ribosomal (r)RNA genes (rDNA) by RNA polymerase I (Pol I). The efficiency of translation is also critical for protein synthesis and is regulated by the mechanistic target of rapamycin (mTOR) signaling pathway during muscle hypertrophy.

Skeletal muscle loss occurs in various wasting conditions. Cancer cachexia, a debilitating syndrome characterized by severe muscle atrophy, leads to significant weight loss and adversely affects patients' quality of life and survival rates. This condition not only reduces muscle mass but also impairs muscle function, leading to fatigue, reduced physical performance, and limitations in daily activities. The study of muscle in cancer cachexia is of great importance for understanding the underlying mechanisms of muscle wasting, metabolic dysfunction, and loss of muscle function in cancer patients. Such insights are essential for developing effective treatments, as current options for cancer cachexia are inadequate. Advancing our knowledge in this area may significantly enhance patient outcomes and quality of life, underscoring its importance in ongoing research. The overarching goal of this dissertation aims to explore how translational capacity and efficiency in skeletal muscle is influenced during cancer cachexia.

Preclinical models have been crucial in elucidating the mechanisms of muscle wasting in lung cancer (LC). In study 1, we examined anabolic deficits and proinflammatory effectors in LP07 and Lewis lung carcinoma (LLC) tumor models. Tumor growth led to significant weakness in LP07 mice but not in LLC mice, despite both models showing similar reductions in gastrocnemius muscle mass. LP07 tumors caused reductions in ribosomal RNA (rRNA) and rRNA gene (rDNA) transcription elongation, while LLC tumors did not affect ribosomal capacity. In the LP07 model, expression of Pol I elongation-associated subunits increased, whereas LLC tumors elevated mRNAs of Pol I elongation-related factors. Both models exhibited similar reductions in ribosomal protein (RP)S6 and 4E-BP1 phosphorylation, independent of mTOR phosphorylation in LP07 mice. Muscle inflammation varied by tumor type. The LLC tumor-bearing mice had increased IL-6 and TNF-α mRNAs, while NLRP3 mRNA upregulation was independent of tumor type. In summary, both models caused muscle wasting, but only the LP07 model showed muscle weakness with reduced ribosomal capacity. Intracellular signaling diverged at the mTOR level, and the LLC model showed a more pronounced increase in proinflammatory factors. This study's findings reveal novel, divergent anabolic deficits and proinflammatory effector expressions in LP07 and LLC lung cancer models.

Study 2 further investigated potential inhibitory effects on anabolic processes in skeletal and cardiac muscles using the Yoshida AH-130 ascites hepatoma model of cancer cachexia in rats. After 7 days of tumor burden, rats exhibited reduced body weight, as well as decreased skeletal muscle and heart weights. These changes coincided with lower levels of rRNA and notable 4E-BP1 hypophosphorylation. Both skeletal and cardiac muscles showed signs of endoplasmic reticulum stress, evidenced by elevated GADD34 mRNA expression. Furthermore, heart tissue exhibited heightened INF-γ mRNA levels, while both skeletal and cardiac muscles

displayed significantly elevated IL-1β mRNA levels. This study's findings suggest that diminished translational capacity and efficiency likely contribute to decreased skeletal muscle and heart masses in the Yoshida AH-130 ascites hepatoma model. Moreover, divergent responses in striated muscle tissues through endoplasmic reticulum stress and production of pro-inflammatory cytokines may also play significant roles in this process. In conclusion, the findings of this dissertation advance the understanding of molecular mechanisms underlying muscle wasting in cancer cachexia.

TABLE OF CONTENTS

LIST OF FIGURES

LIST OF TABLES

LIST OF ABBREVIATIONS

4E-BP1	eIF4E binding protein 1
ATF4	activating transcription factor 4
ATF6	activating transcription factor 6
BiP	binding immunoglobulin protein
BW	body weight
CHOP	c transcription factor called CCAAT/enhancer-binding protein homologous protein
CSA	cross-sectional area
EDL	extensor digitorum longus
eIF2α	alpha-subunit of eukaryotic translation initiation factor 2
eIF4E	eukaryotic translation initiation factor 4E
eIF4F	eukaryotic translation initiation factor 4F
eIF4G	eukaryotic translation initiation factor 4G
ER	endoplasmic reticulum
ERK	extracellular signal-regulated kinase
ETS	external transcribed spacer
FACT	facilitates chromatin transcription
FBW	final body weight
GAPDH	glyceraldehyde 3-phosphate dehydrogenase
GAST	gastrocnemius
GRP78	glucose-regulated protein 78
IBW	initial body weight

IL-1	interleukin-1
IL-18	interleukin-18
IL-1β	interleukin-1 beta
IL-6	interleukin-6
IP	intraperitoneal
IRE1	inositol-requiring enzyme 1
ITS	internal transcribed spacer
LARP1	La-related protein 1
LC	lung cancer
LLC	Lewis lung-cell carcinoma
LP07	LP07 lung adenocarcinoma
mRNA	messenger ribonucleic acid
mTOR	mechanistic target of rapamycin
mTORC1	mechanistic target of rapamycin complex 1
MuRF1	muscle-specific ring finger protein 1
MyHC	myosin heavy chain
NIH	National Institutes of Health
NLRP3	nucleotide-binding oligomerization domain-like receptor family and pyrin domain containing 3
NSCLC	non-small cell lung cancer
PCR	polymerase chain-reaction
PERK	protein kinase R-like ER kinase
PL	plantaris

qPCR	quantitative PCR
rDNA	ribosomal DNA
RNA	ribonucleic acid
RP	ribosomal protein
RPS6	ribosomal protein S6
rRNA	ribosomal ribonucleic Acid
RT	room temperature
S6K1	ribosomal protein S6 kinase 1
SD	standard deviation
SE	standard error
SEM	standard error mean
SOL	soleus
sXBP1	spliced XBP1
TA	tibialis anterior
TNF-α	tumor necrosis factor-alpha
UBTF	upstream binding transcription factor
UPR	unfolded protein response
UPS	ubiquitin-proteasomal system
XBP1	X-box-binding protein 1

ACKNOWLEDGEMENTS

I would first like to thank my mentor Dr. Gustavo Nader for his guidance throughout this journey. Thank you for taking me into the lab and allowing me to expand my knowledge and skillset under your mentorship. I am also grateful to my committee members, Dr. Scot Kimball, Dr. Burt Staniar, and Dr. Robert Paulson, for their support and insight during my time at Penn State. I want to thank my current lab mates, Nina Kim and Julia Olivant, for their help and support over the past year or two. It has been a pleasure to fight with antibody companies with you when their products inevitably don't work properly. A special thanks to my former lab mates, Bin Guo and Hyo Gun Kim, for teaching me much of my current lab skills, and to our former postdoc, Deva Bennet, who is sadly no longer with us. I also want to thank my former FAU lab mates, Hector Paez and Jessica Halle, for their willingness to exchange ideas, protocols, and troubleshooting tips. I would also like to thank my girlfriend Ali for her unwavering love and support during the most stressful and demanding years of my studies, my parents Saundra Jankowski and Dan Belcher for always believing in me, and all the friends I have made and kept in touch with across the four states I've lived in thus far. Lastly, I dedicate this dissertation to my grandparents, Carl Jankowski and Phillis Belcher, who unfortunately passed during my time at Penn State and were unable to see me complete my degree. I love and miss you both. I would also like to acknowledge the Huck Institutes' Microscopy Core Facility (RRID:SCR_024457) for use of the Olympus BX61 Microscope and thank Gang "Greg" Ning for helpful discussions on its use. This doctoral dissertation is based upon work supported through the National Institutes of Health (NIH) by R01AR078430. The content is solely the responsibility of the author and does not necessarily represent the official views of any funding agency.

CHAPTER 1. INTRODUCTION

1.1. SKELETAL MUSCLE PHYSIOLOGY

Skeletal muscle is a highly plastic and dynamic connective tissue that comprises approximately 30-40% of total body weight (1). Muscle is primarily comprised of water (75%), protein (20%), and several smaller substrates to include lipids, carbohydrates, and minerals (5%) (1). The maintenance of muscle mass is determined by a balance between protein synthesis and breakdown (2). This balance can be shifted to favor either hypertrophy or atrophy in response to nutrition, physical activity, hormonal balance, injury, or disease. Skeletal muscle is predominantly responsible for force generation and bodily movement, posture maintenance, basal energy metabolism, storage of carbohydrates and amino acids, heat production, and general quality of life (1, 3).

The sliding filament theory of muscle contraction has been a fundamental concept in the field of muscle physiology for decades. Based on the independent findings by A.F. Huxley and R. Niedergerke (4) and H.E. Huxley and J. Hanson (5) in 1954, this theory suggests that muscle contraction occurs through the sliding of actin and myosin filaments past each other within the sarcomere (6). The classical sliding filament theory has since been expanded to include the role of titin, a giant elastic protein found in muscle sarcomeres. Studies show that titin is activated during muscle contraction and may contribute to the overall force production of skeletal muscle (7). Additionally, this proposed three-filament sarcomere model, which includes the thin actin filaments, thick myosin filaments, and titin, has been suggested as a more comprehensive explanation for the mechanisms of muscle contraction (8). While the sliding filament theory has been fundamental in understanding muscle contraction, this theory alone cannot explain this

phenomenon. For example, the enhanced state of titin during active stretch and eccentric contractions in skeletal muscle is not accounted for by the classical understanding of the sliding filament theory (7). Overall, research in muscle physiology has evolved to encompass a multidisciplinary approach to understanding the mechanisms that regulate muscle function.

1.1.1. Skeletal muscle structure

The structure of skeletal muscle is characterized by a specific and well-defined arrangement of muscle fibers and associated connective tissue. At the gross tissue level, muscle size is determined by the number and size of individual muscle fibers (9). Muscle fibers are multinucleated and exist in a terminally differentiated post-mitotic state once fully developed (10). Skeletal muscle is primarily comprised of three major connective tissue layers, the endomysium, perimysium, and epimysium. These layers support the structure of the skeletal muscle and provide essential mechanical and chemical environments (11). The innermost layer, the endomysium, surrounds the individual muscle fibers. These fibers are grouped into muscle fascicles by the middle layer, the perimysium, and the outermost layer, the epimysium, encases the entire muscle. These layers, collectively known as the extracellular matrix, are crucial for the development and growth of skeletal muscle (11, 12). The extracellular matrix is essential for forming functional muscle units by guiding muscle cell growth (11) and participates in the transduction of mechanical force into intracellular signaling pathways (12). Together, the extracellular matrix not only facilitates force transduction but also organizes muscle fibers into cohesive muscle structures.

Satellite cells, the stem cells of skeletal muscle, are located between the sarcolemma and the basal lamina. These cells contribute to muscle growth, repair, and regeneration. When

activated by myogenic factors, the satellite cells proliferate and differentiate into new muscle fibers (13). A single muscle fiber is ~100 μm in diameter and 1 cm in length and is encased by the sarcolemma (1). The sarcolemma is associated with a complex of various proteins that link to the internal myofilament structure. This is predominately made up of the thin filament actin protein, and the thick filament, myosin, both of which play a crucial role in muscle contraction and are essential for maintaining muscle strength and integrity (1, 6). Two other proteins that contribute to the mechanical and physiological properties of muscle are titin (7, 8) and nebulin (14). Titin is a large ~4,000kDa elastic protein that attaches to the Z disk of the sarcomere and to myosin to stabilize and align the thick myosin filament. While nebulin is integrated into the thin actin filaments and facilitates the alignment of the Z disk (14). In addition to actin and myosin, these proteins contribute to the integrity of the sarcomere, maintain passive tension, and assist in the assembly of myofibrils (1).

The composition of muscle fibers plays a crucial role in various physiological functions. There are two main types of fibers in skeletal muscle, type I and type II, each with distinct characteristics and functions. These fiber types are identified by the type of myosin heavy chain (MyHC) protein they express (15). Type I muscle fibers are rich in mitochondria, highly oxidative, and are fatigue-resistant with a slower contractile rate (16). In contrast, type II muscle fibers are known for their fast contraction capabilities, are often associated with muscle power and strength, and maintain a higher capacity for growth (16). Type II fibers can be further classified into type IIA, which has a more oxidative phenotype, and type IIx, which are highly glycolytic and quick to fatigue (1).

Skeletal muscles contain a heterogeneous combination of both type I and type II fibers, varying by muscle to support a variety of tasks and movements (16). For example, in C57BL6J

mice, the soleus muscle is composed of approximately 37% type I and 67% type II fibers, while the gastrocnemius comprises around 6% type I and 94% type II fibers (17). This heterogeneous mix of fiber types is predominantly associated with the specific functions of each muscle (16). The smaller soleus muscle is responsible for maintaining posture and stability, and thus more resistant to fatigue. While the larger gastrocnemius muscle is primarily engaged in dynamic and rapid movements such as running or jumping. Thus, the arrangement of mixed fiber types is dependent on the muscle's function and its role in locomotion.

1.2. REGULATION OF SKELETAL MUSCLE MASS

Skeletal muscle responds to external stimuli in ways that influence its biochemical and mechanical properties, as well as its size. The mass of skeletal muscle is determined by the balance between protein synthesis and degradation (2). In response to external stimuli such as resistance exercise, mechanical loading, nutrients, and growth factors, the regulation of protein turnover in skeletal muscle demonstrates remarkable adaptability. This allows the skeletal muscle to respond quickly and adjust appropriately to various conditions (18). Muscle hypertrophy occurs when the rate of protein synthesis significantly exceeds the rate of degradation, resulting in a net accumulation of protein (2). Conversely, external stimuli such as immobilization, nutrient deprivation, inflammation, viral infection, and tumors can negatively affect protein turnover and lead to muscle atrophy. In this instance, when the rate of protein degradation exceeds the rate of synthesis, the net outcome is a loss in muscle mass (2). Understanding these mechanisms is crucial for developing strategies to maintain or enhance muscle health under different conditions.

1.2.1. Protein Synthesis and Muscle Hypertrophy

In myocytes, proteins are synthesized through the ribosomal translation of messenger (m) ribonucleic acids (RNA), which determines the rate of protein synthesis (19). In mammalian cells, ribosomes are composed of the 40S small and 60S large ribosomal subunits. These subunits are assembled from four ribosomal (r)RNAs and approximately 80 different ribosomal proteins (20). During translation, rRNA is responsible for catalyzing the formation of peptide bonds in the ribosome (21). This suggests that the transcription of the rRNA genes (rDNA) is critical for producing new ribosomes, often referred to as translational capacity, which is the maximum capability of the cell to synthesize proteins.

Ribosomes are the essential machinery that translates genetic information into functional proteins, therefore, a sufficient population of ribosomes is necessary to support muscle protein synthesis. Proper ribosomal synthesis requires all three RNA polymerases (Pol I, II, and III) (22), with Pol I being the most critical of the three (23). Pol I transcription is considered a rate-limiting step in ribosome biogenesis (23, 24). The rDNA is transcribed by Pol I to produce the 45S pre-rRNA, a long, single-stranded RNA molecule that contains the sequences for 18S, 5.8S, and 28S rRNAs, along with external and internal transcribed spacers (ETS and ITS). The 45S pre-rRNA is then processed into the mature 28S, 18S, and 5.8S rRNAs (25). The role of Pol II is to generate the mRNAs encoding the ribosomal proteins and processing factors, while Pol III is responsible for 5S rRNA transcription in the nucleoplasm (25). The mature rRNAs along with the ribosomal proteins are then assembled and processed into 40S and 60S subunits, and transported to the cytoplasm to be assembled into mature ribosomes (26) (Fig. 1.2.). While any impairments to the process of ribosome biogenesis will reduce overall translational capacity, transcription of rDNA by Pol I is the most critical step in this process (23). Previous studies in

rats showed an increase in RNA concentration in the soleus muscle during overload-induced hypertrophy, which corresponded with significant increases in protein synthesis (27). Since rRNA constitutes about 80% of all total RNA (28), the increase in RNA concentration reflects enhancements to rDNA transcription. The functional overload of skeletal muscle in mice has been shown to enhance early rDNA transcription, increase rRNA content, and induce hypertrophic growth (29). These results indicate that enhanced rDNA transcription subsequently leads to an increase in translational capacity.

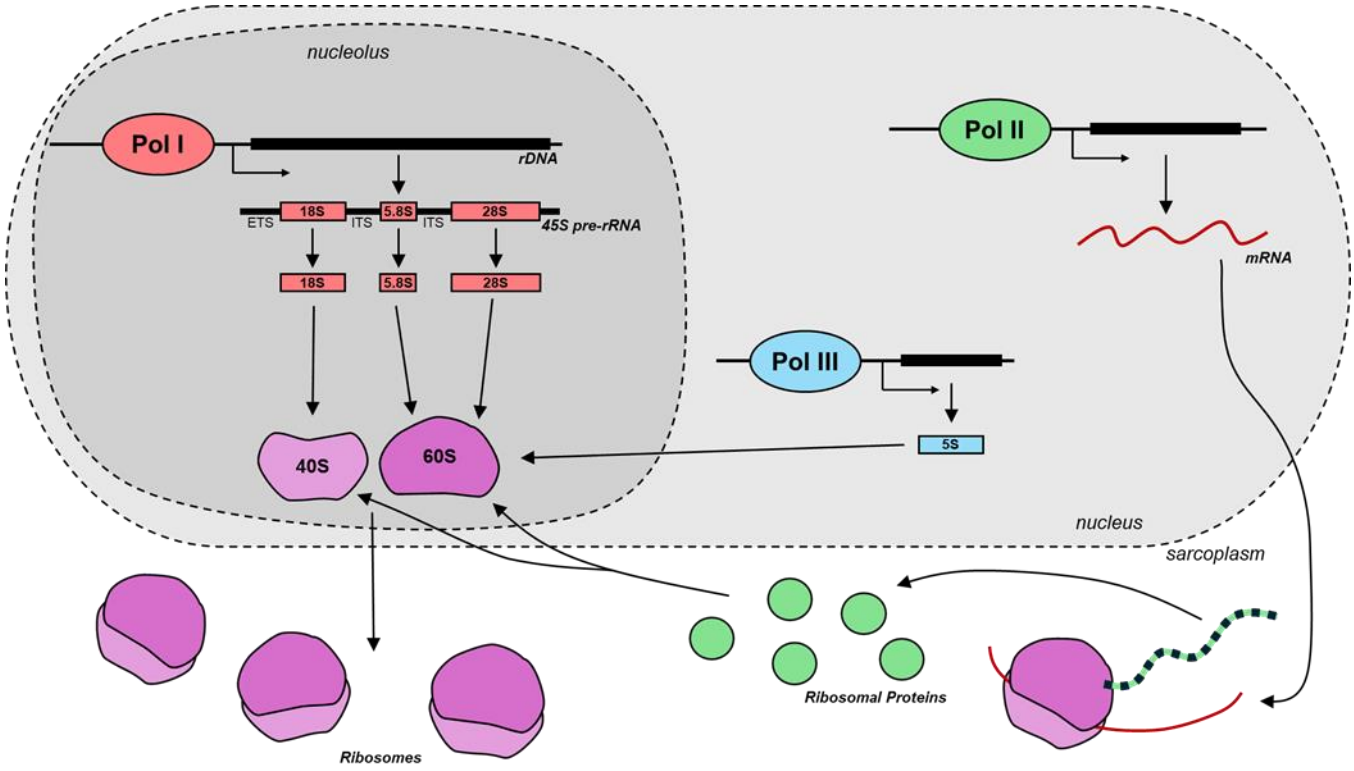

Figure 1.2. Translational Capacity

Schematic representation of ribosome production coordinated by all three RNA polymerases.

In addition to translational capacity, the efficiency of translation is crucial for promoting protein synthesis. Translational efficiency is defined as the rate of mRNA translation into proteins within cells (Fig. 1.1.). In skeletal muscle, this is predominantly regulated by the

mechanistic target of rapamycin complex 1 (mTORC1) signaling pathway (30). The makeup of mTORC1 comprises the mTOR kinase, regulatory associated protein of mTOR (raptor), DEP domain-containing mTOR-interacting protein (DEPTOR), 40 kDa proline-rich Akt substrate (PRAS40), and mammalian lethal with SEC13 protein 8 (mLST8) (31). In skeletal muscle, mTORC1 activation by insulin growth factor 1 (IGF-1)/insulin receptor substrate-1 (IRS-1) signaling is essential for hypertrophy (32, 33). This pathway operates through Akt activation via phosphoinositide 3-kinase (PI3K)s phosphorylation of phosphatidylinositol 4,5-bisphosphate (PIP2) to phosphatidylinositol 3,4,5-triphosphate (PIP3) (34). Active Akt phosphorylates the tuberous sclerosis complex (TSC)1/2, inhibiting its GTPase-activating protein (GAP) activity towards the small G protein Rheb. The GTP-bound Rheb activates mTORC1, which then phosphorylates eIF4E binding protein 1 (4E-BP1) and the 70kDa ribosomal subunit protein S6 kinase 1 (S6K1). Once phosphorylated, 4E-BP1 releases its inhibition of the eukaryotic translation initiation factor 4E (eIF4E), facilitating the recruitment of eIF4G, eIF4A, and the poly(A) binding protein (PABP) into the translation initiation complex, eIF4F (35). Activation of S6K1 by mTORC1 then leads to phosphorylation of ribosomal protein (RP)S6, subsequently increasing mRNA translation and protein synthesis (36, 37). Additionally, mTORC1 phosphorylates other components of the translation initiation machinery, such as eIF4G (38) and eukaryotic translation elongation factor 2 kinase (eEF2K) (39). Signaling through the mTORC1 pathway plays a crucial role in facilitating muscle hypertrophy. Genetic overexpression of Akt in mice significantly increased muscle fiber cross-sectional area (CSA), which was blocked by the mTOR inhibitor rapamycin (33). This was also marked by increased S6K1 phosphorylation, indicating a key role for mTORC1 in muscle hypertrophy. The activation of mTOR also plays a role in rRNA synthesis (40) and producing ribosomal proteins via the RNA binding protein La

ribonucleoprotein 1 (LARP1) (41). When LARP1 is phosphorylated by mTOR and S6K1, it alleviates its inhibition on ribosomal protein mRNA translation specifically (42). Additionally, mTOR regulates rRNA synthesis by promoting rDNA transcription (30, 40, 43).

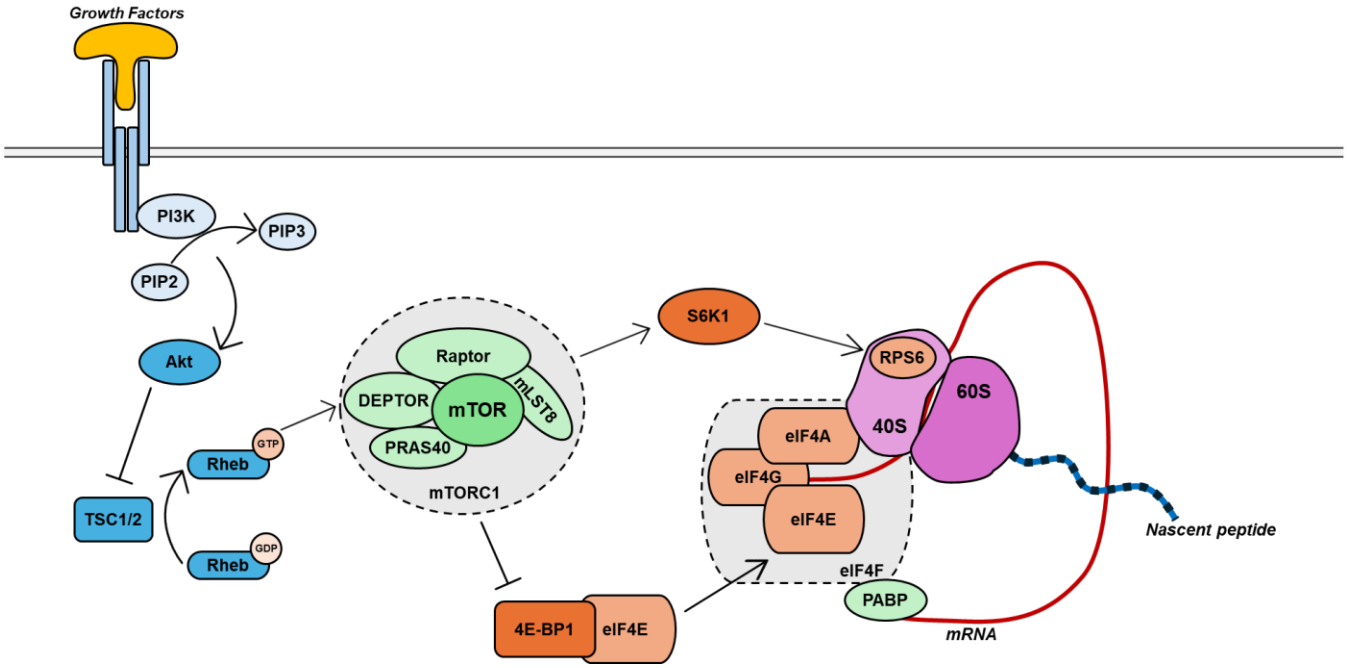

Figure 2.1. Translational Efficiency

Schematic representation of mTORC1 signaling to the translational machinery via growth factor stimulation.

Collectively, both translational capacity and efficiency determine the rate of protein synthesis in skeletal muscle cells. Ultimately, understanding these mechanisms provides critical insight into how muscle cells adapt to various stimuli and achieve growth through translational efficiency and capacity.

1.2.2. Protein Degradation and Muscle Atrophy

In contrast to skeletal muscle hypertrophy, a loss of skeletal muscle mass is observed under many different conditions including disuse, various disease states (sepsis, cancer, and renal

failure), and aging. Accordingly, the proteolytic systems involved in muscle atrophy are responsive to a number of different triggers such as immobilization and disuse, transforming growth factors (TGF) such as myostatin, inflammatory cytokines, endoplasmic reticulum (ER) stress, and nutrient availability. Each of these factors or conditions can facilitate increases in protein degradation.

The primary process involved in the breakdown of muscle proteins is the ubiquitin-proteasomal system (UPS), which centers around the 26S proteasome tasked with degrading ubiquitin-tagged proteins (44). The UPS is crucial for protein degradation across all cell types and plays a fundamental role in normal physiology. The addition of ubiquitin molecules by ubiquitin activating enzymes (E1s), ubiquitin conjugating enzymes (E2s), and ubiquitin targeting enzymes (E3s) serves as the canonical signal for degradation by the 26S proteasome (45). Two muscle-specific E3 ligases, muscle-specific ring finger protein 1 (MuRF1) and atrogin-1 (also known as muscle atrophy F-box), have been extensively studied in the context of muscle atrophy. MuRF1 has been specifically identified as a mediator of muscle protein degradation (46). It preferentially interacts with structural muscle proteins such as MyHC, myosin light chain-1 (MLC1), and MLC2, promoting their degradation (47). Increased expression of MuRF1 is commonly observed during conditions associated with muscle wasting, such as cancer cachexia (48, 49). Atrogin-1, on the other hand, promotes the suppression of protein synthesis through degradation of a critical translation initiation factor complex, eukaryotic initiation factor 3 subunit 5 (eIF3-f) (50). Similarly, atrogin-1 also targets myogenin for polyubiquitination and degradation during myotube atrophy and disrupts muscle regeneration (51). These studies suggest that although MuRF1 and atrogin-1 function through different regulatory pathways to impede muscle mass, they do work in concert to facilitate muscle protein degradation.

Skeletal muscle wasting conditions are often associated with systemic and local increases in proinflammatory cytokines such as interleukin-1 (IL-1α and IL-1β), interleukin-6 (IL-6), tumor necrosis factor (TNF-α), and interferon-γ (IFN-γ). These elevated cytokine levels promote inflammation by binding to and signaling through their respective receptors, leading to the local activation of protein catabolism (52). Increased production of pro-inflammatory cytokines such as TNF-α, IL-1β, or IL-6, may also contribute to the local pro-inflammatory environment, increasing muscle-specific cytokine production, thereby promoting muscle wasting (53–56). Much evidence suggests that TNF-α and IL-6 play a significant role in muscle wasting conditions such as cancer cachexia and sepsis (56–60). The treatment with recombinant TNF-α resulted in significant muscle mass and muscle protein content loss in rats (53). Overexpression of IL-6 impaired muscle growth during early adolescence and caused substantial muscle loss in adult mice and involved increased expression of both MuRF1 and atrogin-1 (61). Both TNF-α and IL-6 often work together to promote muscle wasting and exacerbate inflammation. For example, treatment of C2C12 myotubes with recombinant TNF-α led to a decrease in total protein content along with an increase in IL-6 (62). Additionally, exposure of myotubes to recombinant IL-6 promoted myosin degradation, suppressed mTOR and p70S6k phosphorylation, and reduced myotube diameter (63). These findings underscore the critical roles of proinflammatory cytokines, particularly TNF-α and IL-6, in driving muscle wasting and inflammation.

Skeletal muscle contains a specialized type of endoplasmic reticulum (ER) known as the sarcoplasmic reticulum. This membrane-bound organelle is crucial for the regulated release of calcium ions into the cytoplasm, triggering muscle contraction (64). In addition to its key role in skeletal muscle calcium homeostasis, the ER also manages the proper folding, packaging, and

trafficking of newly synthesized proteins from the ribosomes. When protein processing in the ER is disrupted, the accumulation of misfolded proteins can cause ER stress. This dysfunction leads to an accumulation of unfolded and misfolded proteins in the ER lumen, potentially affecting cellular function and creating a toxic environment that can result in cell death (64–66). To mitigate this stress, the unfolded protein response (UPR) temporarily halts protein synthesis and increases the production of ER chaperones to clear the damaged proteins (64–66). The UPR is initiated by three ER transmembrane sensors: activating transcription factor-6 (ATF6), inositol-requiring enzyme 1 (IRE1) α, and protein kinase R-like ER kinase (PERK) (66).

During ER stress, the ER chaperone 78 kDa glucose-regulated protein (GRP78), also known as binding immunoglobulin protein (BiP), dissociates from the intraluminal domain of these transmembrane proteins to bind to the misfolded/unfolded proteins in the ER lumen (67). Once GRP78/BiP is released, PERK auto-phosphorylates, leading to a cascade of signals including the direct phosphorylation of the α-subunit of eukaryotic translation initiation factor 2 (eIF2α) and the translation of activating transcription factor-4 (ATF4), which induces a pro-apoptotic transcription factor called CCAAT/enhancer-binding protein homologous protein (CHOP) (66, 67). Another ER transmembrane sensor, IRE1α, also becomes activated by autophosphorylation during ER stress. Through its endonuclease activity, IRE1α promotes the splicing of a 26-base intron from X-box-binding protein 1 (XBP1) mRNA (68). Once translated, the spliced XBP1 (sXBP1) protein acts as an active transcription factor, inducing the expression of ER chaperones and other UPR components to enhance the ER's folding capacity. Lastly, once activated, ATF6 is transported from the ER to the Golgi apparatus, where it is cleaved and functions as an active transcription factor that moves to the nucleus to increase the expression of UPR proteins (69). The induction of the UPR genes through these pathways enhances the cell's

protein folding capacity and decreases the load of misfolded/unfolded proteins. However, excessive activation of the UPR can lead to apoptosis through each of the three pathways (64, 67). Recent studies on the role of the UPR and ER stress in muscle wasting conditions have clarified their complex involvement in regulating muscle mass. In the atrophied muscle of Lewis lung-cell carcinoma (LLC) mice, increased expression of sXBP1, CHOP, and ATF4, along with elevated phosphorylation of eIF2α, was observed (70, 71). However, inhibiting the UPR with 4-phenylbutyrate (4-PBA) only served to exacerbate muscle wasting in both the control and LLC tumor-bearing mice (70). This suggests that while excessive UPR activation may contribute to muscle atrophy, the UPR is also essential for maintaining basal skeletal muscle mass.

1.3. MUSCLE WASTING IN CANCER CACHEXIA

Cancer cachexia is a debilitating condition that is underscored by severe muscle atrophy. This multifactorial syndrome is characterized by significant muscle wasting and weight loss, profoundly affecting patients' quality of life and survival rates (72). Cancer cachexia not only reduces muscle mass but also impairs muscle function, contributing to fatigue, decreased physical performance, and an impairment to overall daily activity. Presently, the etiology of cancer cachexia is still being uncovered. Losses of muscle mass and function are currently understood to be a result of disruptions in muscle homeostasis, particularly in muscle protein turnover. This involves an acceleration in protein catabolism and suppression of anabolism (72). These disruptions arise from a complex interplay of tumor-derived factors, systemic inflammation, and metabolic changes. Pro-inflammatory cytokines such as TNF-α, IL-6, and IFN-γ play a central role in promoting muscle protein breakdown and inhibiting protein synthesis during cachexia (73). Additionally, the upregulation of the ubiquitin-proteasome pathway and the

autophagy-lysosome system leads to increased muscle protein degradation (74). Significant reductions in translational signaling (75–77) and translational capacity (75, 78) have also been observed in cachectic muscle; however, the mechanisms behind these anabolic deficits remain poorly understood. Although no treatments are currently approved for the treatment of cancer cachexia, enhancing our understanding of the mechanisms behind cachexia-induced muscle wasting, metabolic alterations, and contractile dysfunction is crucial. This knowledge is essential for developing effective therapeutic interventions in the future.

1.3.1. Lung Cancer Cachexia

Lung cancer (LC) is one of the most prevalent cachexia-inducing malignancies in the United States and carries a higher risk of inpatient death than all other cancers combined (79, 80). Current treatment options for LC-associated cachexia have shown limited effectiveness in preventing muscle wasting, largely due to an incomplete understanding of the underlying mechanisms. Preclinical animal models of LC have helped identify several molecular mechanisms that promote muscle wasting.

Much of the existing knowledge about muscle wasting mechanisms in LC has been generated using the Lewis lung carcinoma (LLC) model and LP07 lung adenocarcinoma model. In xenografted LLC tumor-bearing mice, muscle wasting is linked to impaired muscle function (77, 81–83), deficits in protein synthesis (81), elevated proteolysis (77, 81, 83, 84), and increased systemic and local inflammation (81, 85). Additionally, the LP07 xenograft model has shown similarities in muscle wasting to the LLC model (86–88) However, despite both tumor types originating in the lung and causing muscle wasting, it is unknown whether they involve similar anabolic disruptions. This is crucial because muscle wasting in cancer is associated with reduced

ribosomal capacity (75, 78, 89, 90). In addition to impairments to translational capacity, alterations in intracellular signaling involved in translational control may also promote muscle wasting in LC (70, 81, 87). In late-stage non-small cell lung cancer (NSCLC) patients, reductions in p70S6k and 4E-BP1 phosphorylation were observed in coordination with severe muscle loss (91). However, the role of translational capacity in LC cachexia has yet to be explored.

1.3.2. Liver Cancer Cachexia

Hepatocellular carcinoma is one of the fastest growing and deadliest cancers in the United States (92). Approximately 25% of patients with hepatocellular carcinoma develop cachexia, significantly increasing mortality rates (93). Additionally, the tissue-wasting effects of cachexia extend beyond skeletal muscle, causing significant impairments in the heart as well. The Yoshida AH-130 ascites hepatoma is a widely studied pre-clinical model for cancer cachexia research. In this aggressive cancer model, rats xenografted with AH-130 tumors rapidly lose skeletal and cardiac muscle mass (78, 94–96). This muscle wasting is often accompanied by systemic and local inflammation, disrupted cellular metabolism, and elevated proteolysis (53, 97, 98).

Elevations in systemic inflammation have also been previously linked to impaired cardiovascular function (55, 99). For example, increases in circulating IL-1b and IL-6 have been observed during heart failure (100, 101). Endogenous production of TNF-α has been found in chronic heart failure patients and an overexpression in the heart leads to cardiovascular complications (102). However, while systemic inflammation has been previously documented in several models of cancer cachexia (53, 97), the effects of local cytokine production in the skeletal and cardiac muscles of AH-130 Yoshida tumor-bearing rat remains unanswered.

Translational efficiency, in addition to capacity, is crucial for muscle mass maintenance. Suppressed anabolic signaling has been observed in cachectic AH-130 tumor-bearing rats (96, 103, 104), but the root cause remains undetermined. One potential contributor is the induction of ER stress, which arises from the accumulation of unfolded or misfolded proteins in the ER. The UPR under this stress represses translational signaling to restore cellular proteostasis (66). ER stress-induced UPR activation has been previously linked to cancer cachexia (70). Increased ER stress markers have been observed in the skeletal muscle of LLC and APCMin/+ cachectic mice (70). However, the role of ER stress in muscle wasting in the Yoshida AH-130 ascites hepatoma model has yet to be fully elucidated.

The study of muscle in cancer cachexia is of paramount importance for understanding the underlying mechanisms of muscle wasting, metabolic dysfunction, and loss of muscle function in cancer patients. Detailed insights into these processes are critical for the development of effective therapeutic strategies, as current treatment options for cancer cachexia are lacking. Advancing our knowledge in this area has the potential to significantly improve patient outcomes and quality of life, making it a vital focus of ongoing research.

1.5. DISSERTATION OBJECTIVES

The objective of this dissertation is to examine the role of translational capacity and efficiency in skeletal muscle during cancer cachexia. This explored through two studies in pre-clinical animal models structured around the following aims:

1. Determine whether muscle wasting in the LP07 and LLC preclinical models of lung cancer-induced cachexia involves similar anabolic deficits and the local expression of proinflammatory factors.

2. Investigate the impact of tumor-burden on translational capacity and efficiency in skeletal and cardiac muscle mass using the Yoshida AH-130 hepatoma model.

1.6. REFERENCES

1. **Frontera WR**, **Ochala J**. Skeletal Muscle: A Brief Review of Structure and Function. *Behav Genet* 45: 183–195, 2015. doi: 10.1007/s00223-014-9915-y.
2. **Millward DJ**, **Garlick PJ**, **Nnanyelugo DO**, **Waterlow JC**. The relative importance of muscle protein synthesis and breakdown in the regulation of muscle mass. *Biochem J* 156: 185–188, 1976. doi: 10.1042/bj1560185.
3. **Trovato FM**, **Imbesi R**, **Conway N**, **Castrogiovanni P**. Morphological and Functional Aspects of Human Skeletal Muscle. *J Funct Morphol Kinesiol 2016, Vol 1, Pages 289-302* 1: 289–302, 2016. doi: 10.3390/JFMK1030289.
4. **Huxley AF**, **Niedergerke R**. Structural changes in muscle during contraction; interference microscopy of living muscle fibres. *Nature* 173: 971–973, 1954. doi: 10.1038/173971A0.
5. **Huxley H**, **Hanson J**. Changes in the cross-striations of muscle during contraction and stretch and their structural interpretation. *Nature* 173: 973–976, 1954. doi: 10.1038/173973A0.
6. **Stephens RE**. ANALYSIS OF MUSCLE CONTRACTION BY ULTRAVIOLET MICROBEAM DISRUPTION OF SARCOMERE STRUCTURE. *J Cell Biol* 25: 129–139, 1965. doi: 10.1083/JCB.25.2.129.
7. **Hessel AL**, **Lindstedt SL**, **Nishikawa KC**. Physiological Mechanisms of Eccentric Contraction and Its Applications: A Role for the Giant Titin Protein. *Front Physiol* 8, 2017. doi: 10.3389/FPHYS.2017.00070.

8. **Qian Z**, **Ping L**, **Xuelin Z**. Re-examining the mechanism of eccentric exercise-induced skeletal muscle damage from the role of the third filament, titin (Review). *Biomed Reports* 20: 14, 2024. doi: 10.3892/BR.2023.1703.

9. **Chalmers GR**, **Roy RR**, **Edgerton VR**. Variation and limitations in fiber enzymatic and size responses in hypertrophied muscle. *https://doi.org/101152/jappl1992732631* 73: 631–641, 1992. doi: 10.1152/JAPPL.1992.73.2.631.

10. **Camarda G**, **Siepi F**, **Pajalunga D**, **Bernardini C**, **Rossi R**, **Montecucco A**, **Meccia E**, **Crescenzi M**. A pRb-independent mechanism preserves the postmitotic state in terminally differentiated skeletal muscle cells. *J Cell Biol* 167: 417–423, 2004. doi: 10.1083/JCB.200408164.

11. **Purslow PP**. The Structure and Role of Intramuscular Connective Tissue in Muscle Function. *Front Physiol* 11: 495, 2020. doi: 10.3389/FPHYS.2020.00495.

12. **Kjær M**. Role of extracellular matrix in adaptation of tendon and skeletal muscle to mechanical loading. *Physiol Rev* 84: 649–698, 2004. doi: 10.1152/PHYSREV.00031.2003.

13. **Yin H**, **Price F**, **Rudnicki MA**. Satellite Cells and the Muscle Stem Cell Niche. *Physiol Rev* 93: 23, 2013. doi: 10.1152/PHYSREV.00043.2011.

14. **Labeit S**, **Ottenheijm CAC**, **Granzier H**. Nebulin, a major player in muscle health and disease. *FASEB J* 25: 822–829, 2011. doi: 10.1096/FJ.10-157412.

15. **Ennion S**, **Sant' Ana Pereira J**, **Sargeant AJ**, **Young A**, **Goldspink G**. Characterization of human skeletal muscle fibres according to the myosin heavy chains they express. *J Muscle Res Cell Motil* 16: 35–43, 1995. doi: 10.1007/BF00125308.

16. **Schiaffino S**, **Reggiani C**. Fiber types in mammalian skeletal muscles. *Physiol Rev* 91:

1447–1531, 2011. doi: 10.1152/PHYSREV.00031.2010.

17. **Augusto V**, **Padovani CR**, **Campos GER**, **Augusto V**, **Padovani CR**, **Campos GER**. Skeletal Muscle Fiber Types in C57BL6J Mice [Online]. *J Morphol Sci* 21: 89–94, 2004. http://www.jms.periodikos.com.br/journal/jms/article/587cb4537f8c9d0d058b45ea [26 Jun. 2024].

18. **Goldberg AL**, **Goodman HM**. Relationship between growth hormone and muscular work in determining muscle size. *J Physiol* 200: 655, 1969. doi: 10.1113/JPHYSIOL.1969.SP008714.

19. **Millward DJ**, **Garlick PJ**, **James WPT**, **Nnanyelugo DO**, **Ryatt JS**. Relationship between protein synthesis and RNA content in skeletal muscle. *Nature* 241: 204–205, 1973. doi: 10.1038/241204a0.

20. **Fromont-Racine M**, **Senger B**, **Saveanu C**, **Fasiolo F**. Ribosome assembly in eukaryotes. *Gene* 313: 17–42, 2003. doi: 10.1016/S0378-1119(03)00629-2.

21. **Jenni S**, **Ban N**. The chemistry of protein synthesis and voyage through the ribosomal tunnel. *Curr Opin Struct Biol* 13: 212–219, 2003. doi: 10.1016/S0959-440X(03)00034-4.

22. **Mayer C**, **Grummt I**. Ribosome biogenesis and cell growth: mTOR coordinates transcription by all three classes of nuclear RNA polymerases. *Oncogene* 25: 6384–6391, 2006. doi: 10.1038/SJ.ONC.1209883.

23. **Laferté A**, **Favry E**, **Sentenac A**, **Riva M**, **Carles C**, **Chédin S**. The transcriptional activity of RNA polymerase I is a key determinant for the level of all ribosome components. *Genes Dev* 20: 2030–2040, 2006. doi: 10.1101/GAD.386106.

24. **Moss T**, **Stefanovsky VY**. Promotion and regulation of ribosomal transcription in eukaryotes by RNA polymerase I. *Prog Nucleic Acid Res Mol Biol* 50: 25–66, 1995. doi:

10.1016/S0079-6603(08)60810-7.

25. **Thomson E**, **Ferreira-Cerca S**, **Hurt E**. Eukaryotic ribosome biogenesis at a glance. *J Cell Sci* 126: 4815–4821, 2013. doi: 10.1242/JCS.111948.

26. **Tschochner H**, **Hurt E**. Pre-ribosomes on the road from the nucleolus to the cytoplasm. *Trends Cell Biol* 13: 255–263, 2003. doi: 10.1016/S0962-8924(03)00054-0.

27. **Hamosh M**, **Lesch M**, **Baron J**, **Kaufman S**. Enhanced Protein Synthesis in a Cell-Free System from Hypertrophied Skeletal Muscle. *Science (80-)* 157: 935–937, 1967. doi: 10.1126/SCIENCE.157.3791.935.

28. **Zak R**, **Rabinowitz M**, **Platt C**. Ribonucleic Acids Associated with Myofibrils. *Biochemistry* 6: 2493–2500, 1967. doi: doi.org/10.1021/bi00860a028.

29. **von Walden F**, **Casagrande V**, **Farrants AKÖ**, **Nader GA**. Mechanical loading induces the expression of a Pol I regulon at the onset of skeletal muscle hypertrophy. *Am J Physiol - Cell Physiol* 302: 1523–1530, 2012. doi: 10.1152/ajpcell.00460.2011.

30. **von Walden F**, **Liu C**, **Aurigemma N**, **Nader GA**. mTOR signaling regulates myotube hypertrophy by modulating protein synthesis, rDNA transcription, and chromatin remodeling. *Am J Physiol - Cell Physiol* 311: C663–C672, 2016. doi: 10.1152/ajpcell.00144.2016.

31. **Yoon MS**. mTOR as a key regulator in maintaining skeletal muscle mass. *Front Physiol* 8: 294538, 2017. doi: doi.org/10.3389/fphys.2017.00788.

32. **Glass DJ**. Signalling pathways that mediate skeletal muscle hypertrophy and atrophy. *Nat Cell Biol* 5: 87–90, 2003. doi: 10.1038/NCB0203-87.

33. **Bodine SC**, **Stitt TN**, **Gonzalez M**, **Kline WO**, **Stover GL**, **Bauerlein R**, **Zlotchenko E**, **Scrimgeour A**, **Lawrence JC**, **Glass DJ**, **Yancopoulos GD**. Akt/mTOR pathway is a

crucial regulator of skeletal muscle hypertrophy and can prevent muscle atrophy in vivo. *Nat Cell Biol 2001 311* 3: 1014–1019, 2001. doi: 10.1038/ncb1101-1014.

34. **Zhao L**, **Vogt PK**. Class I PI3K in oncogenic cellular transformation. *Oncogene* 27: 5486–5496, 2008. doi: 10.1038/ONC.2008.244.

35. **Hay N**, **Sonenberg N**. Upstream and downstream of mTOR. *Genes Dev* 18: 1926–1945, 2004. doi: 10.1101/GAD.1212704.

36. **Fingar DC**, **Salama S**, **Tsou C**, **Harlow E**, **Blenis J**. Mammalian cell size is controlled by mTOR and its downstream targets S6K1 and 4EBP1/eIF4E. *Genes Dev* 16: 1472–1487, 2002. doi: 10.1101/GAD.995802.

37. **Ruvinsky I**, **Sharon N**, **Lerer T**, **Cohen H**, **Stolovich-Rain M**, **Nir T**, **Dor Y**, **Zisman P**, **Meyuhas O**. Ribosomal protein S6 phosphorylation is a determinant of cell size and glucose homeostasis. *Genes Dev* 19: 2199, 2005. doi: 10.1101/GAD.351605.

38. **Raught B**, **Gingras AC**, **Gygi SP**, **Imataka H**, **Morino S**, **Gradi A**, **Aebersold R**, **Sonenberg N**. Serum-stimulated, rapamycin-sensitive phosphorylation sites in the eukaryotic translation initiation factor 4GI. *EMBO J* 19: 434–444, 2000. doi: 10.1093/EMBOJ/19.3.434.

39. **Wang X**, **Li W**, **Williams M**, **Terada N**, **Alessi DR**, **Proud CG**. Regulation of elongation factor 2 kinase by p90(RSK1) and p70 S6 kinase. *EMBO J* 20: 4370–4379, 2001. doi: 10.1093/EMBOJ/20.16.4370.

40. **Mayer C**, **Zhao J**, **Yuan X**, **Grummt I**. mTOR-dependent activation of the transcription factor TIF-IA links rRNA synthesis to nutrient availability. *Genes Dev* 18: 423, 2004. doi: 10.1101/GAD.285504.

41. **Rosario FJ**, **Powell TL**, **Gupta MB**, **Cox L**, **Jansson T**. mTORC1 Transcriptional

Regulation of Ribosome Subunits, Protein Synthesis, and Molecular Transport in Primary Human Trophoblast Cells. *Front Cell Dev Biol* 8: 583801, 2020. doi: 10.3389/fcell.2020.583801.

42. **Hong S**, **Freeberg MA**, **Han T**, **Kamath A**, **Yao Y**, **Fukuda T**, **Suzuki T**, **Kim JK**, **Inoki K**. LARP1 functions as a molecular switch for mTORC1-mediated translation of an essential class of mRNAs. *Elife* 6: e25237, 2017. doi: 10.7554/ELIFE.25237.

43. **Hannan KM**, **Brandenburger Y**, **Jenkins A**, **Sharkey K**, **Cavanaugh A**, **Rothblum L**, **Moss T**, **Poortinga G**, **McArthur GA**, **Pearson RB**, **Hannan RD**. mTOR-dependent regulation of ribosomal gene transcription requires S6K1 and is mediated by phosphorylation of the carboxy-terminal activation domain of the nucleolar transcription factor UBF. *Mol Cell Biol* 23: 8862–8877, 2003. doi: 10.1128/MCB.23.23.8862-8877.2003.

44. **Murton AJ**, **Constantin D**, **Greenhaff PL**. The involvement of the ubiquitin proteasome system in human skeletal muscle remodelling and atrophy. *Biochim Biophys Acta* 1782: 730–743, 2008. doi: 10.1016/J.BBADIS.2008.10.011.

45. **Grice GL**, **Nathan JA**. The recognition of ubiquitinated proteins by the proteasome. *Cell Mol Life Sci C* 73: 3497, 2016. doi: 10.1007/S00018-016-2255-5.

46. **Bodine SC**, **Latres E**, **Baumhueter S**, **Lai VKM**, **Nunez L**, **Clarke BA**, **Poueymirou WT**, **Panaro FJ**, **Erqian Na**, **Dharmarajan K**, **Pan ZQ**, **Valenzuela DM**, **Dechiara TM**, **Stitt TN**, **Yancopoulos GD**, **Glass DJ**. Identification of ubiquitin ligases required for skeletal muscle atrophy. *Science* 294: 1704–1708, 2001. doi: 10.1126/SCIENCE.1065874.

47. **Peris-Moreno D**, **Taillandier D**, **Polge C**. MuRF1/TRIM63, Master Regulator of Muscle

Mass. *Int J Mol Sci* 21: 1–39, 2020. doi: 10.3390/IJMS21186663.

48. **Silva KAS**, **Dong J**, **Dong Y**, **Dong Y**, **Schor N**, **Tweardy DJ**, **Zhang L**, **Mitch WE**. Inhibition of Stat3 activation suppresses caspase-3 and the ubiquitin-proteasome system, leading to preservation of muscle mass in cancer cachexia. *J Biol Chem* 290: 11177–11187, 2015. doi: 10.1074/jbc.M115.641514.

49. **Cai D**, **Frantz JD**, **Tawa NE**, **Melendez PA**, **Oh BC**, **Lidov HGW**, **Hasselgren PO**, **Frontera WR**, **Lee J**, **Glass DJ**, **Shoelson SE**. IKKβ/NF-κB activation causes severe muscle wasting in mice. *Cell* 119: 285–298, 2004. doi: 10.1016/j.cell.2004.09.027.

50. **Lagirand-Cantaloube J**, **Offner N**, **Csibi A**, **Leibovitch MP**, **Batonnet-Pichon S**, **Tintignac LA**, **Segura CT**, **Leibovitch SA**. The initiation factor eIF3-f is a major target for Atrogin1/MAFbx function in skeletal muscle atrophy. *EMBO J* 27: 1266–1276, 2008. doi: 10.1038/emboj.2008.52.

51. **MacPherson PCD**, **Wang X**, **Goldman D**. Myogenin Regulates Denervation-Dependent Muscle Atrophy in Mouse Soleus Muscle. *J Cell Biochem* 112: 2149, 2011. doi: 10.1002/JCB.23136.

52. **Ji Y**, **Li M**, **Chang M**, **Liu R**, **Qiu J**, **Wang K**, **Deng C**, **Shen Y**, **Zhu J**, **Wang W**, **Xu L**, **Sun H**. Inflammation: Roles in Skeletal Muscle Atrophy. *Antioxidants* 11, 2022. doi: 10.3390/ANTIOX11091686.

53. **Lang CH**, **Frost RA**, **Nairn AC**, **MacLean DA**, **Vary TC**. TNF-α impairs heart and skeletal muscle protein synthesis by altering translation initiation. *Am J Physiol - Endocrinol Metab* 282: E336–E347, 2002. doi: 10.1152/ajpendo.00366.2001.

54. **Luo G**, **Hershko DD**, **Robb BW**, **Wray CJ**, **Hasselgren P-O**. IL-1β stimulates IL-6 production in cultured skeletal muscle cells through activation of MAP kinase signaling

pathway and NF-κB. *Am J Physiol Integr Comp Physiol* 284: R1249–R1254, 2003. doi: 10.1152/ajpregu.00490.2002.

55. **Webster JM**, **Kempen LJAP**, **Hardy RS**, **Langen RCJ**. Inflammation and Skeletal Muscle Wasting During Cachexia. *Front Physiol* 11: 597675, 2020. doi: 10.3389/fphys.2020.597675.

56. **Frost RA**, **Nystrom GJ**, **Lang CH**. Lipopolysaccharide regulates proinflammatory cytokine expression in mouse myoblasts and skeletal muscle. *Am J Physiol Integr Comp Physiol* 283: R698–R709, 2002.

57. **Kayacan O**, **Karnak D**, **Beder S**, **Güllü E**, **Tutkak H**, **Şenler FÇ**, **Köksal D**. Impact of TNF-α and IL-6 levels on development of cachexia in newly diagnosed NSCLC patients. *Am J Clin Oncol Cancer Clin Trials* 29: 328–335, 2006. doi: 10.1097/01.COC.0000221300.72657.E0.

58. **Goodman MN**. Interleukin-6 Induces Skeletal Muscle Protein Breakdown in Rats. *https://doi.org/103181/00379727-205-43695* 205: 182–185, 1994. doi: 10.3181/00379727-205-43695.

59. **Damas P**, **Ledoux D**, **Nys M**, **Vrindts Y**, **De Groote D**, **Franchimont P**, **Lamy M**. Cytokine serum level during severe sepsis in human IL-6 as a marker of severity. *Ann Surg* 215: 356, 1992. doi: 10.1097/00000658-199204000-00009.

60. **Op den Kamp CM**, **Langen RC**, **Minnaard R**, **Kelders MC**, **Snepvangers FJ**, **Hesselink MK**, **Dingemans AC**, **Schols AM**. Pre-cachexia in patients with stages I-III non-small cell lung cancer: Systemic inflammation and functional impairment without activation of skeletal muscle ubiquitin proteasome system. *Lung Cancer* 76: 112=117, 2012. doi: 10.1016/j.lungcan.2011.09.012.

61. **Pelosi L**, **Berardinelli MG**, **Forcina L**, **Ascenzi F**, **Rizzuto E**, **Sandri M**, **De Benedetti F**, **Scicchitano BM**, **Musarò A**. Sustained Systemic Levels of IL-6 Impinge Early Muscle Growth and Induce Muscle Atrophy and Wasting in Adulthood. *Cells* 10, 2021. doi: 10.3390/CELLS10071816.

62. **Alvarez B**, **Quinn LBS**, **Busquets S**, **López-Soriano FJ**, **Argilés JM**. TNF-α modulates cytokine and cytokine receptors in C2C12 myotubes. *Cancer Lett* 175: 181–185, 2002. doi: 10.1016/S0304-3835(01)00717-0.

63. **Pelosi M**, **De Rossi M**, **Barberi L**, **Musarò A**. IL-6 impairs myogenic differentiation by downmodulation of p90RSK/eEF2 and mTOR/p70S6K axes, without affecting AKT activity. *Biomed Res Int* 2014, 2014. doi: 10.1155/2014/206026.

64. **Bohnert KR**, **McMillan JD**, **Kumar A**. Emerging roles of ER stress and unfolded protein response pathways in skeletal muscle health and disease. *J Cell Physiol* 233: 67–78, 2018. doi: 10.1002/JCP.25852.

65. **Doyle KM**, **Kennedy D**, **Gorman AM**, **Gupta S**, **Healy SJM**, **Samali A**. Unfolded proteins and endoplasmic reticulum stress in neurodegenerative disorders. *J Cell Mol Med* 15: 2025, 2011. doi: 10.1111/J.1582-4934.2011.01374.X.

66. **Preston AM**, **Hendershot LM**. Examination of a second node of translational control in the unfolded protein response. *J Cell Sci* 126: 4253–4261, 2013. doi: 10.1242/jcs.130336.

67. **Gallot YS**, **Bohnert KR**. Confounding Roles of ER Stress and the Unfolded Protein Response in Skeletal Muscle Atrophy. *Int J Mol Sci* 22: 1–18, 2021. doi: 10.3390/IJMS22052567.

68. **Gebert M**, **Sobolewska A**, **Bartoszewska S**, **Cabaj A**, **Crossman DK**, **Króliczewski J**, **Madanecki P**, **Dąbrowski M**, **Collawn JF**, **Bartoszewski R**. Genome-wide mRNA

profiling identifies X-box-binding protein 1 (XBP1) as an IRE1 and PUMA repressor. *Cell Mol Life Sci C* 78: 7061, 2021. doi: 10.1007/S00018-021-03952-1.

69. **Tam AB**, **Roberts LS**, **Chandra V**, **Rivera IG**, **Nomura DK**, **Forbes DJ**, **Niwa M**. The UPR Activator ATF6 Responds to Proteotoxic and Lipotoxic Stress by Distinct Mechanisms. *Dev Cell* 46: 327, 2018. doi: 10.1016/J.DEVCEL.2018.04.023.

70. **Bohnert KR**, **Gallot YS**, **Sato S**, **Xiong G**, **Hindi SM**, **Kumar A**. Inhibition of ER stress and unfolding protein response pathways causes skeletal muscle wasting during cancer cachexia. *FASEB J* 30: 3053–3068, 2016. doi: 10.1096/fj.201600250RR.

71. **Bohnert KR**, **Goli P**, **Roy A**, **Sharma AK**, **Xiong G**, **Gallot YS**, **Kumar A**. The Toll-Like Receptor/MyD88/XBP1 Signaling Axis Mediates Skeletal Muscle Wasting during Cancer Cachexia. *Mol Cell Biol* 39: e00184-19, 2019. doi: 10.1128/mcb.00184-19.

72. **Argilés JM**, **Busquets S**, **Stemmler B**, **López-Soriano FJ**. Cancer cachexia: Understanding the molecular basis. *Nat Rev Cancer* 14: 754–762, 2014. doi: 10.1038/nrc3829.

73. **Ma JF**, **Sanchez BJ**, **Hall DT**, **Tremblay AK**, **Di Marco S**, **Gallouzi I**. STAT 3 promotes IFN γ/ TNF α-induced muscle wasting in an NF -κB-dependent and IL -6-independent manner. *EMBO Mol Med* 9: 622–637, 2017. doi: 10.15252/emmm.201607052.

74. **Zhang Y**, **Wang J**, **Wang X**, **Gao T**, **Tian H**, **Zhou D**, **Zhang L**, **Li G**, **Wang X**. The autophagic-lysosomal and ubiquitin proteasome systems are simultaneously activated in the skeletal muscle of gastric cancer patients with cachexia. *Am J Clin Nutr* 111: 570–579, 2020. doi: 10.1093/ajcn/nqz347.

75. **Kim H-G**, **Huot J**, **Pin F**, **Guo B**, **Bonetto A**, **Nader G**. Reduced rDNA transcription

diminishes skeletal muscle ribosomal capacity and protein synthesis in cancer cachexia. *FASEB* 35: e21335, 2021. doi: 10.1096/fj.202002257R.

76. **White JP**, **Baynes JW**, **Welle SL**, **Kostek MC**, **Matesic LE**, **Sato S**, **Carson JA**. The regulation of skeletal muscle protein turnover during the progression of cancer cachexia in the Apc Min/+ mouse. *PLoS One* 6, 2011. doi: 10.1371/journal.pone.0024650.

77. **Brown JL**, **Lee DE**, **Rosa-Caldwell ME**, **Brown LA**, **Perry RA**, **Haynie WS**, **Huseman K**, **Sataranatarajan K**, **Van Remmen H**, **Washington TA**, **Wiggs MP**, **Greene NP**. Protein imbalance in the development of skeletal muscle wasting in tumour-bearing mice. *J Cachexia Sarcopenia Muscle* 9: 987–1002, 2018. doi: 10.1002/jcsm.12354.

78. **Baracos VE**, **DeVivo C**, **Hoyle DH**, **Goldberg AL**. Activation of the ATP-ubiquitin-proteasome pathway in skeletal muscle of cachectic rats bearing a hepatoma. *Am J Physiol Metab* 268: E996–E1006, 1995. doi: 10.1152/ajpendo.1995.268.5.E996.

79. **Arthur ST**, **Van Doren BA**, **Roy D**, **Noone JM**, **Zacherle E**, **Blanchette CM**. Cachexia among US cancer patients. *J Med Econ* 19: 874–880, 2016. doi: 10.1080/13696998.2016.1181640.

80. **Siegel RL**, **Miller KD**, **Jemal A**. Cancer statistics, 2019. *CA Cancer J Clin* 69: 7–34, 2019. doi: 10.3322/caac.21551.

81. **Puppa MJ**, **Gao S**, **Narsale AA**, **Carson JA**. Skeletal muscle glycoprotein 130's role in Lewis lung carcinoma-induced cachexia. *FASEB J* 28: 998–1109, 2014. doi: 10.1096/fj.13-240580.

82. **Brown JL**, **Rosa-Caldwell ME**, **Lee DE**, **Blackwell TA**, **Brown LA**, **Perry RA**, **Haynie WS**, **Hardee JP**, **Carson JA**, **Wiggs MP**, **Washington TA**, **Greene NP**. Mitochondrial degeneration precedes the development of muscle atrophy in progression of cancer

cachexia in tumour-bearing mice. *J Cachexia Sarcopenia Muscle* 8: 926–938, 2017. doi: 10.1002/jcsm.12232.

83. **Lim S**, **Deaver JW**, **Rosa-Caldwell ME**, **Haynie WS**, **Morena da Silva F**, **Cabrera AR**, **Schrems ER**, **Saling LW**, **Jansen LT**, **Dunlap KR**. Development of metabolic and contractile alterations in development of cancer cachexia in female tumor-bearing mice. *J Appl Physiol* 132: 58–72, 2022. doi: 10.1152/japplphysiol.00660.2021.

84. **Hain BA**, **Xu H**, **VanCleave AM**, **Gordon BS**, **Kimball SR**, **Waning DL**. REDD1 deletion attenuates cancer cachexia in mice. *J Appl Physiol* 131: 1718–1730, 2021. doi: 10.1152/japplphysiol.00536.2021.

85. **Ohe Y**, **Podack ER**, **Olsen KJ**, **Miyahara Y**, **Miura K**, **Saito H**, **Koishihara Y**, **Ohsugi Y**, **Ohira T**, **Nishio K**, **Saijo N**. Interleukin-6 cdna transfected lewis lung carcinoma cells show unaltered net tumour growth rate but cause weight loss and shorten survival in syngenic mice. *Br J Cancer* 67: 939–944, 1993. doi: 10.1038/bjc.1993.174.

86. **Chacon-Cabrera A**, **Fermoselle C**, **Urtreger AJ**, **Mateu-Jimenez M**, **Diament MJ**, **de Kier Joffé EDB**, **Sandri M**, **Barreiro E**. Pharmacological Strategies in Lung Cancer-Induced Cachexia: Effects on Muscle Proteolysis, Autophagy, Structure, and Weakness. *J Cell Physiol* 229: 1660–1672, 2014. doi: 10.1002/jcp.24611.

87. **Chacon-Cabrera A**, **Mateu-Jimenez M**, **Langohr K**, **Fermoselle C**, **García-Arumí E**, **Andreu AL**, **Yelamos J**, **Barreiro E**. Role of PARP activity in lung cancer-induced cachexia: Effects on muscle oxidative stress, proteolysis, anabolic markers, and phenotype. *J Cell Physiol* 232: 3744–3761, 2017. doi: 10.1002/jcp.25851.

88. **Chacon-Cabrera A**, **Fermoselle C**, **Salmela I**, **Yelamos J**, **Barreiro E**. MicroRNA expression and protein acetylation pattern in respiratory and limb muscles of Parp-1-/- and

Parp-2-/- mice with lung cancer cachexia. *Biochim Biophys Acta - Gen Subj* 1850: 2530–2543, 2015. doi: 10.1016/j.bbagen.2015.09.020.

89. **Emery PW**, **Edwards RHT**, **Rennie MJ**. Protein synthesis in muscle measured in vivo in cachectic patients with cancer. *Br Med J* 289: 584–586, 1984. doi: 10.1136/bmj.289.6445.584.

90. **Goodlad GAJ**, **Clark CM**. Response of skeletal muscle RNA polymerases I and II to tumour growth. *Biochim Biophys Acta (BBA)-Gene Struct Expr* 950: 296–302, 1988. doi: 10.1016/0167-4781(88)90125-x.

91. **Murton AJ**, **Maddocks M**, **Stephens FB**, **Marimuthu K**, **England R**, **Wilcock A**. Consequences of Late-Stage Non–Small-Cell Lung Cancer Cachexia on Muscle Metabolic Processes. *Clin Lung Cancer* 18: e1–e11, 2017. doi: 10.1016/j.cllc.2016.06.003.

92. **McGlynn KA**, **Petrick JL**, **El-Serag HB**. Epidemiology of Hepatocellular Carcinoma. *Hepatology* 73: 4–13, 2021. doi: 10.1002/hep.31288.

93. **Wolf E**, **Rich NE**, **Marrero JA**, **Parikh ND**, **Singal AG**. Use of Hepatocellular Carcinoma Surveillance in Patients With Cirrhosis: A Systematic Review and Meta-Analysis. *Hepatology* 73, 2021. doi: 10.1002/hep.31309.

94. **Salazar-Degracia A**, **Busquets S**, **Argilés JM**, **Bargalló-Gispert N**, **López-Soriano FJ**, **Barreiro E**. Effects of the beta2 agonist formoterol on atrophy signaling, autophagy, and muscle phenotype in respiratory and limb muscles of rats with cancer-induced cachexia. *Biochimie* 149: 79–91, 2018. doi: 10.1016/j.biochi.2018.04.009.

95. **Yuan L**, **Springer J**, **Palus S**, **Busquets S**, **Jové Q**, **Alves de Lima Junior E**, **Anker MS**, **von Haehling S**, **Álvarez Ladrón N**, **Millman O**, **Oosterlee A**, **Szymczyk A**,

López-Soriano FJ, **Anker SD**, **Coats AJS**, **Argiles JM**. The atypical β-blocker S-oxprenolol reduces cachexia and improves survival in a rat cancer cachexia model. *J Cachexia Sarcopenia Muscle* 14: 653–660, 2023. doi: 10.1002/jcsm.13116.

96. **Toledo M**, **Springer J**, **Busquets S**, **Tschirner A**, **López-Soriano FJ**, **Anker SD**, **Argilés JM**. Formoterol in the treatment of experimental cancer cachexia: effects on heart function. *J Cachexia Sarcopenia Muscle* 5: 315–320, 2014. doi: 10.1007/s13539-014-0153-y.

97. **White JP**, **Puppa MJ**, **Gao S**, **Sato S**, **Welle SL**, **Carson JA**. Muscle mTORC1 suppression by IL-6 during cancer cachexia: A role for AMPK. *Am J Physiol - Endocrinol Metab* 304: E1042-1052, 2013. doi: 10.1152/ajpendo.00410.2012.

98. **Argilés JM**, **López-Soriano FJ**. The role of cytokines in cancer cachexia. *Med Res Rev* 19: 223–248, 1999. doi: 10.1002/(sici)1098-1128(199905)19:3<223::aid-med3>3.0.co;2-n.

99. **Chen L**, **Deng H**, **Cui H**, **Fang J**, **Zuo Z**, **Deng J**, **Li Y**, **Wang X**, **Zhao L**. Inflammatory responses and inflammation-associated diseases in organs. *Oncotarget* 9: 7204–7218, 2018. doi: 10.18632/oncotarget.23208.

100. **Testa M**, **Yeh M**, **Lee P**, **Fanelli R**, **Loperfido F**, **Berman JW**, **LeJemtel TH**. Circulating levels of cytokines and their endogenous modulators in patients with mild to severe congestive heart failure due to coronary artery disease or hypertension. *J Am Coll Cardiol* 28: 964–971, 1996. doi: 10.1016/S0735-1097(96)00268-9.

101. **Deswal A**, **Petersen NJ**, **Feldman AM**, **Young JB**, **White BG**, **Mann DL**. Cytokines and cytokine receptors in advanced heart failure: An analysis of the cytokine database from the Vesnarinone Trial (VEST). *Circulation* 103: 2055–2059, 2001. doi:

10.1161/01.CIR.103.16.2055.

102. **Sack MN**. Tumor necrosis factor-α in cardiovascular biology and the potential role for anti-tumor necrosis factor-α therapy in heart disease. *Pharmacol Ther* 94: 123–135, 2002. doi: 10.1016/S0163-7258(02)00176-6.

103. **Springer J**, **Tschirner A**, **Haghikia A**, **Von Haehling S**, **Lal H**, **Grzesiak A**, **Kaschina E**, **Palus S**, **Pötsch M**, **Von Websky K**, **Hocher B**, **Latouche C**, **Jaisser F**, **Morawietz L**, **Coats AJS**, **Beadle J**, **Argiles JM**, **Thum T**, **Földes G**, **Doehner W**, **Hilfiker-Kleiner D**, **Force T**, **Anker SD**. Prevention of liver cancer cachexia-induced cardiac wasting and heart failure. *Eur Heart J* 35: 932–941, 2014. doi: 10.1093/eurheartj/eht302.

104. **Padrão AI**, **Moreira-Gonçalves D**, **Oliveira PA**, **Teixeira C**, **Faustino-Rocha AI**, **Helguero L**, **Vitorino R**, **Santos LL**, **Amado F**, **Duarte JA**, **Ferreira R**. Endurance training prevents TWEAK but not myostatin-mediated cardiac remodelling in cancer cachexia. *Arch Biochem Biophys* 567: 13–21, 2015. doi: 10.1016/j.abb.2014.12.026.

CHAPTER 2. LP07 AND LLC PRE-CLINICAL MODELS OF LUNG CANCER INDUCE DIVERGENT ANABOLIC DEFICITS AND EXPRESSION OF PRO-INFLAMMATORY EFFECTORS OF MUSCLE WASTING

This chapter is published:

Belcher DJ, Guitart M, Hain B, Kim HG, Waning D, Barreiro E, Nader GA. LP07 and LLC preclinical models of lung cancer induce divergent anabolic deficits and expression of pro-inflammatory effectors of muscle wasting. *J Appl Physiol* 133: 1260–1272, 2022. doi: 10.1152/japplphysiol.00246.2022.

2.1 ABSTRACT

Pre-clinical models have been instrumental in elucidating the mechanisms underlying muscle wasting in lung cancer (LC). We investigated anabolic deficits and the expression of pro-inflammatory effectors of muscle wasting in the LP07 and Lewis lung carcinoma (LLC) tumor models. Tumor growth resulted in significant weakness in LP07 but not in LLC mice despite similar reductions in gastrocnemius muscle mass in both models. The LP07 tumors caused a reduction in ribosomal (r)RNA and a decrease in rRNA gene (rDNA) transcription elongation, while no changes in ribosomal capacity were evident in LLC tumor bearing mice. Expression of RNA Polymerase I (Pol I) elongation-associated subunits Polr2f, PAF53, and Znrd1 mRNAs was significantly elevated in the LP07 model, while Pol I elongation-related factors FACT and Spt4/5 mRNAs were elevated in the LLC mice. Reductions in RPS6 and 4E-BP1 phosphorylation were

similar in both models but was independent of mTOR phosphorylation in LP07 mice. Muscle inflammation was also tumor-specific, IL-6 and TNF-α mRNA increased with LLC tumors, but upregulation of NLRP3 mRNA was independent of tumor type. In summary, while both models caused muscle wasting, only the LP07 model displayed muscle weakness with reductions in ribosomal capacity. Intracellular signaling diverged at the mTOR level with similar reductions in RPS6 and 4E-BP1 phosphorylation regardless of tumor type. The increase in pro-inflammatory factors was more pronounced in the LLC model. Our results demonstrate novel divergent anabolic deficits and expression of pro-inflammatory effectors of muscle wasting in the LP07 and LLC pre-clinical models of lung cancer.

2.2 INTRODUCTION

Lung cancer (LC) is one the most prevalent cachexia-inducing malignancies in the United States, with a greater risk for inpatient death than all other cancers combined (1, 2). Current treatment options for LC-associated cachexia have shown limited effectiveness at preventing muscle wasting, in part, due to the limited understanding of the mechanisms underlying this condition. The use of pre-clinical models of LC has facilitated the identification of several molecular mechanisms promoting muscle wasting, yet their use continues to pose unique challenges. Differences in host genetic background, immune status, tumor origin, administration route, differential onset of tumor growth, and tumor burden can introduce confounding variables that limit the elucidation of the mechanism driving muscle wasting in LC (3–10). In addition to the scarcity of human clinical data on LC-induced muscle wasting, these limitations may hinder progress towards the development of therapeutic interventions to prevent or reverse muscle wasting in cancer cachexia (11).

Much of the current knowledge about the mechanisms promoting muscle wasting in LC was generated using the Lewis lung carcinoma (LLC) model (5, 6, 8, 12–14). Following LLC tumor development, muscle wasting is associated with impaired muscle function (5, 6, 8, 9, 14), deficits in protein synthesis and elevated proteolysis (5, 6, 14, 15), increased systemic and local inflammation (5, 9), and mitochondrial dysfunction (8, 14). More recently, the LP07 lung adenocarcinoma (LP07) model revealed myopathogenic similarities with the LLC model (3, 4, 10). However, despite both tumor types originating from the lung and producing muscle wasting, whether they involve similar anabolic deficits remains unknown. This is an important problem as muscle wasting in cancer is associated with a reduction in ribosomal capacity (16–19). Anabolic impairments play a critical role in muscle wasting because muscle mass is largely determined by alterations in protein synthesis rates, which in turn depends on the ribosomal capacity of the muscle (20, 21). In addition to a lower ribosomal production, alterations in intracellular signaling involved in translational control may also promote muscle wasting in LC (4, 5, 13). Whether these anabolic mechanisms are similarly affected in skeletal muscle of LP07 and LLC tumor models remains to be investigated.

Congruent with the alterations in protein metabolism, an increase in systemic pro-inflammatory cytokines is often associated with tumor burden (16), and has been consistently demonstrated in pre-clinical models (5–7, 17) and late-stage LC patients with muscle wasting (23–26). Based on their effects on whole body metabolism, systemic cytokines can be classified as pro- (e.g. IL-1b, IL6, TNF-α) or anti-cachectic (e.g. IL-4, IL-10, IL-13) (27), and can play a role in local cytokine production to promote muscle wasting (28–30). A potential mediator of *in situ* cytokine production is the nucleotide-binding oligomerization domain-like receptor family and pyrin domain containing 3 (NLRP3) inflammasome. In response to inflammatory insults, NLRP3

mediates IL-1β and IL-18 production (31) to control local tissue inflammation (32). Currently, there are no data available about the involvement of the NLRP3 inflammasomes in cancer-induced muscle wasting. Because of the potential inflammatory responses to different tumor types, and the role of NLRP3 in modulating local muscle low-grade chronic inflammation during the progression of muscle wasting, we asked whether the different models of LC could elicit the coordinated expression of NLRP3 and downstream cytokines IL-1β and IL-18.

The goal of this study was to examine whether muscle wasting in the LP07 and LLC pre-clinical models of LC involved similar anabolic deficits and the local expression of pro-inflammatory factors. We hypothesized that muscle wasting following LP07 or LLC tumor implantation will be associated with a reduction in ribosomal capacity as a consequence of lower rDNA transcription together with alterations in mTOR and downstream signaling involved in translational control. Additionally, we sought to determine whether the expression of local pro-inflammatory effectors of muscle wasting was similar regardless of tumor type. Our findings revealed that despite the LP07 and LLC tumor cells originating from the lung and producing similar levels of muscle wasting, the LP07 model resulted in a larger reduction in force production. Anabolic deficits involved a specific decline in rDNA transcription elongation in the LP07 model. A reduction in mTOR phosphorylation was only evident in the LLC model, but RPS6 and 4E-BP1 phosphorylation was negatively affected regardless of the tumor type. Muscle expression of the pro-inflammatory cytokines IL-6 and TNF-α was higher in LLC mice, and while NLRP3 expression was similar in LP07 and LLC models, IL-1β and IL-18 were not induced in either model. Overall, our findings show that despite producing a similar muscle wasting phenotype, these pre-clinical models of LC induce muscle wasting via divergent anabolic deficits, neuromuscular, and pro-inflammatory mechanisms.

2.3 METHODS

2.3.1. Animals

All animal experiments were approved by both the animal care and use committees of the Universitat Pompeu Fabra and Pennsylvania State University for the LP07 and LLC models respectively, in accordance with the ethical standards set in the 1964 Declaration of Helsinki. The LP07 model was generated as previously described (4). Briefly, $4x10^5$ LP07 tumor cells (RRID: CVCL_W868) resuspended in 200µl MEM were subcutaneously inoculated under anesthesia into the right flank of 8-week-old randomly selected female BALB/c mice and 200µl MEM alone was injected in control mice. The LLC model was generated as recently described (15) by injecting $5x10^5$ LLC cells (RRID: CVCL_4358, CRL-1642, ATCC, Manassas, VA) in 100 µL sterile PBS subcutaneously into the right flank of 8-week-old randomly selected female C57BL6/129mice. Control mice were injected with 100µL of sterile PBS. Both LP07 and LLC models were monitored for tumor growth over a 28-30-day period, and upon euthanasia, the gastrocnemius muscles were excised, frozen and stored at -80°C for subsequent analysis. Age matched BALB/c or C57BL6/129 mice were used as controls for the LP07 and LLC models respectively.

2.3.2. Determination of muscle function

Forelimb force production was determined via the grip strength test prior to tumor cell inoculation and prior to euthanasia as previously described (3, 33). Briefly, mice were allowed to grasp a wire mesh attached to a force transducer (Bioseb, Vitrolles, France) while held by the base of the tail. Three pulls were recorded with 5 seconds of rest between trials and absolute grip strength was calculated as the average of the peak forces from the three trials.

2.3.3. RNA Extraction and Real-time Quantitative Polymerase Chain Reaction

Total RNA was extracted using Direct-zol RNA MiniPrep kit (Cat. No. R2051, Zymo Research, Irvin, CA) following manufacturer instructions as previously described (16). Briefly, following extraction, RNA was quantified spectrophotometrically using a CLARIOstar Microplate Reader with a LVis Plate (BMG Labtech, Ortenberg, Germany) and cDNA synthesized through reverse transcription PCR using the SuperScript VILO cDNA synthesis kit (Cat. No. 11756500, Zymo Research, Irvin, CA). The cDNA products were then used to quantify the respective mRNA and rRNA quantities via qRT-PCT (BioRad CX384) utilizing GoTaq qPCR Master (Cat. No. A6002, Promega, Madison, WI). The full list of qRT-PCR primers is found in Table 2.1. All analyzed transcripts via qPCR were normalized to GAPDH by the comparative Ct (ΔΔCt) method.

Table 2.1. qPCR primers

Target	Forward Sequence 5'-3'	Reverse Sequence 5'-3'
45S pre-rRNA (ETS)	CCAAGTGTTCATGCCACGTG	CGAGCGACTGCCACAAAAA
45S pre-rRNA (ITS)	CCGGCTTGCCCGATTT	GCCAGCAGGAACGAAACG
UBTF	CGCGCAGCATACAAAGAATACA	GTTTGGGCCTCGGAGCTT
SSRP1	CAGAGACATTGGAGTTCAACGA	GCCCGTCTTGCTGTTCTTAAAG
Spt16	TGGGACCTCGCGTGATTCTC	GCCACGTCTGTAAGGCAGTTG
Spt4	AGTGGCAGCGAGTCAGTAAC	AGTGGCAGCGAGTCAGTAAC
Spt5	CTGGAGAAAGAAGAGATTGAAGCC	TCAGACCCTCCATACACCGT
Twtstnb	CTGAGCCTGGGCAGACGTTA	CAGGCTTAGGGATAGAGGCGT
PAF-53	CTCGGTTCTCCTGCCCTCC	AGAAAGAGGTACACGCCGCC
Znrd1	TCACACCAGACAGATGCGCT	AAAGCATGGTAGCCGGAGGG
Polr2f	TCGACGGCGACGACTTTGAT	GGCCCGCTCATACTTGGTCA
IL-6	AGCCAGAGTCCTTCAGAGAGA	GGAGAGCATTGGAAATTGGGG
TNF-α	GTCCCCAAAGGGATGAGAAGT	TTTGCTACGACGTGGGCTAC
NLRP3	AGAGTGGATGGGTTTGCTGG	CGTGTAGCGACTGTTGAGGT
IL-1β	TGCCAAAAGGAAGATGATGCT	ACCCTCCCCACCTAACTTTG
IL-18	GCACCTTCTTTTCCTTCATCTTTG	GTTGTTCATCTCGGAGCCTGT
Myostatin	TGGCCATGATCTTGCTGTAA	CCTTGACTTCTAAAAAGGGATTCA
GAPDH	ACTGAGCAAGAGAGGCCCTA	TATGGGGGTCTGGGATGGAA

2.3.4. Western Blot Analysis

Samples were homogenized and extracted in RIPA lysis buffer (50mM Tris pH 8.0, 150mM NaCl, 1% Triton X-100, 0.1% SDS) supplemented with Pierce™ Protease and Phosphatase Inhibitor Mini Tablets (Cat. No. A32959, Thermo Fisher Scientific, Waltham, MA). The extracted proteins (10μg) were separated by SDS-PAGE on polyacrylamide gels, transferred to PVDF membranes as previously described (16), and subjected immunoblotting using the following antibodies: 4E-BP1 (1:2000, Cell Signaling Technology [CST] Cat. No. 9644, RRID: AB_2097841); Phospho-S6 Ribosomal Protein (S235/236) (1:2000, CST Cat. No. 2211, RRID: AB_331679), S6 Ribosomal Protein (1:2000, CST Cat. No. 2217, RRID: AB_331355), mTOR (1:2000, CST Cat. No. 2983, RRID: AB_2105622), Phospho-mTOR (Ser2448) (1:1000, CST Cat.

No. 2971, RRID: AB_330970). All blots were verified for equal loading using whole membrane staining with 0.2% India ink in PBS (Alfa Aesar™ Cat. No. J61007AP, Thermo Fisher Scientific, Waltham, MA).

2.3.5. Statistical Analysis

All data are reported as means ± standard deviation (SD) or mean standard error (SE) where appropriate and represented as either fold change or as percentage change from control. To reduce variability, potential outliers were identified by a ROUT test with the maximum false discovery rate set to 1%. A two-tail unpaired t-test was used when comparing the model tumor weights and tumor to BW ratios. All other comparisons were analyzed by a two-way (model x tumor) ANOVA. A planned Tukey's multiple comparison was performed in the event that there was a significant interaction or main effect. *P* values ≤ 0.05 were considered significant. Correlations between the changes in muscle mass and rRNA, elongation subunits, pol I subunits, translational signaling factors, and cytokine mRNA expression were calculated using Pearson product-moment correlation coefficients where appropriate. All statistical analyses were performed and graphically represented using GraphPad Prism 8 (GraphPad Prism, RRID: SCR_002798, San Diego, CA).

2.4. RESULTS

2.4.1. Skeletal muscle wasting is similar in LP07 and LLC models of cachexia

Changes in tumor-free body weight relative to initial body weight revealed a significant decrease in the LLC tumor group only (*P*=0.008) (Fig. 2.1A). Additionally, analyses of both raw tumor weight (*P*=0.001) (Fig. 2.1B) and the percentage of the tumor weight relative to whole body weight (*P*=0.023) (Fig. 2.1C) were significantly higher in the LLC model when compared to the

LP07. Relative gastrocnemius muscle mass was significantly lower in both the LP07 (P=0.026) and LLC (P<0.002) tumor mice (Fig. 2.1D). Gastrocnemius wet muscle weight was also significantly decreased in both the LP07 (P=0.031) and the LLC (P<0.001) models. However, despite similar reductions in relative muscle weight, the LP07 tumor model experienced a decline in forelimb grip strength (P<0.001) which was not apparent in the LLC model (P=0.645) (Fig 2.1F).

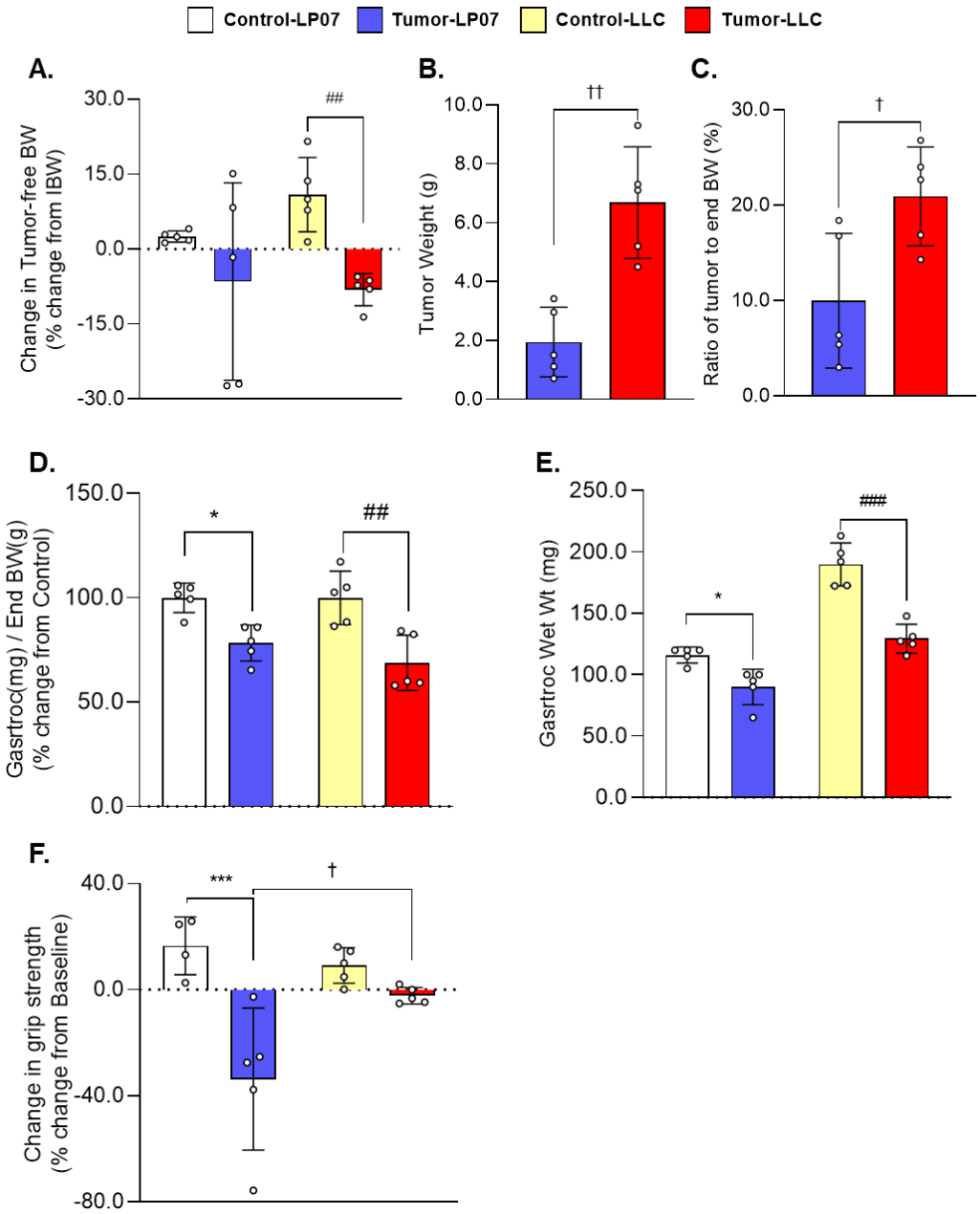

Figure 2.3. Skeletal muscle wasting is similar in LP07 and LLC models of cachexia

A: change in body weight (BW) was calculated as the percentage difference between initial and tumor-free end endpoint BW in grams. **B**: tumor weights are expressed in grams. **C**: the ratio of tumor weights was divided by the end BW and expressed in percentages. **D**: end gastrocnemius wet weight in milligrams was normalized as a percentage relative to their respective control. E: end gastrocnemius wet weight in milligrams. F: change in forelimb grip strength was calculated as the percent difference between initial and endpoint force in Newtons. Data are expressed as means ± SD. A two-way ANOVA followed by a Tukey's multiple-comparisons test was performed for the change in tumor-free BW, relative muscle weight, and grip strength; and an unpaired two-tail t test was used for tumor weight and ratio of tumor to total end BW. Significant difference from LP07 control: **P < 0.01; from LLC control: ##P < 0.01, ###P < 0.001; between tumor groups: †P < 0.05, ††P < 0.01, †††P < 0.001. gastroc, gastrocnemius; LLC, Lewis lung carcinoma.

2.4.2. LP07 tumors reduced rRNA levels and rDNA transcription elongation

Losses in total rRNA content occurred in the LP07 tumor mice (P=0.008), while no observable differences were found in the LLC model *(*P=0.916) (Fig. 2.2A). When compared to their LLC counterparts, we found that total rRNA content was approximately 60% lower in the tumor-bearing LP07 mice (P=0.002), and strongly correlated with losses in muscle mass (LP07: r=0.708, P=0.022) (Fig. 2.2B). While no alterations were found in 45S pre-rRNA 5' external transcribed spacer (ETS) transcription, a reduction in the 45S pre-RNA internal transcribed spacer 1 (ITS) was observed in LP07 mice when compared to controls (P=0.007) and no detectable differences in either ETS or ITS transcripts in the LLC model (Fig. 2.2C).

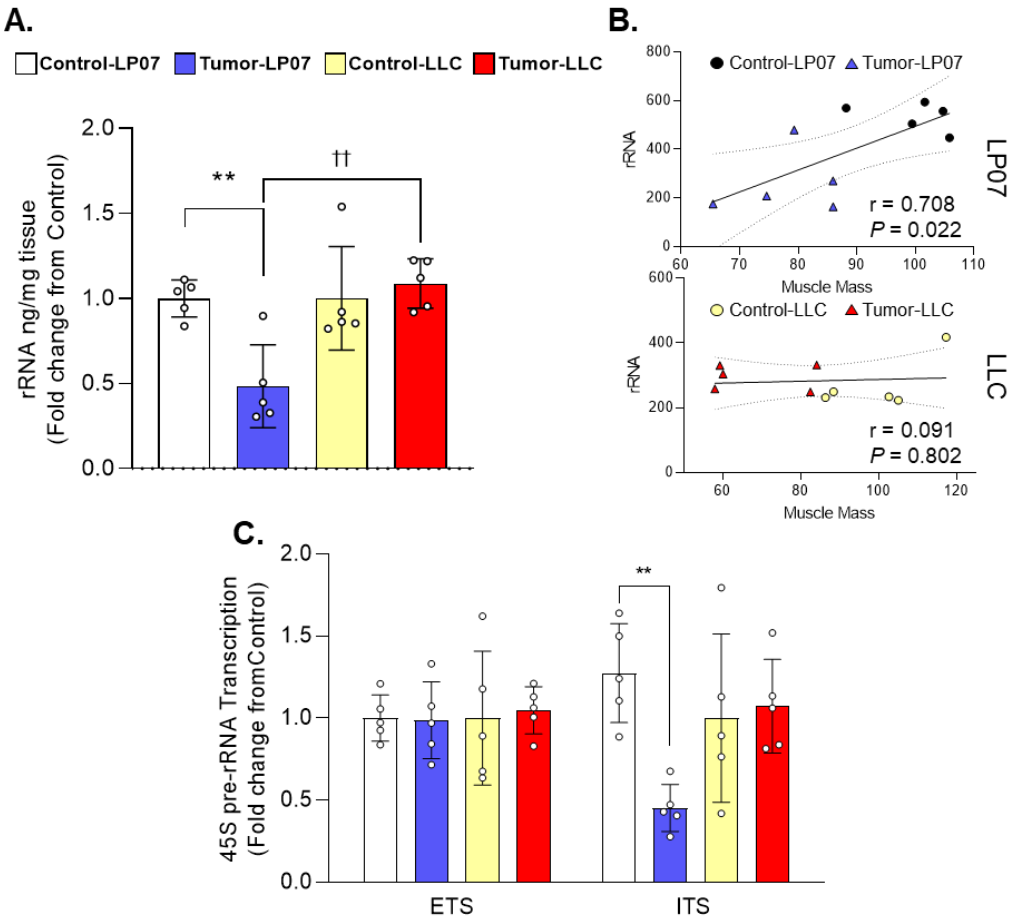

Figure 4.2. Tumor-bearing LP07 mice exhibited significantly lower ribosomal (r)RNA and 45S pre-rRNA internal transcribed spacer (ITS) compared with controls and LLC tumor mice

A: quantification of total rRNA. **B**: Pearson's product-moment correlations between rRNA and gastrocnemius muscle mass in LP07 and Lewis lung carcinoma (LLC) inoculated mice. **C**: expression of 45S pre-rRNA 5' external transcribed spacer (ETS) and ITS. Data are expressed as fold-change from controls ± SE. A two-way ANOVA followed by a Tukey's multiple-comparisons test was performed for all direct comparisons. Correlations were calculated using Pearson's product-moment correlation. Significant difference from LP07 control: $*P < 0.05$; between tumor groups: $\dagger P < 0.05$.

2.4.3. RNA pol I elongation-related subunits are upregulated in LP07 tumor bearing mice

To further investigate possible explanations for the loss of rRNA and ITS transcripts observed in the LP07 model, we next analyzed the mRNA expression of pol I subunits associated with 45S pre-rRNA elongation. Examination of pol I subunit mRNA showed significant increases in Polr2f in LP07 tumor mice compared to both control (P=0.006) and LLC tumor bearing mice (P=0.001) and significantly which negatively correlated to muscle mass loss (r=-0.785, P=0.007). Additionally, increased PAF53 (P=0.022) and Znrd1 (P=0.004) mRNA transcripts were uncovered in the LP07 model only (Fig. 2.3A) with significant correlations to muscle mass (PAF53: r=-0.720, P=0.019; Znrd1: r=-0.865, P=0.001) (Fig. 2.3B).

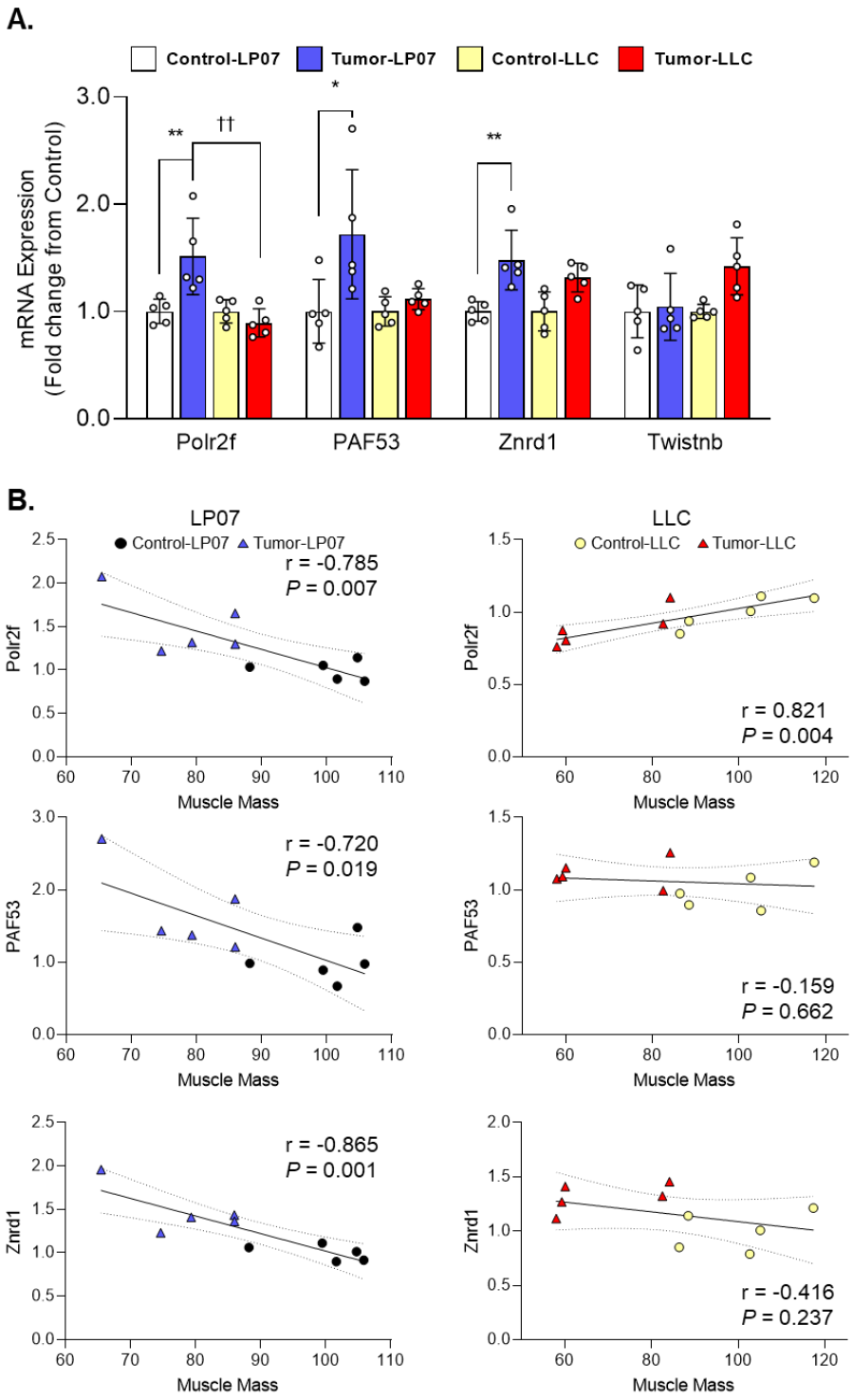

Figure 2.5. RNA pol I subunit mRNA expression was increased in LP07 model

A: expression of RNA pol I elongation associated subunit mRNAs. **B**: correlations between RNA pol I elongation associated subunit mRNAs and gastrocnemius muscle mass. Data are expressed as mean fold-change from controls ± SE. A two-way ANOVA followed by a Tukey's multiple-comparisons test was performed for all direct comparisons. Correlations were calculated using Pearson's product-moment correlation. Significant differences from LP07 controls: *$P < 0.05$, **$P < 0.01$; between tumor groups: ††$P < 0.01$

2.4.4. RNA pol I-associated elongation factors are significantly elevated in the LLC tumor bearing mice

Due to the disruption in rDNA transcription in 45S pre-rRNA elongation, we next examined several RNA pol I associated elongation factors. Of the five factors evaluated, only SSRP1, Spt4, and Spt16 mRNA transcripts were significantly elevated in LLC tumor-bearing mice when compared to controls (Spt16: P=0.049; SSRP1: P=0.024; Spt4: P=0.010), while no changes were observed in the LP07 (Fig. 2.4A). Further analyses revealed strong correlations between Spt16 (r=-0.763, P=0.046), SSRP1(r=-0.730, P=0.017), and Spt4 (r=-0.713, P=0.021) and the losses in muscle mass in the LLC model (Fig. 2.4B).

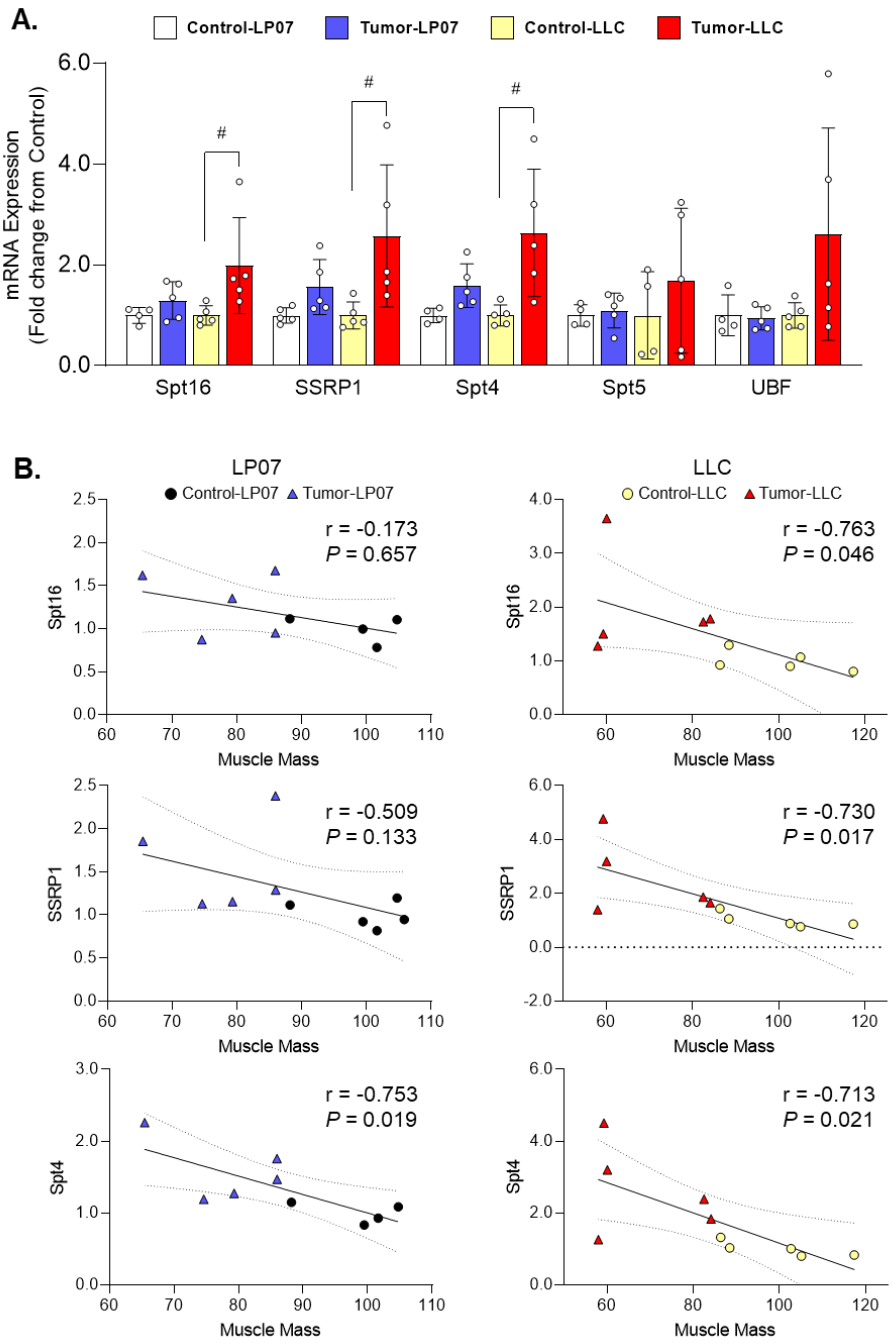

Figure 2.6. An increase in RNA polymerase I (RNA pol I) elongation factors was found in the Lewis Lung Carcinoma (LLC) model for Spt16, SSRP1, and Spt4 mRNA transcripts

A: expression of Spt16, SSRP1, Spt4, Spt5, and UBTF mRNA. **B**: Pearson's product-moment correlations between RNA pol I elongation factor mRNA and gastrocnemius muscle mass in LP07 and LLC inoculated mice. Data are expressed as mean fold-change from controls ± SE. A two-way ANOVA followed by a Tukey's multiple-comparisons test was performed for all direct comparison. Correlations were calculated using Pearson's product-moment correlation. Significant differences from LLC control: #$P < 0.05$.

2.4.5. Phosphorylation status of translational control factors differs between LP07 and LLC models

We then investigated the anabolic deficits in the LP07 and LLC models by examining changes in translational control factor signaling. Western blots were used to compare the phosphorylation status of $mTOR^{(S2448)}$ relative to total mTOR, the gamma band of 4E-BP1 relative to total 4E-BP1 as a surrogate for phosphorylation, and the phosphorylation status of $RPS6^{(S235/236)}$ relative to total RPS6. Here, we show a significant reduction in mTOR phosphorylation in the tumor-bearing LLC mice when compared to their controls (P=0.042) and the LP07 tumor-bearing group (P=0.036) (Fig. 2.5A) that strongly correlated to losses in muscle mass (r=0.929, P<0.001) (Fig. 2.5C). Downstream of mTORC1, we uncovered similar decreases in RPS6 phosphorylation (LP07: P=0.020; LLC: P=0.003) and 4E-BP1 phosphorylation (LP07: P<0.001; LLC: P<0.001) (Fig. 5A) with significant correlations to lower muscle mass in both models (RPS6: r=0.827, P=0.011; 4E-BP1: r=0.792, P=0.019) (Fig. 2.5C).

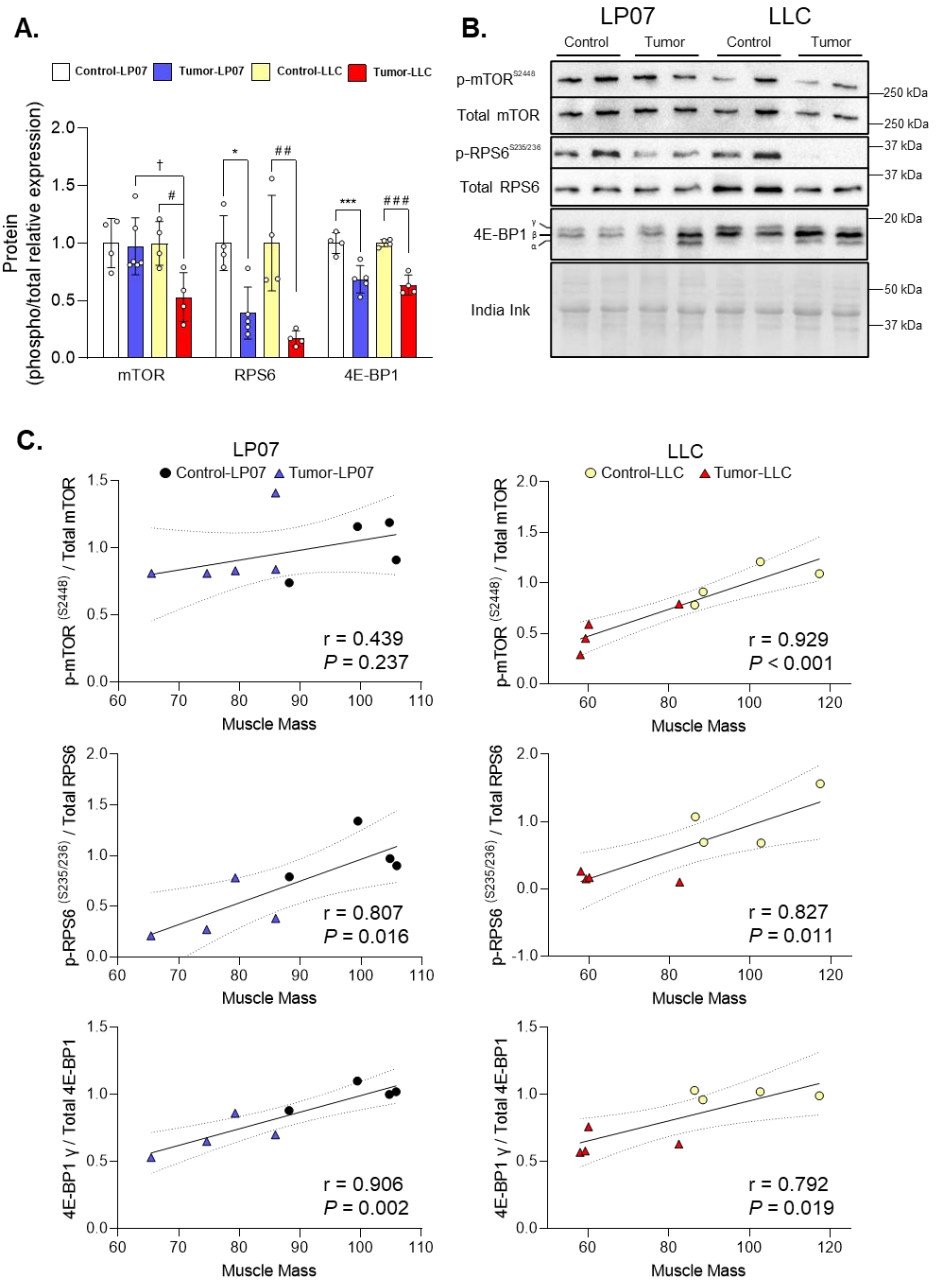

Figure 2.7. Phosphorylation Status of Translational Control Factors Differs between LP07 and LLC Models

A: quantification of mTOR, RPS6, and 4E-BP1 Western blots. **B**: representative Western blots for mTOR, RPS6, and 4E-BP1. The 4E-BP1 γ subunit was normalized to total 4E-BP1 and phosphorylated ribosomal protein S6 at S235/236 (p-RPS6(S235/236)) was normalized to total RPS6 to assess protein phosphorylation status. **C**: correlations between mTOR, RPS6, and 4E-BP1 Western blots and gastrocnemius muscle mass. Data are expressed as mean fold-change from controls ± SD. A two-way ANOVA followed by a Tukey's multiple-comparisons test was performed for all direct comparisons. Correlations were calculated using Pearson's product-moment correlation. Significant differences from LP07 controls: *P < 0.05, ***P < 0.001; from LLC controls: ###P < 0.001. LLC, Lewis lung carcinoma.

2.4.6. IL-6 and TNF-α mRNA are significantly elevated in LLC mice while NLRP3 mRNA is induced regardless of tumor type

To assess specific pro-inflammatory cytokine profile in these models, we examined the mRNA levels of selected effectors of muscle wasting. In the LLC tumor mice, muscle IL-6 and TNF-α mRNA levels were significantly elevated when compared to both their respective control groups (IL-6: $P<0.001$; TNF-α: $P<0.001$) and the LP07 group (IL-6: $P<0.001$; TNF-α: $P=0.028$) (Fig. 2.6A), and negatively correlated with reductions in muscle mass (IL-6: r=-0.787, $P=0.007$; TNF-α: r=-0.562, $P=0.091$) (Fig. 2.6B). Expression of the NLRP3 inflammasome, IL-1β and IL-18 did not differ between models. However, NLRP3 mRNA levels were elevated in the tumor-bearing mice of both models (LP07: $P<0.001$; LLC: $P=0.004$). The expression of myostatin remained unaltered in either tumor model at the time points studied (Fig. 2.6A).

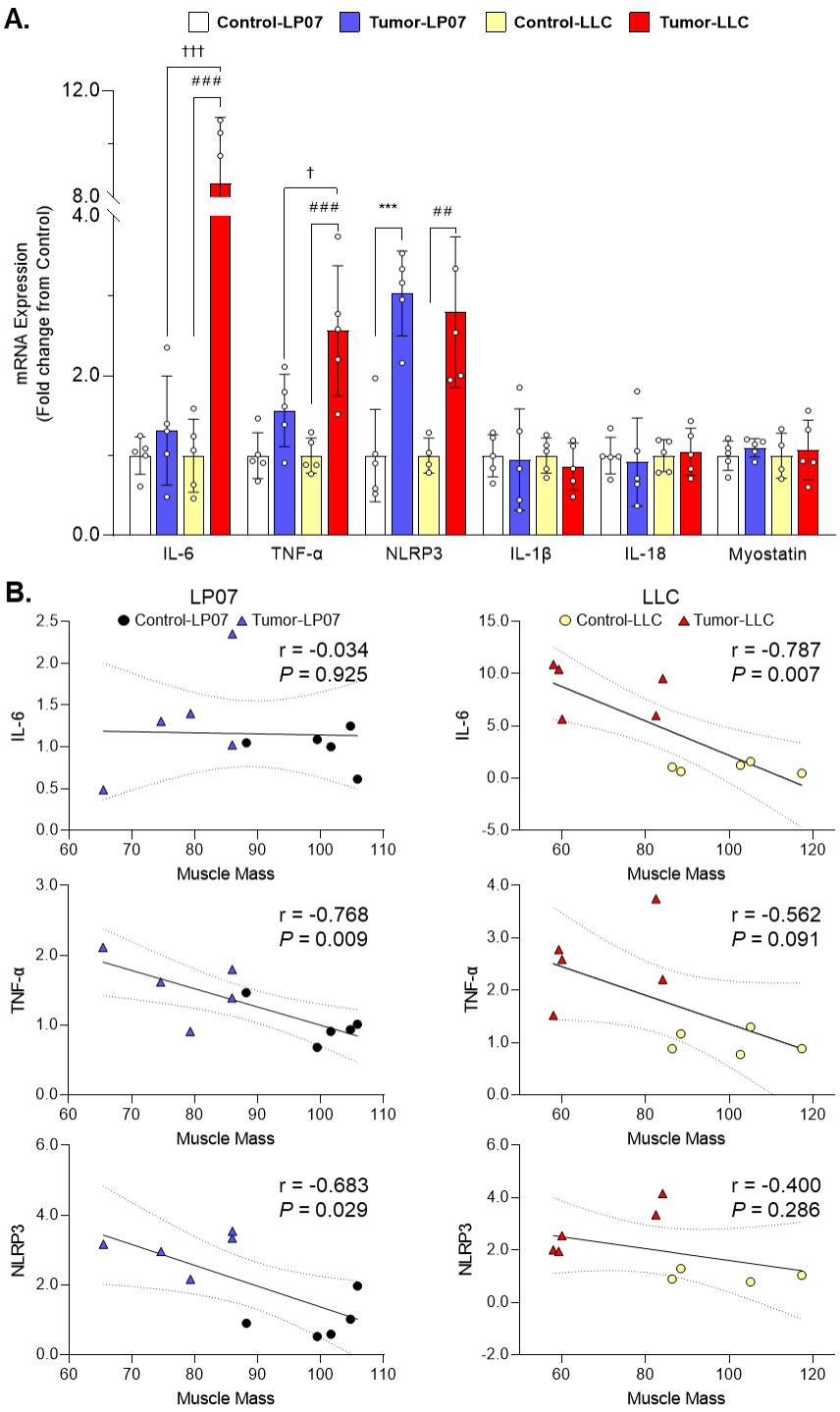

Figure 2.8. Proinflammatory cytokine mRNA expression was only elevated in the skeletal muscle of cachectic LLC mice

A: expression of proinflammatory cytokines (IL-6, TNF-α, NLRP3, IL-1β, and IL-18) and myostatin mRNA. **B**: correlations between proinflammatory cytokine mRNA levels and gastrocnemius muscle mass. Data are expressed as mean fold-change from controls ± SE. A two-way ANOVA followed by a Tukey's multiple-comparisons test was performed for all direct comparisons. Correlations were calculated using Pearson's product-moment correlation. Significant differences from LP07 controls: *P < 0.05, ***P < 0.001; from LLC controls: ###P < 0.001. LLC, Lewis lung carcinoma.

2.5. DISCUSSION

We investigated key mechanisms underlying anabolic deficits and the expression of pro-inflammatory cytokines using two established pre-clinical models of LC with muscle wasting. Clinically, cancer cachexia is defined by a loss of body weight, weakness, and wasting of skeletal muscle and adipose tissue that is not reversible by nutritional interventions (34–36). The emergence of new pre-clinical models of cancer cachexia has raised awareness about potential differences that may challenge their translational relevance for the understanding of muscle wasting in humans (11, 37). This motivated us to determine if tumors originating from the same tissue involved similar mechanisms of muscle wasting or whether they entail tumor-specific mechanisms. LP07 tumors have been previously shown to cause a significant reduction in body (~8%), gastrocnemius (~25%), and diaphragm (~25%) mass (3), while LLC tumor bearing mice also experienced reductions in lean body mass (~10%), tibialis anterior (~25%), extensor digitorum longus (~15%), soleus (~25%), and gastrocnemius (~20%) mass (15). Contrary to our hypothesis, we report findings demonstrating divergent anabolic deficits and local expression of pro-inflammatory cytokines in these established pre-clinical models of LC-associated muscle wasting.

Impaired force production often accompanies muscle wasting and is a hallmark of cancer cachexia (34, 36). We found that although both tumor types caused similar levels of muscle wasting, the LP07 tumors resulted in a severe reduction in grip strength while the LLC tumor bearing mice remained unaffected. This suggests that either the LP07 tumor impacts the neuromuscular system in a tumor-specific manner, or that the Balb/c mouse strain is more susceptible to neuromuscular impairments following an oncogenic challenge. Recent findings from two independent laboratories using the C26, MC38, or HCT116 tumors as models of

colorectal cancer reported that muscle wasting was associated with disruptions of neuromuscular junctions (38, 39). The underlying cause of the force deficits was a defect in presynaptic axon terminal morphology, which did not appear to show any tumor selectivity in the CD2F1 mouse strain (39). Thus, while it seems likely that force deficits in the LP07 may be a consequence defective neuromuscular remodeling, it remains to be determined whether the LLC tumors can impact the neuromuscular junction in a similar manner at a later time point, or whether the C57BL6/129 mice are resistant to tumor-induced neuromuscular junction alterations.

Reduced skeletal muscle anabolism has been consistently reported in pre-clinical models of cancer (16–19), and is largely determined by a diminished ribosomal capacity (15). Here, we report that muscle rRNA levels were significantly reduced in LP07 but not in the LLC tumor-bearing mice. The reduction in rRNA was consistent with our recent findings in the ES-2 ovarian cancer model (16), but in the LP07 model, the deficit in rRNA production was a consequence of decreased rDNA elongation as reflected by a lower (~40%) ITS signal. Because disruptions in Pol I elongation can impair rRNA processing and hence rRNA levels (40), we examined the expression of Pol I subunits and associated elongation factors to find out if the deficit in Pol I elongation was a consequence of a reduced expression of these factors. The Pol I holoenzyme is composed of 13 subunits, of which Polr2f, PAF53, Znrd1, and Twistnb promote efficient transcription elongation (41, 42). For example, mutations in rpa49 (yeast ortholog of PAF53) results in defective Pol I elongation (41), and ablation of the core Pol I subunit ABC23 (yeast ortholog of Polr2f), leads to the loss of rpa43 (Twistnb), reduces rpa14 stability, and consequently impairs rRNA elongation (42). Contrary to our assumption, we found that the expression of Pol I subunits involved in transcription elongation was higher in LP07 tumor-bearing mice. This intriguing finding resembles the expression pattern of Pol I subunits previously reported in the ES-2 model with reduced rDNA

transcription, where the expression of Pol I factors was elevated in response to lower rRNA production (16). In the LP07 model, the specific response involved the upregulation of selected Pol I elongation subunits, likely to counter the reduction in rDNA transcription elongation. Another contrasting finding was the elevated expression of Pol I-associated elongation factors in the LLC model. Due to the specific reduction in ITS levels, we focused on two complexes involved in Pol I elongation. The **Fa**cilitates **C**hromatin **T**ranscription (FACT) complex is a heterotrimeric protein complex composed of the Spt16 and SSRP1 subunits (43), and is responsible for maintaining the euchromatic state to facilitate transcription elongation (44). The Spt4/5 complex interacts with Pol I to promote processivity along the rDNA repeat (45). While we did not find any differences in the LP07 group, the expression level of Spt16, SSRP1, and Spt5 mRNA was significantly elevated in the LLC tumor bearing mice. Clearly, while the LP07 tumor impaired transcription elongation, the LLC model appears to maintain rRNA levels likely via the upregulation of elongation-specific factors. These observations suggest that model specific regulatory mechanisms exist at the level of rDNA transcription elongation that either impair (LP07) or maintain (LLC) rRNA production. This is in contrast with our previous findings in the ES-2 ovarian cancer model where deficits in rDNA transcription occurred at the initiation level (16).

In addition to the discrepant alterations in ribosomal capacity, the LP07 and LLC models also produced dissimilar changes in muscle intracellular signaling. A reduction in mTOR phosphorylation was only apparent in LLC mice, however a significant reduction in RPS6 and 4E-BP1 phosphorylation was detectable in both models. While our results are consistent with previous findings in cachectic LLC mice (5, 6, 13), a recent clinical investigation of late-stage non-small cell lung cancer (NSCLC) patients reported reductions in p70S6k and 4E-BP1 phosphorylation independent of changes in mTOR phosphorylation (23). Thus, it appears that the phosphorylation

patterns induced by the LP07 model resemble those described in muscle from LC patients. The dissociation in mTOR phosphorylation from its downstream targets is intriguing because mTOR is recognized as the putative upstream modulator of RPS6$^{(S235/236)}$ and 4E-BP1. A possible explanation for the discrepancy between mTOR phosphorylation and downstream targets is the input from Ras/Raf/ERK signaling, which may be operant in parallel to mTOR (6, 46). For example, pharmacological inhibition of ERK with the MEK inhibitor U0126 can reduce RPS6$^{(S235/236)}$ phosphorylation to a greater extent than rapamycin (46), and the ERK inhibitor LY-294002 can significantly reduce 4E-BP1 phosphorylation. Thus it is possible that ERK signaling may operate along with mTOR to modulate RPS6 and 4E-BP1 phosphorylation (47), which suggests that dysregulation of ERK signaling also contributes to the reduction in RPS6 and 4E-BP1 phosphorylation in LC independent of mTOR. Whereas both LP07 and LLC tumor bearing mice experienced a reduction in RPS6 and 4E-BP1 phosphorylation, a clear detrimental signaling effect exists at the level of mTOR phosphorylation in the LLC tumor bearing mice.

Changes in systemic pro-inflammatory cytokines have been consistently associated with muscle wasting in cancer (27, 35). Specifically in late stage LC patients, elevated TNF-α and IL-6 levels are concurrent with the progression of cachexia (23, 24) and can aggravate the pro-inflammatory milieu by stimulating *in situ* cytokine production (48). Increased systemic inflammation has been well-documented in both LP07 and LLC models (4, 5, 9), however, it is unclear if local skeletal muscle cytokine expression is conserved in these models (48, 49). We found that LLC tumors induced a significant increase in muscle IL-6 and TNF-α mRNA, but the LP07 tumor model did not significantly alter the expression of these cytokines. NLRP3, considered to be important for local cytokine production via the inflammasome (31), was similar in both models, but the pro-inflammatory cytokines IL-1β and IL-18 were not induced in either model.

This was intriguing and contrary to our hypothesis that NLRP3, IL-1β, and IL-18 are transcriptionally co-regulated. One possible explanation is that the elevation in NLRP3 mRNA may serve as a priming mechanism for IL-1β and IL-18 processing, therefore once these cytokines are produced, NLRP3 facilitates their maturation into active cytokines. Previous studies have shown that sepsis-induced muscle wasting stimulates local NLRP3-dependent IL-1β production (32). However, because the expression of these cytokines is transient and most severe following acute insults (32, 50), the lack of changes in IL-1β or IL-18 mRNA suggests that these cytokines may be induced during the acute phase of the wasting process rather than at this later stage. This interpretation is consistent with recent findings demonstrating downregulation of pro-inflammatory cytokines during the late stages (4 weeks) of muscle wasting in LLC tumor bearing mice (51). We also examined if the LP07 and LLC tumors caused any changes in myostatin, a potent negative regulator of muscle growth (52). Myostatin mRNA expression was not induced by either tumor, which is in line with clinical findings showing that myostatin mRNA was unaltered in muscle biopsies from late-stage NSCLC patients (23, 24). Together with the lack of changes in IL-1β and IL-18 expression, our results suggest that myostatin may play a more prominent role in the early stages of the wasting process (53). Altogether, the cytokine findings suggest that while IL-6 and TNF-α appear to contribute to muscle wasting in a tumor specific manner (i.e. elevated in LLC), the specific responses of other pro-inflammatory and growth suppressing factors may be conserved but at earlier time points. The fact that NLRP3 expression was similar in both models suggests that inflammasome-mediated local cytokine production may be a general response to tumors. Clearly, while the LP07 and LLC pre-clinical models of LC exhibit divergent pro-inflammatory phenotypes, more research is warranted to establish their temporal involvement in these two models of LC-induced muscle wasting.

In summary, although both the LP07 and LLC pre-clinical models of LC resulted in significant muscle wasting, clear differences in anabolic deficits, neuromuscular function, intracellular signaling, and pro-inflammatory cytokine profiles demonstrate tumor specific mechanisms of action that promote muscle wasting and loss of function. A limitation of this study is that we were not able to define the role of tumor burden because we utilized two tumor types in different genetic backgrounds. However, it is important to highlight that the LLC developed into larger tumors compared to the LP07 with a ~2-fold higher tumor weight to body mass ratio. Yet, muscle wasting was relatively similar in the two models studied. Further investigations designed to address the role of tumor burden will help clarify how different tumor types induce anabolic deficits and the expression of pro-inflammatory effectors in pre-clinical models of muscle wasting.

2.6. REFERENCES

1. **Arthur ST**, **Van Doren BA**, **Roy D**, **Noone JM**, **Zacherle E**, **Blanchette CM**. Cachexia among US cancer patients. *J Med Econ* 19: 874–880, 2016. doi: 10.1080/13696998.2016.1181640.
2. **Siegel RL**, **Miller KD**, **Jemal A**. Cancer statistics, 2019. *CA Cancer J Clin* 69: 7–34, 2019. doi: 10.3322/caac.21551.
3. **Chacon-Cabrera A**, **Fermoselle C**, **Urtreger AJ**, **Mateu-Jimenez M**, **Diament MJ**, **de Kier Joffé EDB**, **Sandri M**, **Barreiro E**. Pharmacological Strategies in Lung Cancer-Induced Cachexia: Effects on Muscle Proteolysis, Autophagy, Structure, and Weakness. *J Cell Physiol* 229: 1660–1672, 2014. doi: 10.1002/jcp.24611.
4. **Chacon-Cabrera A**, **Mateu-Jimenez M**, **Langohr K**, **Fermoselle C**, **García-Arumí E**, **Andreu AL**, **Yelamos J**, **Barreiro E**. Role of PARP activity in lung cancer-induced

cachexia: Effects on muscle oxidative stress, proteolysis, anabolic markers, and phenotype. *J Cell Physiol* 232: 3744–3761, 2017. doi: 10.1002/jcp.25851.

5. **Puppa MJ**, **Gao S**, **Narsale AA**, **Carson JA**. Skeletal muscle glycoprotein 130's role in Lewis lung carcinoma-induced cachexia. *FASEB J* 28: 998–1109, 2014. doi: 10.1096/fj.13-240580.

6. **Brown JL**, **Lee DE**, **Rosa-Caldwell ME**, **Brown LA**, **Perry RA**, **Haynie WS**, **Huseman K**, **Sataranatarajan K**, **Van Remmen H**, **Washington TA**, **Wiggs MP**, **Greene NP**. Protein imbalance in the development of skeletal muscle wasting in tumour-bearing mice. *J Cachexia Sarcopenia Muscle* 9: 987–1002, 2018. doi: 10.1002/jcsm.12354.

7. **Zhang G**, **Liu Z**, **Ding H**, **Miao H**, **Garcia JM**, **Li YP**. Toll-like receptor 4 mediates Lewis lung carcinoma-induced muscle wasting via coordinate activation of protein degradation pathways. *Sci Rep* 7: 1–8, 2017. doi: 10.1038/s41598-017-02347-2.

8. **Brown JL**, **Rosa-Caldwell ME**, **Lee DE**, **Blackwell TA**, **Brown LA**, **Perry RA**, **Haynie WS**, **Hardee JP**, **Carson JA**, **Wiggs MP**, **Washington TA**, **Greene NP**. Mitochondrial degeneration precedes the development of muscle atrophy in progression of cancer cachexia in tumour-bearing mice. *J Cachexia Sarcopenia Muscle* 8: 926–938, 2017. doi: 10.1002/jcsm.12232.

9. **Ohe Y**, **Podack ER**, **Olsen KJ**, **Miyahara Y**, **Miura K**, **Saito H**, **Koishihara Y**, **Ohsugi Y**, **Ohira T**, **Nishio K**, **Saijo N**. Interleukin-6 cdna transfected lewis lung carcinoma cells show unaltered net tumour growth rate but cause weight loss and shorten survival in syngenic mice. *Br J Cancer* 67: 939–944, 1993. doi: 10.1038/bjc.1993.174.

10. **Chacon-Cabrera A**, **Fermoselle C**, **Salmela I**, **Yelamos J**, **Barreiro E**. MicroRNA expression and protein acetylation pattern in respiratory and limb muscles of Parp-1-/- and

Parp-2-/- mice with lung cancer cachexia. *Biochim Biophys Acta - Gen Subj* 1850: 2530–2543, 2015. doi: 10.1016/j.bbagen.2015.09.020.

11. **Ballarò R**, **Costelli P**, **Penna F**. Animal models for cancer cachexia. *Curr Opin Support Palliat Care* 10: 281–287, 2016. doi: 10.1097/SPC.0000000000000233.

12. **Rosa-Caldwell ME**, **Fix DK**, **Washington TA**, **Greene NP**. Muscle alterations in the development and progression of cancer-induced muscle atrophy: a review. *J Appl Physiol* 128: 25–41, 2020. doi: 10.1152/japplphysiol.00622.2019.

13. **Bohnert KR**, **Gallot YS**, **Sato S**, **Xiong G**, **Hindi SM**, **Kumar A**. Inhibition of ER stress and unfolding protein response pathways causes skeletal muscle wasting during cancer cachexia. *FASEB J* 30: 3053–3068, 2016. doi: 10.1096/fj.201600250RR.

14. **Lim S**, **Deaver JW**, **Rosa-Caldwell ME**, **Haynie WS**, **Morena da Silva F**, **Cabrera AR**, **Schrems ER**, **Saling LW**, **Jansen LT**, **Dunlap KR**. Development of metabolic and contractile alterations in development of cancer cachexia in female tumor-bearing mice. *J Appl Physiol* 132: 58–72, 2022. doi: 10.1152/japplphysiol.00660.2021.

15. **Hain BA**, **Xu H**, **VanCleave AM**, **Gordon BS**, **Kimball SR**, **Waning DL**. REDD1 deletion attenuates cancer cachexia in mice. *J Appl Physiol* 131: 1718–1730, 2021. doi: 10.1152/japplphysiol.00536.2021.

16. **Kim H-G**, **Huot J**, **Pin F**, **Guo B**, **Bonetto A**, **Nader G**. Reduced rDNA transcription diminishes skeletal muscle ribosomal capacity and protein synthesis in cancer cachexia. *FASEB* 35: e21335, 2021. doi: 10.1096/fj.202002257R.

17. **Emery PW**, **Edwards RHT**, **Rennie MJ**. Protein synthesis in muscle measured in vivo in

cachectic patients with cancer. *Br Med J* 289: 584–586, 1984. doi: 10.1136/bmj.289.6445.584.

18. **Baracos VE**, **DeVivo C**, **Hoyle DH**, **Goldberg AL**. Activation of the ATP-ubiquitin-proteasome pathway in skeletal muscle of cachectic rats bearing a hepatoma. *Am J Physiol Metab* 268: E996–E1006, 1995. doi: 10.1152/ajpendo.1995.268.5.E996.
19. **Goodlad GAJ**, **Clark CM**. Response of skeletal muscle RNA polymerases I and II to tumour growth. *Biochim Biophys Acta (BBA)-Gene Struct Expr* 950: 296–302, 1988. doi: 10.1016/0167-4781(88)90125-x.
20. **Millward DJ**, **Garlick PJ**, **Nnanyelugo DO**, **Waterlow JC**. The relative importance of muscle protein synthesis and breakdown in the regulation of muscle mass. *Biochem J* 156: 185–188, 1976. doi: 10.1042/bj1560185.
21. **Millward DJ**, **Garlick PJ**, **James WPT**, **Nnanyelugo DO**, **Ryatt JS**. Relationship between protein synthesis and RNA content in skeletal muscle [15]. *Nature* 241: 204–205, 1973. doi: 10.1038/241204a0.
22. **Gao S**, **Durstine JL**, **Koh HJ**, **Carver WE**, **Frizzell N**, **Carson JA**. Acute myotube protein synthesis regulation by IL-6-related cytokines. *Am J Physiol - Cell Physiol* 313: C487–C500, 2017. doi: 10.1152/ajpcell.00112.2017.
23. **Murton AJ**, **Maddocks M**, **Stephens FB**, **Marimuthu K**, **England R**, **Wilcock A**. Consequences of Late-Stage Non–Small-Cell Lung Cancer Cachexia on Muscle Metabolic Processes. *Clin Lung Cancer* 18: e1–e11, 2017. doi: 10.1016/j.cllc.2016.06.003.
24. **Op Den Kamp CM**, **Langen RC**, **Snepvangers FJ**, **De Theije CC**, **Schellekens JM**, **Laugs F**, **Dingemans AMC**, **Schols AM**. Nuclear transcription factor κB activation and

protein turnover adaptations in skeletal muscle of patients with progressive stages of lung cancer cachexia. *Am J Clin Nutr* 98: 738–748, 2013. doi: 10.3945/ajcn.113.058388.

25. **Paval DR**, **Patton R**, **McDonald J**, **Skipworth R**, **Gallagher I**, **Laird B**. A systematic review examining the relationship between cytokines and cachexia in incurable cancer. *J Cachexia Sarcopenia Muscle* 13: 824–838, 2022. doi: 10.1002/jcsm.12912.
26. **Pelosi M**, **De Rossi M**, **Barberi L**, **Musarò A**. IL-6 impairs myogenic differentiation by downmodulation of p90RSK/eEF2 and mTOR/p70S6K axes, without affecting AKT activity. *Biomed Res Int* 2014, 2014. doi: 10.1155/2014/206026.
27. **Argilés JM**, **López-Soriano FJ**. The role of cytokines in cancer cachexia. *Med Res Rev* 19: 223–248, 1999. doi: 10.1002/(sici)1098-1128(199905)19:3<223::aid-med3>3.0.co;2-n.
28. **Webster JM**, **Kempen LJAP**, **Hardy RS**, **Langen RCJ**. Inflammation and Skeletal Muscle Wasting During Cachexia. *Front Physiol* 11, 2020. doi: 10.3389/fphys.2020.597675.
29. **Podbregar M**, **Lainscak M**, **Prelovsek O**, **Mars T**. Cytokine response of cultured skeletal muscle cells stimulated with proinflammatory factors depends on differentiation stage. *Sci World J* 2013, 2013. doi: 10.1155/2013/617170.
30. **Luo G**, **Hershko DD**, **Robb BW**, **Wray CJ**, **Hasselgren P-O**. IL-1β stimulates IL-6 production in cultured skeletal muscle cells through activation of MAP kinase signaling pathway and NF-κB. *Am J Physiol Integr Comp Physiol* 284: R1249–R1254, 2003. doi: 10.1152/ajpregu.00490.2002.
31. **Martinon F**, **Burns K**, **Tschopp J**. The Inflammasome: A molecular platform triggering

activation of inflammatory caspases and processing of proIL-β. *Mol Cell* 10: 417–426, 2002. doi: 10.1016/S1097-2765(02)00599-3.

32. **Huang N**, **Kny M**, **Riediger F**, **Busch K**, **Schmidt S**, **Luft FC**, **Slevogt H**, **Fielitz J**. Deletion of Nlrp3 protects from inflammation-induced skeletal muscle atrophy. *Intensive Care Med Exp* 5: 1–15, 2017. doi: 10.1186/s40635-016-0115-0.

33. **Bonetto A**, **Andersson DC**, **Waning DL**. Assessment of muscle mass and strength in mice. *Bonekey Rep* 4: 732, 2015. doi: 10.1038/bonekey.2015.101.

34. **Fearon K**, **Strasser F**, **Anker SD**, **Bosaeus I**, **Bruera E**, **Fainsinger RL**, **Jatoi A**, **Loprinzi C**, **MacDonald N**, **Mantovani G**, **Davis M**, **Muscaritoli M**, **Ottery F**, **Radbruch L**, **Ravasco P**, **Walsh D**, **Wilcock A**, **Kaasa S**, **Baracos VE**. Definition and classification of cancer cachexia: An international consensus. *Lancet Oncol* 12: 489–495, 2011. doi: 10.1016/S1470-2045(10)70218-7.

35. **Argilés JM**, **Busquets S**, **Stemmler B**, **López-Soriano FJ**. Cancer cachexia: Understanding the molecular basis. *Nat Rev Cancer* 14: 754–762, 2014. doi: 10.1038/nrc3829.

36. **Vanhoutte G**, **Van De Wiel M**, **Wouters K**, **Sels M**, **Bartolomeeussen L**, **De Keersmaecker S**, **Verschueren C**, **De Vroey V**, **De Wilde A**, **Smits E**, **Cheung KJ**, **De Clerck L**, **Aerts P**, **Baert D**, **Vandoninck C**, **Kindt S**, **Schelfhaut S**, **Vankerkhoven M**, **Troch A**, **Ceulemans L**, **Vandenbergh H**, **Leys S**, **Rondou T**, **Dewitte E**, **Maes K**, **Pauwels P**, **De Winter B**, **Van Gaal L**, **Ysebaert D**, **Peeters M**. Cachexia in cancer: what is in the definition? *BMJ Open Gastroenterol* 3: e000097, 2016. doi: 10.1136/bmjgast-2016-000097.

37. **Penna F**, **Busquets S**, **Argilés JM**. Experimental cancer cachexia: Evolving strategies for

getting closer to the human scenario. *Semin Cell Dev Biol* 54: 20–27, 2016. doi: 10.1016/j.semcdb.2015.09.002.

38. **Sartori R**, **Hagg A**, **Zampieri S**, **Armani A**, **Winbanks CE**, **Viana LR**, **Haidar M**, **Watt KI**, **Qian H**, **Pezzini C**. Perturbed BMP signaling and denervation promote muscle wasting in cancer cachexia. *Sci Transl Med* 13: eaay9592, 2021. doi: 10.1126/scitranslmed.aay9592.

39. **Huot JR**, **Pin F**, **Bonetto A**. Muscle weakness caused by cancer and chemotherapy is associated with loss of motor unit connectivity. *Am J Cancer Res* 11: 2990–3001, 2021.

40. **Schneider DA**, **Michel A**, **Sikes ML**, **Vu L**, **Dodd JA**, **Salgia S**, **Osheim YN**, **Beyer AL**, **Nomura M**. Transcription Elongation by RNA Polymerase I Is Linked to Efficient rRNA Processing and Ribosome Assembly. *Mol Cell* 26: 217–229, 2007. doi: 10.1016/j.molcel.2007.04.007.

41. **Albert B**, **Léger-Silvestre I**, **Normand C**, **Ostermaier MK**, **Pérez-Fernández**, **Panov KI**, **Zomerdijk JCBM**, **Schultz P**, **Gadal O**. RNA polymerase I-specific subunits promote polymerase clustering to enhance the rRNA gene transcription cycle. *J Cell Biol* 192: 277–293, 2011. doi: 10.1083/jcb.201006040.

42. **Lanzendörfer M**, **Smid A**, **Klinger C**, **Schultz P**, **Sentenac A**, **Carles C**, **Riva M**. A shared subunit belongs to the eukaryotic core RNA polymerase. *Genes Dev* 11: 1037–1047, 1997. doi: 10.1101/gad.11.8.1037.

43. **Orphanides G**, **LeRoy G**, **Chang C-H**, **Luse DS**, **Reinberg D**. FACT, a factor that facilitates transcript elongation through nucleosomes. *Cell* 92: 105–116, 1998. doi: 10.1016/s0092-8674(00)80903-4.

44. **Birch JL**, **Tan BCM**, **Panov KI**, **Panova TB**, **Andersen JS**, **Owen-Hughes TA**, **Russell**

J, **Lee SC**, **Zomerdijk JCBM**. FACT facilitates chromatin transcription by RNA polymerases i and III. *EMBO J* 28: 854–865, 2009. doi: 10.1038/emboj.2009.33.

45. **Schneider DA**, **French SL**, **Osheim YN**, **Bailey AO**, **Vu L**, **Dodd J**, **Yates JR**, **Beyer AL**, **Nomura M**. RNA polymerase II elongation factors Spt4p and Spt5p play roles in transcription elongation by RNA polymerase I and rRNA processing. *Proc Natl Acad Sci U S A* 103: 127070–12712, 2006. doi: 10.1073/pnas.0605686103.

46. **Roux PP**, **Shahbazian D**, **Vu H**, **Holz MK**, **Cohen MS**, **Taunton J**, **Sonenberg N**, **Blenis J**. RAS/ERK signaling promotes site-specific ribosomal protein S6 phosphorylation via RSK and stimulates cap-dependent translation. *J Biol Chem* 282: 14056–14064, 2007. doi: 10.1074/jbc.M700906200.

47. **Le Plénier S**, **Goron A**, **Sotiropoulo A**, **Archambault E**, **Guihenneuc C**, **Walrand S**, **Salles J**, **Jourdan M**, **Neveux N**, **Cynober L**, **Moinard C**. Citrulline directly modulates muscle protein synthesis via the PI3K/MAPK/4E-BP1 pathway in a malnourished state: Evidence from in vivo, ex vivo, and in vitro studies. *Am J Physiol - Endocrinol Metab* 312: E27–E36, 2017. doi: 10.1152/ajpendo.00203.2016.

48. **Webster JM**, **Kempen LJAP**, **Hardy RS**, **Langen RCJ**. Inflammation and Skeletal Muscle Wasting During Cachexia. *Front Physiol* 11, 2020. doi: 10.3389/fphys.2020.597675.

49. **Argilés JM**, **Stemmler B**, **López-Soriano FJ**, **Busquets S**. Inter-tissue communication in cancer cachexia. *Nat Rev Endocrinol* 15: 9–20, 2018. doi: 10.1038/s41574-018-0123-0.

50. **Voss JG**, **Shagal AG**, **Tsuji JM**, **MacDonald JW**, **Bammler TK**, **Farin FM**, **St Pierre Schneider B**. Time Course of Inflammatory Gene Expression Following Crush Injury in Murine Skeletal Muscle. *Nurs Res* 66: 63–74, 2017. doi:

10.1097/NNR.0000000000000209.

51. **Blackwell TA**, **Cervenka I**, **Khatri B**, **Brown JL**, **Rosa-Caldwell ME**, **Lee DE**, **Perry Jr RA**, **Brown LA**, **Haynie WS**, **Wiggs MP**. Transcriptomic analysis of the development of skeletal muscle atrophy in cancer-cachexia in tumor-bearing mice. *Physiol Genomics* 50: 1071–1082, 2018. doi: 10.1152/physiolgenomics.00061.2018.

52. **Wang DT**, **Yang YJ**, **Huang RH**, **Zhang ZH**, **Lin X**. Myostatin Activates the Ubiquitin-Proteasome and Autophagy-Lysosome Systems Contributing to Muscle Wasting in Chronic Kidney Disease. *Oxid Med Cell Longev* 2015: 1–18, 2015. doi: 10.1155/2015/684965.

53. **Busquets S**, **Toledo M**, **Orpí M**, **Massa D**, **Porta M**, **Capdevila E**, **Padilla N**, **Frailis V**, **López-Soriano FJ**, **Han HQ**, **Argilés JM**. Myostatin blockage using actRIIB antagonism in mice bearing the Lewis lung carcinoma results in the improvement of muscle wasting and physical performance. *J Cachexia Sarcopenia Muscle* 3: 37–43, 2012. doi: 10.1007/s13539-011-0049-z.

CHAPTER 3. ANABOLIC DEFICITS AND DIVERGENT UNFOLDED PROTEIN RESPONSE UNDERLIE MUSCLE AND HEART GROWTH IMPAIRMENTS IN THE YOSHIDA HEPATOMA TUMOR MODEL OF CANCER CACHEXIA

This chapter has been submitted for publication and is pending peer-review in *Physiological Reports*:

Belcher DJ, Kim N, Navarro B, Möller M, López-Soriano FJ, Busquets S, Nader GA. Anabolic deficits and divergent unfolded protein response underlie muscle and heart growth impairments in the Yoshida hepatoma tumor model of cancer cachexia. *Physiol Rep: (Under Peer-Review)*

3.1. ABSTRACT

Cancer cachexia manifests as whole body wasting, however, the precise mechanisms governing the alterations in tissue anabolism remain incompletely understood. In this study, we explored the potential suppression of anabolic processes in both skeletal and cardiac muscles of the Yoshida AH-130 ascites hepatoma model of cancer cachexia. After 7 days, tumor-bearing rats displayed lower body, skeletal muscle, and heart weights. These deficiencies were associated with decreased ribosomal (r)RNA, and significant 4E-BP1 hypophosphorylation. Indications of endoplasmic reticulum stress were evident by elevated GADD34 mRNA expression in both skeletal and cardiac muscles, and increased ATF4 expression in the skeletal, but not in heart muscle. Increased tissue INF-γ mRNA was uncovered in the heart, while IL-1β mRNA was

significantly elevated in both skeletal and cardiac muscles. Our results indicate that lower skeletal muscle and heart masses in the Yoshida AH-130 ascites hepatoma model likely involves a marked reduction translational capacity and efficiency, and divergent alterations in endoplasmic reticulum stress and tissue production of pro-inflammatory cytokines.

3.2. INTRODUCTION

Cachexia is a multifaceted bodily wasting condition that increases overall mortality and morbidity of cancer patients (1–3). Reductions in fat and skeletal muscle mass and strength are hallmarks of this condition (1, 3). Also prevalent is the loss of cardiac mass, which leads to impaired heart function and reduced physical capacity (4). Collectively, these deteriorations severely reduce quality of life and shorten lifespan of cancer patients. (1, 3, 4).

Hepatocellular carcinoma is one of the fastest growing and deadliest forms of cancer in the U.S (5). Approximately 25% of hepatocellular carcinoma patients develop cachectic symptoms, contributing to the increased rate of mortality (6). The Yoshida AH-130 ascites hepatoma is one of the most extensively studied pre-clinical models of cancer cachexia in hepatocellular carcinoma research. As a highly aggressive form of cancer, rats carrying the AH-130 tumor experience a rapid loss in skeletal and cardiac muscle mass (7–10). This wasting is often accompanied by systemic and local inflammation (11, 12), disrupted cellular metabolism (13, 14), and elevated proteolysis (10, 13, 14). The intrinsic maintenance of skeletal and cardiac muscle mass relies on the balance of protein turnover (15). Disruption to this equilibrium from a suppression in protein synthesis, an elevation in protein degradation, or a combination of both leads to tissue wasting. We recently showed that disruptions to anabolism in skeletal muscle coincides with cancer-induced muscle wasting (16–18). This led to an overall reduction in

ribosomal content, effectively suppressing the rate at which protein synthesis can occur (19). Despite this understanding in skeletal muscle, the impact of cachexia on translational capacity in the heart remains elusive.

In addition to the importance of translational capacity, translational efficiency also plays a significant role in the maintenance of muscle mass. While a suppression in anabolic signaling has been observed in cachectic AH-130 tumor-bearing rats (10, 20, 21), the root cause of this deficiency remains undetermined. A potential contributor to this deficiency may be through the induction of endoplasmic reticulum (ER) stress. This manifests through an accumulation of unfolded or misfolded proteins that aggregate and clog the lumen of the ER (22). The unfolded protein response (UPR), by ER stress, represses translational signaling to restore cellular proteostasis (23). ER-stress induced UPR activation has been linked to several atrophying conditions such as sarcopenia, inflammatory myopathies, muscular dystrophy, and cancer cachexia (24). Increased expression of multiple ER stress markers have previously been observed in the skeletal muscle of LLC and $APC^{Min/+}$ cachectic mice (25). However, whether ER stress is a significantly contributes to wasting in skeletal and cardiac muscle of Yoshida AH-130 ascites hepatoma model of cachexia remains to be elucidated.

Muscle wasting is often linked to systemic elevations in pro-inflammatory cytokines in cancer (26–29). Cytokines, based on their impact on their organ and tissue effects, can be categorized as pro- or anti-inflammatory (29). Increased production of pro-inflammatory cytokines such as TNF-α, IL-1β, or IL-6, may also contribute to the local pro-inflammatory environment, thereby promoting muscle wasting (26, 30, 31). Elevations in systemic inflammation have also been previously linked to impaired cardiovascular function (32, 33). For example, increases in circulating IL-1 β and IL-6 have been observed during heart failure (34,

35). Endogenous production of TNF-α has been found in chronic heart failure patients and an overexpression in the heart leads to cardiovascular complications (36). However, while systemic inflammation has been previously documented in several models of cancer cachexia (26–28, 37), the effects of the local cytokine production in the skeletal and cardiac muscles of AH-130 Yoshida tumor-bearing rat remains unanswered.

Our goal in the present study was to determine whether reductions in translational capacity and efficiency underlie impediments to skeletal and cardiac muscle mass in the Yoshida AH-130 hepatoma model, and whether the induction of the unfolded protein response (UPR) and local tissue expression of pro-inflammatory cytokines were modulated in this model of cachexia. We demonstrate that inoculation with Yoshida AH-130 tumor cells caused a reduction in ribosomal capacity and 4E-BP1 phosphorylation in both skeletal and cardiac muscle. Wasting was associated with ATF4 and GADD34 gene expression in skeletal muscle, but the latter only in the heart. Local IL-1β expression was detected in both skeletal and cardiac muscle of cachectic rats and was accompanied by a marked increase in IFN-γ expression in the heart but not in skeletal muscle. Overall, these findings suggest that Yoshida AH-130 tumor-bearing rats undergo skeletal and cardiac muscle wasting, in part, via a reduction in translational capacity, dysregulated translational control signaling, UPR induction, and the expression of tissue pro-inflammatory cytokines.

3.3. METHODS

3.3.1. Animals and tumor inoculation

Male Wistar rats (8-week-old) were housed in a controlled environment with a temperature of 22±2°C and a normal dark cycle of 12 hours with lights on from 08:00 a.m. to 08:00 p.m. All

animal experiments were made in accordance with the European Community guidelines for the use of laboratory animals (38), and The Bioethical Committee of the University of Barcelona approved the experimental protocol. Rats were randomly divided into control (n=6) or tumor groups (n=7). Animals in the tumor group received an intraperitoneal (i.p.) inoculation of 10^8 AH-130 Yoshida ascites hepatoma cells, while those in the control group received an equal volume of saline. After 7 days, animals were weighed and anesthetized with an i.p. injection of ketamine/xylazine mixture (3:1) (Imalgene® and Rompun®, respectively). Throughout the duration of the study, food and water were supplied ad libitum. In both animal groups, food intake and body weight were determined on Day 0 and immediately before sacrifice on Day 7. Food intake was calculated by: (food weight on Day 7 – food weight on Day 0)/initial body weight on Day 0 × 100. Tumors were carefully extracted from the peritoneal cavity to assess tumor volume and cell density. The gastrocnemius muscles and heart tissues were rapidly excised, weighed, frozen in liquid nitrogen, and stored at -80° C until further analysis.

3.3.2. RNA Extraction and Quantitative Polymerase Chain Reaction

Total RNA extraction from gastrocnemius and heart tissues were performed as previously described (18). Briefly, tissues were homogenized in TRIzol reagent (Cat. No. 15596026, Ambion, Thermo Fisher Scientific, Waltham, MA), RNA was extracted using Direct-zol RNA MiniPrep kit (Cat. No. R2051, Zymo Research, Irvin, CA) following the manufacturer's instructions, and quantified spectrophotometrically using a CLARIOstar Microplate Reader and a LVis Plate (BMG Labtech, Ortenberg, Germany). Next, cDNA was synthesized from 1µg of RNA through reverse transcription PCR using the SuperScript™ IV VILO™ cDNA synthesis kit (Cat. No. 11756500, Invitrogen, Thermo Fisher Scientific, Waltham, MA). Analysis of mRNA and rRNA was

performed via qPCR (BioRad CX384) with GoTaq qPCR Master (Cat. No. A6002, Promega, Madison, WI) and primers listed in table 3.1. All transcripts were normalized to the average of GAPDH and β-actin by the comparative Ct (ΔΔCt) method and represented as fold-change from controls. XBP1 splicing (sXBP1) was determined as described previously (39) using primers targeting the 26 base pair intron cleaved by IRE1 and normalized to total XBP1 (t-XBP1) mRNA.

Table 3.1. qPCR primers

Target	**Forward Sequence 5'-3'**	**Reverse Sequence 5'-3'**
ATF4	GTTTGACTTCGATGCTCTGTTTC	GGGCTCCTTATTAGTCTCTTGG
GADD34	CTCTGAAGGGTAGAAAGGTGC	TCGATCTCGTGCAAACTGCT
sXBP1	GCTGAGTCCGCAGCAGGT	CAGGGTCCAACTTGTCCAGAAT
t-XBP1	TGGCCGGGTCTGCTGAGTCCG	ATCCATGGGAAGATGTTCTGG
IL-1β	CAGCTTTCGACAGTGAGGAGA	TGTCGAGATGCTGCTGTGAG
IL-6	CTCTCCGCAAGAGACTTCCA	GGTCTGTTGTGGGTGGTATCC
IFN-γ	GCCCTCTCTGGCTGTTACTG	CCAAGAGGAGGCTCTTTCCT
TNF-α	GATCGGTCCCAACAAGGAGG	CTTGGTGGTTTGCTACGACG
GAPDH	AGTGCCAGCCTCGTCTCATA	CGTTGAACTTGCCGTGGGTA
β-Actin	CACCCGCGAGTACAACCTTCT	CGTCATCCATGGCGAACTGGT

3.3.3. Western Blot Analysis

All tissue samples were homogenized and extracted in RIPA lysis buffer (50 mM Tris pH 8.0, 150 mM NaCl, 1% Triton X-100, 0.1% SDS) supplemented with Pierce Protease and Phosphatase Inhibitor Mini Tablets (Cat. No. A32959, Thermo Fisher Scientific, Waltham, MA) using 1 tablet per 10mL of lysis buffer. Protein (10-30 µg) was separated by SDS-PAGE on polyacrylamide gels, transferred to PVDF membranes as previously described (18), and immunoblotted using the following antibodies: 4E-BP1 [1:4,000, Cell Signaling Technology (CST); Cat. No. 9644, RRID: AB_2097841]; Phospho-S6 Ribosomal Protein (S235/236; 1:1,000, CST; Cat. No. 2211, RRID: AB_331679), S6 Ribosomal Protein (1:2,000, CST; Cat. No. 2217,

RRID: AB_331355), eIF4E (1:2,000, CST; Cat. No. 2067 RRID: AB_2097675). Immunoblots for phosphorylated and total RPS6, 4E-BP1, and eIF4E were performed on the same membrane, respectively. All blots were verified for equal loading using the respective whole lane of Ponceau S stains (Cat. No. J63139.K2, Thermo Fisher Scientific, Waltham, MA). The phosphorylated RPS6 was normalized to its total RPS6 singal, the upper gamma band of 4E-BP1 was normalized to the total 4E-BP1 signal, and eIF4E was normalized to the respective whole lane of Ponceau S stains.

3.3.4. Statistical Analysis

All data are reported as means ± standard deviation (SD) or mean standard error (SEM) where appropriate. Percentage differences between groups were calculated as: $|V_1 - V_2| / [(V_1 - V_2) / 2] \times 100$ and rounded to the nearest whole number. Potential outliers were identified by a ROUT test with the maximum false discovery rate set to 1%. All comparisons were analyzed via a two-tail unpaired t test. P values ≤ 0.05 were considered significant. Correlations between the changes in skeletal or cardiac muscle mass and rRNA were calculated using Pearson's product-moment correlation coefficients. All statistical analyses were performed and graphically represented using GraphPad Prism 10 (GraphPad Prism, San Diego, CA, RRID: SCR_002798).

3.4. RESULTS

3.4.1. Yoshida AH-130 ascites-induced skeletal and cardiac muscle wasting involves a reduction in ribosomal capacity

Mean tumor volume in the inoculated rats was 62.68 ± 3.92 mL, with an average tumor cell count of 5877.00 ± 279.13. Normalized food intake over the study duration was significantly

lower in the tumor-bearing rats compared to controls (-15%, *P*=0.002). The presence of Yoshida AH-130 hepatoma tumors resulted in a significant reduction in final tumor-free body weight (FBW) relative to initial body weights (IBW) that was 89% lower than the control treated rats (*P*<0.001; Fig. 3.1A). Skeletal muscle mass was 25% lower (*P*<0.001; Fig. 1B) and heart mass was 17% lower (*P*<0.001) relative to IBW (Fig. 3.1C) in tumor inoculated rats. In skeletal muscle, rRNA was ~40% (*P*=0.002) lower in tumor-bearing rats (Fig. 3.2A), and 37% (*P*=0.074) lower in the heart when compared to controls (Fig. 3.2B). The reduction in rRNA was significantly correlated with muscle weight (r=0.628, P=0.021; Fig. 3.2A) and cardiac weight (r=0.557, P=0.048; Fig. 3.2B).

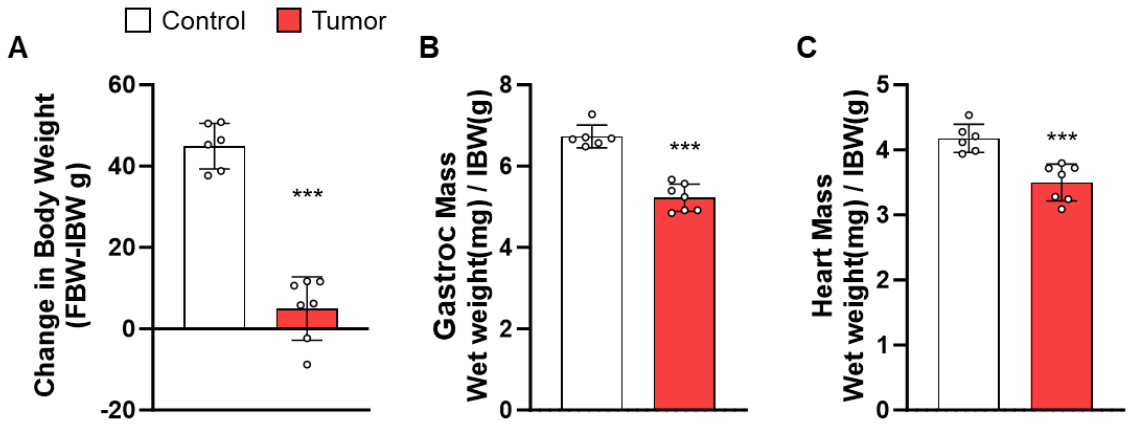

Figure 3.9. Yoshida AH-130 tumor inoculation yields a loss in body weight, skeletal muscle, and heart mass

A: Change in tumor-free body weight (FBW) relative to initial body weight (IBW) in grams for control and tumor-bearing rats. **B**: End-point gastrocnemius muscle mass in milligrams was normalized to IBW in grams. **C**: Heart mass in milligrams was normalized to IBW in grams. Data are expressed as the mean ± SD. Statistical significance was determined by a two-tailed unpaired t-test. Significant difference from control: ***$P < 0.001$. gastroc, gastrocnemius.

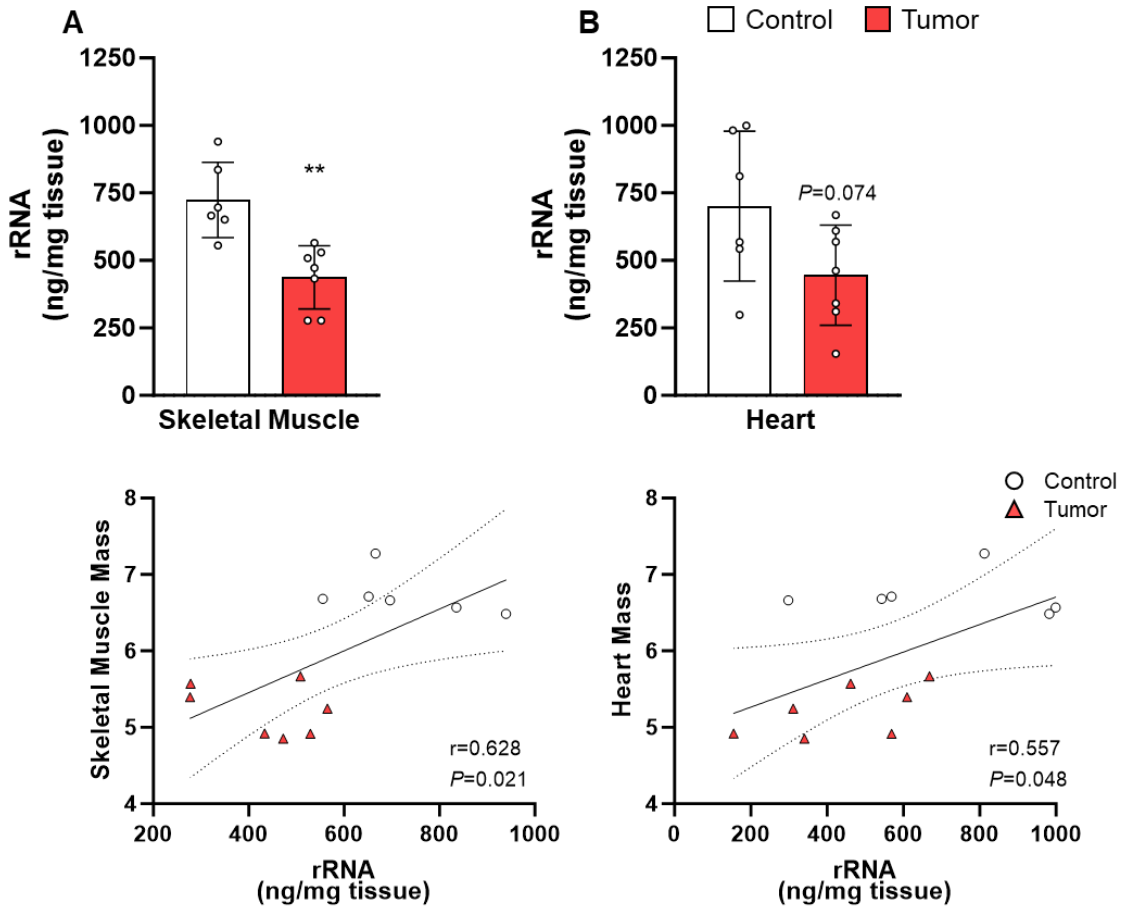

Figure 3.10. AH-130 tumor inoculation induces a loss in rRNA that is associated with reductions in skeletal and cardiac muscle mass

A: quantification of total RNA in skeletal muscle (top). Pearson's product-moment correlations between rRNA and skeletal muscle mass (bottom). **B**: quantification of total rRNA in the heart (top). Pearson's product-moment correlations between rRNA and heart mass (bottom). Data are expressed as the mean ± SD. Statistical significance was determined by a two-tailed unpaired t-test for total RNA. Correlations were calculated using Pearson's product-moment correlation coefficients. Significant difference from control: $^{**}P < 0.01$.

3.4.2. Yoshida AH-130 ascites hepatoma modulate translational initiation factor phosphorylation in both skeletal and cardiac muscle

In addition to a reduction in translational capacity, the inoculation with Yoshida AH-130 ascites hepatoma cells caused a significant reduction in 4E-BP1 phosphorylation in both skeletal (-74%, $P<0.001$) and cardiac (-81%, $P=0.004$) muscles (Fig. 3.3A & 3.3B). The eIF4E protein levels were elevated in the skeletal muscle of AH-130 tumor rats (206%, $P=0.004$; Fig. 3.3A), but no difference was found in the heart (Fig. 3.3B). No significant differences in RPS6 phosphorylation (Ser 235/236) were found in either skeletal muscle or heart (Fig. 3.3A & 3.3B).

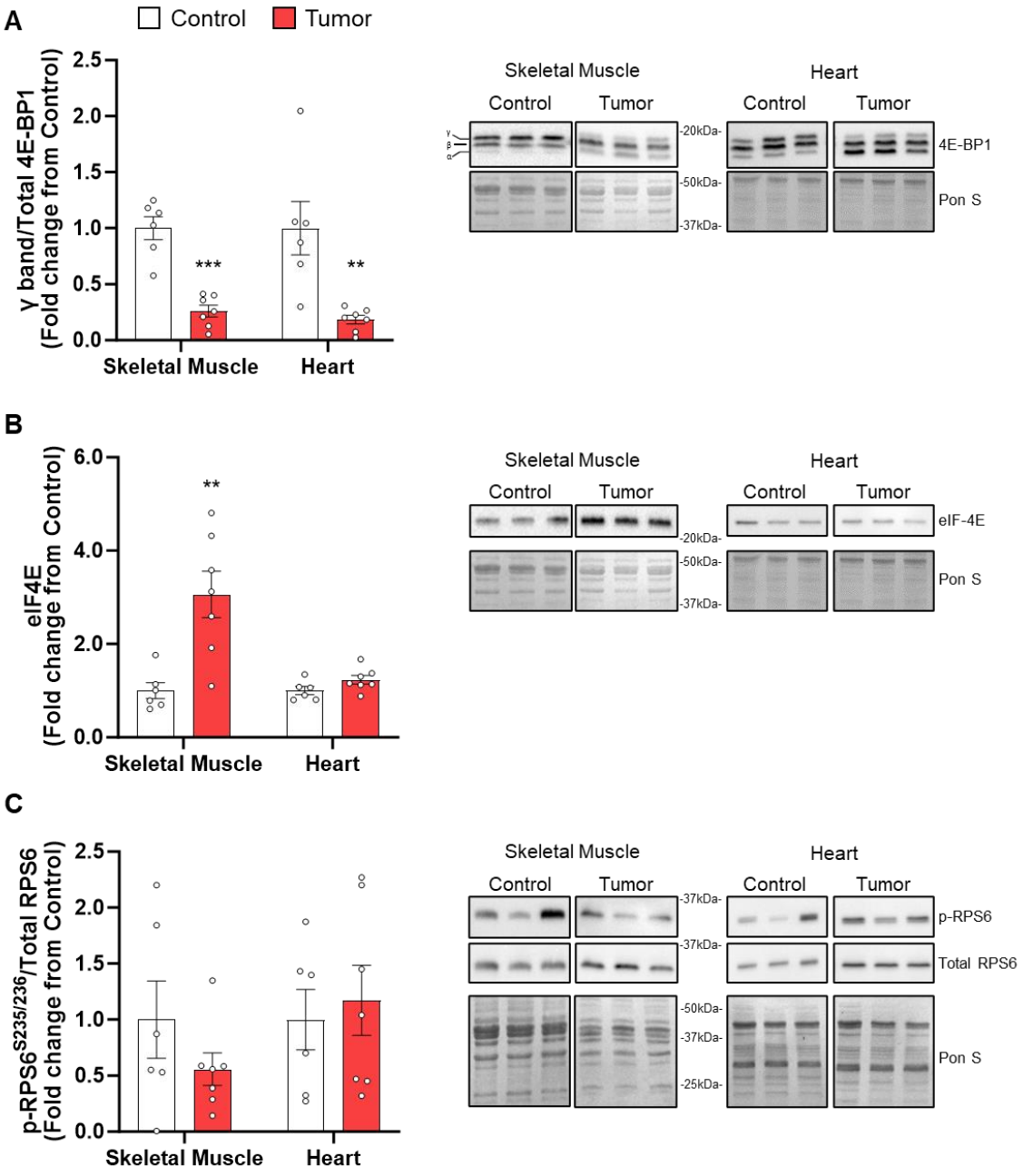

Figure 3.11. Translational control factor 4E-BP1 is hypophosphorylated in both the skeletal and heart muscle of tumor-bearing rats

A: Quantification of 4E-BP1 Western blots and representative blots using 10µg per lane in the skeletal muscle and heart. The 4E-BP1 γ subunit was normalized to total 4E-BP1 to assess protein hypophosphorylation status. **B**: Quantification of eIF4E Western blots and representative blots using 10µg per lane in the skeletal muscle and heart. Total eIF4E was normalized to the respective whole Ponceau S-stained lane. **C**: Quantification of phosphorylated ribosomal protein S6 at S235/236 (p-RPS6) normalized to total RPS6 Western blots and representative blots using 30µg per lane in skeletal muscle and 10µg per lane in the heart. Representative images of all Western blots were cropped for final presentation and are accompanied by cropped representative Ponceau S (Pon S) staining images that were used for normalization. Data are expressed as mean fold-change from controls ± SD. Statistical significance was determined by a two-tailed unpaired t-test. Significant difference from control: $^{**}P < 0.01$, $^{***}P < 0.001$.

3.4.3. UPR gene expression is elevated in Yoshida AH-130 treated rats

Tumor presence increased mRNA levels of ATF4 (88%, $P<0.001$) and GADD34 (301%, $P<0.001$) in skeletal muscle (Fig. 3.4A) but only GADD34 mRNA expression was induced in the heart (48%, $P=0.033$; Fig. 3.4B). XBP1 splicing (sXBP1) was significantly decreased in the cardiac muscle (-42%, $P=0.005$), and trended towards significance in the skeletal muscle (-26%, $P=0.067$) of tumor-bearing rats (Fig. 3.4A & 3.4B).

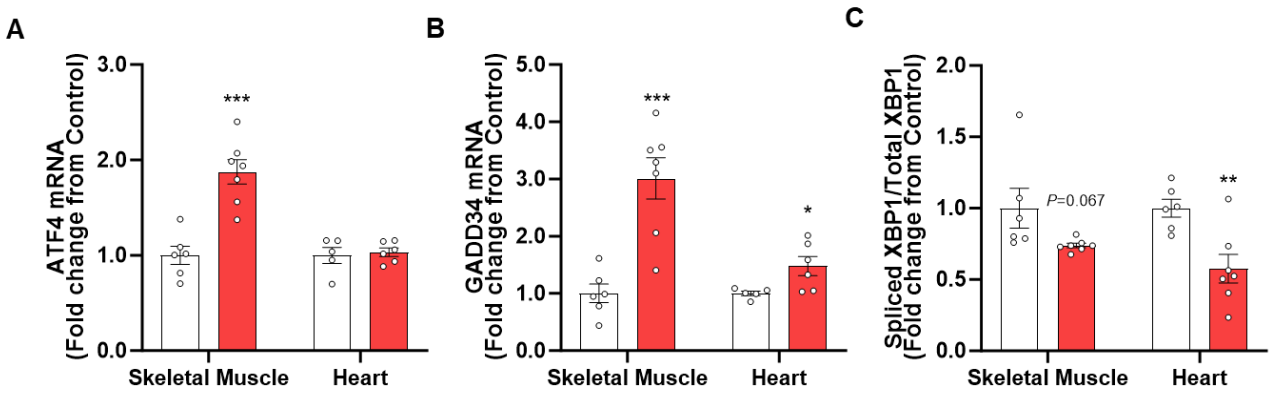

Figure 3.12. Expression of ER-stress mRNA suggests dysregulation of the UPR in the skeletal and heart muscles of Yoshida AH-130 rats.

A: Expression of ATF4 mRNA in skeletal muscle and heart. The ROUT test for outliers removed 1 sample from tumor group of the heart (n=6). **B**: Expression of GADD34 mRNA in the skeletal muscle and heart. The ROUT test for outliers removed 1 sample from the control (n=5) and tumor (n=6) groups respectively of the heart. **C**: Expression of spliced XBP1 normalized to total XBP1 mRNA in skeletal muscle and heart. Data are presented as mean fold-change from controls ± SEM. Statistical significance was determined by a two-tailed unpaired t-test. Significant differences from control are indicated by asterisks: *$P \leq 0.05$, **$P < 0.01$, ***$P < 0.001$.

3.4.4. Yoshida AH-130 induced skeletal and cardiac muscle wasting involve the expression of local pro-inflammatory cytokines

Following tumor inoculation, tissue IL-6 mRNA levels were on average higher in skeletal (137%, $P=0.065$) and cardiac (143%, $P=0.073$) muscle, respectively, but failed to reach significance (Fig. 3.5A & 3.5B). In the skeletal muscle, IL-1β mRNA expression was elevated in

the tumor group by 80% (P=0.012; Fig. 3.5A), and by 117% (P=0.002) in the heart (Fig. 3.5B). Average IFN-γ mRNA in the skeletal muscle was not different from control, but it was significantly elevated in the heart by 75% (P=0.008; Fig. 3.5B). TNF-α mRNA levels in skeletal muscle were not affected by the tumor, but heart levels increase on average without being statistically significant (Fig. 3.5A & 3.5B).

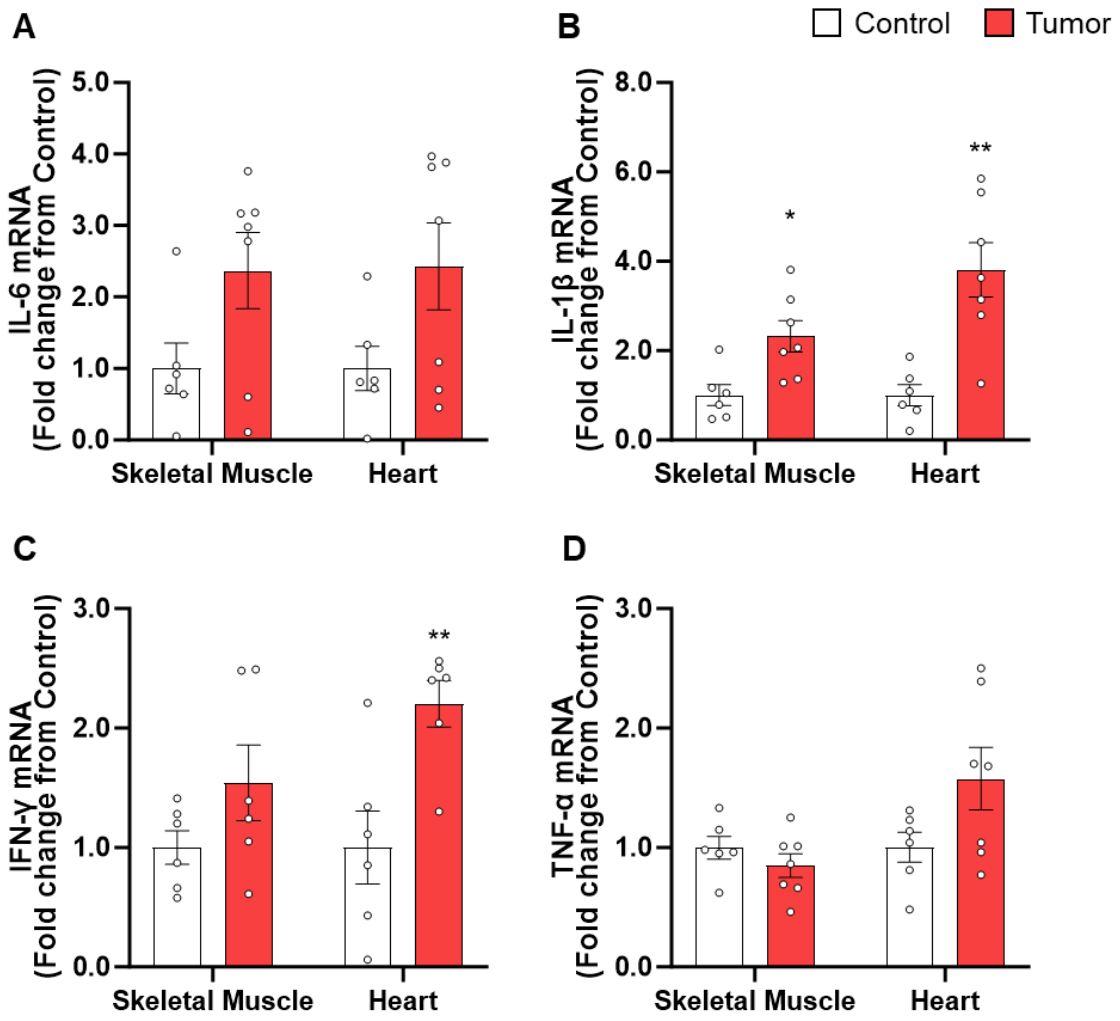

Figure 3.13. Local tissue expression of inflammatory mRNA is increased in cachectic rats

A: Expression of IL-6 mRNA in skeletal muscle and heart. **B**: Expression of IL-1β in skeletal muscle and heart. **C**: Expression of IFN-γ mRNA in the skeletal muscle and heart. The ROUT test for outliers removed 1 sample from the control (n=5) group of skeletal muscle and the tumor (n=6) group of the heart. **D**: Expression of TNF-α mRNA in skeletal muscle and heart. Data are presented as mean fold-change from controls ± SEM. Statistical significance was determined by a two-tailed unpaired t-test. Significant differences from control are indicated by asterisks: *$P \leq 0.05$, **$P < 0.01$.

3.5. DISCUSSION

We investigated skeletal and cardiac muscle wasting related mechanisms in the Yoshida AH-130 rat hepatoma tumor model. Inoculation with tumor cells resulted in skeletal and cardiac muscle wasting, anabolic deficits, increases in the UPR and tissue expression of pro-inflammatory cytokines. Consistent with our previous findings in ovarian, lung, and colon cancer models (16–18), Yoshida AH-130 tumor cells caused a reduction in translational capacity in both skeletal and cardiac muscle, although the decline in the heart did not reach statistical significance at the time point studied. This finding aligns with earlier investigations using this model (7), and support the interpretation that anabolic deficits play a central role in muscle wasting (16–18, 40). While the loss of skeletal muscle is well-defined in cachexia, the impact of this condition on cardiac anabolism is less clear. In this model, cardiac rRNA levels were reduced by ~36% following tumor inoculation. Despite not achieving statistical significance, the reduction in translation capacity strongly correlated with the alterations in cardiac mass. This indicates that, like in skeletal muscle, the loss of ribosomes may play a critical role in cardiac muscle wasting. Another finding indicating defective protein anabolism is the clear reduction in cap-dependent translation signaling. Consistent with other models of cancer cachexia (41–43), we observed a significant decrease in 4E-BP1 phosphorylation in both skeletal and cardiac muscle of tumor-bearing rats. Hypophosphorylation of 4E-BP1 increases its binding affinity for eIF4E, this in turn prevents the formation of the translation initiation complex eIF4F and reduces protein synthesis (44). In contrast with 4E-BP1 hypophosphorylation, skeletal muscle eIF4E protein was significantly elevated in tumor-bearing rats, a response that was not mirrored in the heart. This may represent a feedback mechanism attempting to restore proteostatic balance in wasting muscle, that is operant in skeletal but not in cardiac muscle. Together, these findings indicate that cachexia involves a

generalized reduction in the ability of striated muscle to synthesize proteins and suggest that both translational capacity and efficiency may underlie the anabolic deficits characteristic of tumor-induced cachexia.

The alterations in translational control mechanisms led us to investigate the UPR. As expected, we observed an increase in ATF4 and GADD34 mRNA levels in skeletal muscle, however only GADD34 was elevated in the heart of tumor-bearing rats. These findings partially align with prior observations showing an increase in ATF4 mRNA levels in skeletal muscle of LLC mice (45), while GADD34 expression remained unchanged (25). This raises the question as to what extent the UPR is conserved across cachexia models. We also examined changes in XBP1 splicing and found a robust reduction in sXBP1 in both skeletal and cardiac muscle, although it did not achieve significance in skeletal muscle. Contrary to the findings in this model, an increase sXBP1 has been previously reported in skeletal muscle of cachectic LLC mice (25, 45). This is intriguing because XBP1 is spliced under cellular stress (i.e. with activation of the UPR) (45). We interpret this discrepancy as the disruption of the UPR being a possible atrophy exacerbating factor. A failure to mount the UPR has been shown to increase muscle wasting, LLC mice treated with the UPR inhibitor 4-Phenylbutyric acid (4-PBA) exhibited a suppressed ER stress response and exacerbated muscle wasting. Similarly, myotubes incubated with LLC conditioned media + 4-PBA displayed a smaller diameter and increased activation of proteolytic markers (25). Thus, the defective UPR may reflect a failure to restore proteostasis in this hepatoma tumor model.

Skeletal and cardiac muscle atrophy in cancer has often been linked to changes in systemic pro-inflammatory cytokines (31, 46, 47), which can stimulate the local expression of pro-inflammatory effectors of muscle wasting (30, 48). Consistent with previous findings (49), we found an increase in IL-6 mRNA in both muscle and heart of cachectic rats. However, this increase

was not significant likely due to experimental variability associated with the Yoshida hepatoma model. The elevation of IL-1β mRNA was similar in skeletal and cardiac muscle. Within skeletal muscle, IL-1β can exert direct autocrine effects and activate the NF-κB pathway, leading to increased protein breakdown and muscle wasting (50). The increase in IL-1β was also evident in the heart indicating a possible conserved response to the tumor in striated muscle. Increased expression of IL-1β in cardiomyocytes of rats with chronic heart failure leads to substantial interstitial fibrosis and impaired cardiac function (51), thus the increase in IL-1β expression may underlie cardiac dysfunction in cachexia. The responses of both IL-6 and IL-1β in striated muscle were opposite to the spleen and the brain, respectively (11), indicating that organs respond differently to the tumor. We also observed a significant increase in IFN-γ mRNA expression in the cardiac muscle where it can cause impairments in cardiac contractility and function by acting in an autocrine fashion (52, 53). Changes in TNF-α were evident and variable but not significant in the skeletal muscle, and are contrary to a previous report indicating elevated TNF-α mRNA in the skeletal muscle of rats bearing Yoshida hepatoma tumors (49). Overall, these findings suggest that skeletal and cardiac muscle display divergent patterns of pro-inflammatory cytokine expression despite undergoing similar atrophy, and that these factors may mediate tissue-specific cancer-related alterations in physiological functions.

In summary, we provide evidence demonstrating that impaired anabolism, UPR, and local production of pro-inflammatory cytokines may converge to facilitate tumor-induced muscle and cardiac wasting. Consistent reductions in translational capacity and efficiency, with divergent proteostatic stress control, and tissue pro-inflammatory cytokine expression in the Yoshida model of hepatocellular carcinoma highlight the need for a more thorough understanding of the multifaceted molecular mechanisms involved in tissue wasting in cancer cachexia.

3.6. REFERENCES

1. **Argilés JM**, **Busquets S**, **Stemmler B**, **López-Soriano FJ**. Cancer cachexia: Understanding the molecular basis. *Nat Rev Cancer* 14: 754–762, 2014. doi: 10.1038/nrc3829.
2. **Orellana López C**, **Leyton Estéfane J**, **Ramos Rosales M**, **Vásquez Ramirez C**, **Manriquez Arriagada C**, **Argilés JM**, **López-Soriano FJ**, **Ortega González F**, **Yañez N**, **Busquets S**. Prevalence of Cachexia in Cancer Patients. *Eur J Cancer Care (Engl)* 2023: 1–9, 2023. doi: 10.1155/2023/5743872.
3. **Baracos VE**, **Martin L**, **Korc M**, **Guttridge DC**, **Fearon KCH**. Cancer-associated cachexia. *Nat Rev Dis Prim* 4: 1–18, 2018. doi: 10.1038/nrdp.2017.105.
4. **Barkhudaryan A**, **Scherbakov N**, **Springer J**, **Doehner W**. Cardiac muscle wasting in individuals with cancer cachexia. *ESC Hear Fail* 4: 458–467, 2017. doi: 10.1002/ehf2.12184.
5. **McGlynn KA**, **Petrick JL**, **El-Serag HB**. Epidemiology of Hepatocellular Carcinoma. *Hepatology* 73: 4–13, 2021. doi: 10.1002/hep.31288.
6. **Wolf E**, **Rich NE**, **Marrero JA**, **Parikh ND**, **Singal AG**. Use of Hepatocellular Carcinoma Surveillance in Patients With Cirrhosis: A Systematic Review and Meta-Analysis. *Hepatology* 73, 2021. doi: 10.1002/hep.31309.
7. **Baracos VE**, **DeVivo C**, **Hoyle DH**, **Goldberg AL**. Activation of the ATP-ubiquitin-proteasome pathway in skeletal muscle of cachectic rats bearing a hepatoma. *Am J Physiol Metab* 268: E996–E1006, 1995. doi: 10.1152/ajpendo.1995.268.5.E996.
8. **Salazar-Degracia A**, **Busquets S**, **Argilés JM**, **Bargalló-Gispert N**, **López-Soriano FJ**, **Barreiro E**. Effects of the beta2 agonist formoterol on atrophy signaling, autophagy, and

muscle phenotype in respiratory and limb muscles of rats with cancer-induced cachexia. *Biochimie* 149: 79–91, 2018. doi: 10.1016/j.biochi.2018.04.009.

9. **Yuan L**, **Springer J**, **Palus S**, **Busquets S**, **Jové Q**, **Alves de Lima Junior E**, **Anker MS**, **von Haehling S**, **Álvarez Ladrón N**, **Millman O**, **Oosterlee A**, **Szymczyk A**, **López-Soriano FJ**, **Anker SD**, **Coats AJS**, **Argiles JM**. The atypical β-blocker S-oxprenolol reduces cachexia and improves survival in a rat cancer cachexia model. *J Cachexia Sarcopenia Muscle* 14: 653–660, 2023. doi: 10.1002/jcsm.13116.

10. **Toledo M**, **Springer J**, **Busquets S**, **Tschirner A**, **López-Soriano FJ**, **Anker SD**, **Argilés JM**. Formoterol in the treatment of experimental cancer cachexia: effects on heart function. *J Cachexia Sarcopenia Muscle* 5: 315–320, 2014. doi: 10.1007/s13539-014-0153-y.

11. **Cernackova A**, **Mikova L**, **Horvathova L**, **Tillinger A**, **Mravec B**. Cachexia induced by Yoshida ascites hepatoma in Wistar rats is not associated with inflammatory response in the spleen or brain. *J Neuroimmunol* 337, 2019. doi: 10.1016/j.jneuroim.2019.577068.

12. **Costelli P**, **Llovera M**, **Carbó N**, **García-Martínez C**, **López-Sorianoq FJ**, **Argilés JM**. Interleukin-1 receptor antagonist (IL-1ra) is unable to reverse cachexia in rats bearing an ascites hepatoma (Yoshida AH-130). *Cancer Lett* 95: 33–38, 1995. doi: 10.1016/0304-3835(95)03858-T.

13. **Barreiro E**, **De La Puente B**, **Busquets S**, **López-Soriano FJ**, **Gea J**, **Argilés JM**. Both oxidative and nitrosative stress are associated with muscle wasting in tumour-bearing rats. *FEBS Lett* 579: 1646–1652, 2005. doi: 10.1016/j.febslet.2005.02.017.

14. **Toledo M**, **Penna F**, **Oliva F**, **Luque M**, **Betancourt A**, **Marmonti E**, **López-Soriano FJ**, **Argilés JM**, **Busquets S**. A multifactorial anti-cachectic approach for cancer cachexia

in a rat model undergoing chemotherapy. *J Cachexia Sarcopenia Muscle* 7: 48–59, 2016. doi: 10.1002/jcsm.12035.

15. **Sugden PH**, **Fuller SJ**. Regulation of protein turnover in skeletal and cardiac muscle. *Biochem J* 273: 21–37, 1991. doi: 10.1042/bj2730021.

16. **Kim HG**, **Huot JR**, **Pin F**, **Belcher DJ**, **Bonetto A**, **Nader GA**. Metastatic or xenograft colorectal cancer models induce divergent anabolic deficits and expression of pro-inflammatory effectors of muscle wasting in a tumor-type-dependent manner. *J Appl Physiol* 133: 1273–1283, 2022. doi: 10.1152/japplphysiol.00247.2022.

17. **Kim H-G**, **Huot J**, **Pin F**, **Guo B**, **Bonetto A**, **Nader G**. Reduced rDNA transcription diminishes skeletal muscle ribosomal capacity and protein synthesis in cancer cachexia. *FASEB* 35: e21335, 2021. doi: 10.1096/fj.202002257R.

18. **Belcher DJ**, **Guitart M**, **Hain B**, **Kim HG**, **Waning D**, **Barreiro E**, **Nader GA**. LP07 and LLC preclinical models of lung cancer induce divergent anabolic deficits and expression of pro-inflammatory effectors of muscle wasting. *J Appl Physiol* 133: 1260–1272, 2022. doi: 10.1152/japplphysiol.00246.2022.

19. **Millward DJ**, **Garlick PJ**, **James WPT**, **Nnanyelugo DO**, **Ryatt JS**. Relationship between protein synthesis and RNA content in skeletal muscle. *Nature* 241: 204–205, 1973. doi: 10.1038/241204a0.

20. **Springer J**, **Tschirner A**, **Haghikia A**, **Von Haehling S**, **Lal H**, **Grzesiak A**, **Kaschina E**, **Palus S**, **Pötsch M**, **Von Websky K**, **Hocher B**, **Latouche C**, **Jaisser F**, **Morawietz L**, **Coats AJS**, **Beadle J**, **Argiles JM**, **Thum T**, **Földes G**, **Doehner W**, **Hilfiker-Kleiner D**, **Force T**, **Anker SD**. Prevention of liver cancer cachexia-induced cardiac wasting and heart failure. *Eur Heart J* 35: 932–941, 2014. doi: 10.1093/eurheartj/eht302.

21. **Padrão AI**, **Moreira-Gonçalves D**, **Oliveira PA**, **Teixeira C**, **Faustino-Rocha AI**, **Helguero L**, **Vitorino R**, **Santos LL**, **Amado F**, **Duarte JA**, **Ferreira R**. Endurance training prevents TWEAK but not myostatin-mediated cardiac remodelling in cancer cachexia. *Arch Biochem Biophys* 567: 13–21, 2015. doi: 10.1016/j.abb.2014.12.026.

22. **Malhotra JD**, **Kaufman RJ**. The endoplasmic reticulum and the unfolded protein response. *Semin Cell Dev Biol* 18: 716–731, 2007. doi: 10.1016/j.semcdb.2007.09.003.

23. **Preston AM**, **Hendershot LM**. Examination of a second node of translational control in the unfolded protein response. *J Cell Sci* 126: 4253–4261, 2013. doi: 10.1242/jcs.130336.

24. **Bohnert KR**, **McMillan JD**, **Kumar A**. Emerging roles of ER stress and unfolded protein response pathways in skeletal muscle health and disease. *J Cell Physiol* 233: 67–78, 2018. doi: 10.1002/JCP.25852.

25. **Bohnert KR**, **Gallot YS**, **Sato S**, **Xiong G**, **Hindi SM**, **Kumar A**. Inhibition of ER stress and unfolding protein response pathways causes skeletal muscle wasting during cancer cachexia. *FASEB J* 30: 3053–3068, 2016. doi: 10.1096/fj.201600250RR.

26. **Lang CH**, **Frost RA**, **Nairn AC**, **MacLean DA**, **Vary TC**. TNF-α impairs heart and skeletal muscle protein synthesis by altering translation initiation. *Am J Physiol - Endocrinol Metab* 282: E336–E347, 2002. doi: 10.1152/ajpendo.00366.2001.

27. **White JP**, **Puppa MJ**, **Gao S**, **Sato S**, **Welle SL**, **Carson JA**. Muscle mTORC1 suppression by IL-6 during cancer cachexia: A role for AMPK. *Am J Physiol - Endocrinol Metab* 304: E1042-1052, 2013. doi: 10.1152/ajpendo.00410.2012.

28. **Consul N**, **Guo X**, **Coker C**, **Lopez-Pintado S**, **Hibshoosh H**, **Zhao B**, **Kalinsky K**, **Acharyya S**. Monitoring metastasis and cachexia in a patient with breast cancer: A case study. *Clin Med Insights Oncol* 10: 83–84, 2016. doi: 10.4137/CMO.S40479.

29. **Argilés JM**, **López-Soriano FJ**. The role of cytokines in cancer cachexia. *Med Res Rev* 19: 223–248, 1999. doi: 10.1002/(sici)1098-1128(199905)19:3<223::aid-med3>3.0.co;2-n.

30. **Luo G**, **Hershko DD**, **Robb BW**, **Wray CJ**, **Hasselgren P-O**. IL-1β stimulates IL-6 production in cultured skeletal muscle cells through activation of MAP kinase signaling pathway and NF-κB. *Am J Physiol Integr Comp Physiol* 284: R1249–R1254, 2003. doi: 10.1152/ajpregu.00490.2002.

31. **Webster JM**, **Kempen LJAP**, **Hardy RS**, **Langen RCJ**. Inflammation and Skeletal Muscle Wasting During Cachexia. *Front Physiol* 11: 597675, 2020. doi: 10.3389/fphys.2020.597675.

32. **Chen L**, **Deng H**, **Cui H**, **Fang J**, **Zuo Z**, **Deng J**, **Li Y**, **Wang X**, **Zhao L**. Inflammatory responses and inflammation-associated diseases in organs. *Oncotarget* 9: 7204–7218, 2018. doi: 10.18632/oncotarget.23208.

33. **Bartekova M**, **Radosinska J**, **Jelemensky M**, **Dhalla NS**. Role of cytokines and inflammation in heart function during health and disease. *Heart Fail Rev* 23: 733–758, 2018. doi: 10.1007/s10741-018-9716-x.

34. **Testa M**, **Yeh M**, **Lee P**, **Fanelli R**, **Loperfido F**, **Berman JW**, **LeJemtel TH**. Circulating levels of cytokines and their endogenous modulators in patients with mild to severe congestive heart failure due to coronary artery disease or hypertension. *J Am Coll Cardiol* 28: 964–971, 1996. doi: 10.1016/S0735-1097(96)00268-9.

35. **Deswal A**, **Petersen NJ**, **Feldman AM**, **Young JB**, **White BG**, **Mann DL**. Cytokines and cytokine receptors in advanced heart failure: An analysis of the cytokine database from the Vesnarinone Trial (VEST). *Circulation* 103: 2055–2059, 2001. doi:

10.1161/01.CIR.103.16.2055.

36. **Sack MN**. Tumor necrosis factor-α in cardiovascular biology and the potential role for anti-tumor necrosis factor-α therapy in heart disease. *Pharmacol Ther* 94: 123–135, 2002. doi: 10.1016/S0163-7258(02)00176-6.

37. **Puppa MJ**, **Gao S**, **Narsale AA**, **Carson JA**. Skeletal muscle glycoprotein 130's role in Lewis lung carcinoma-induced cachexia. *FASEB J* 28: 998–1109, 2014. doi: 10.1096/fj.13-240580.

38. **European Parliament Council of the European Union**. Directive 2010/63/EU of the European Parliament and of the Council of 22 September 2010 on the protection of animals used for scientific purposes Text with EEA relevance. *Off J Eur Union* 53, 2010.

39. **Yoon S Bin**, **Park YH**, **Choi SA**, **Yang HJ**, **Jeong PS**, **Cha JJ**, **Lee S**, **Lee SH**, **Lee JH**, **Sim BW**, **Koo BS**, **Park SJ**, **Lee Y**, **Kim YH**, **Hong JJ**, **Kim JS**, **Jin YB**, **Huh JW**, **Lee SR**, **Song BS**, **Kim SU**. Real-time PCR quantification of spliced X-box binding protein 1 (XBP1) using a universal primer method. *PLoS One* 14, 2019. doi: 10.1371/journal.pone.0219978.

40. **Bhogal AS**, **Lorite ML**, **Tisdale MJ**. Changes in nucleic acid and protein levels in atrophying skeletal muscle in cancer cachexia. *Anticancer Res* 26: 4149–4154, 2006.

41. **White JP**, **Baynes JW**, **Welle SL**, **Kostek MC**, **Matesic LE**, **Sato S**, **Carson JA**. The regulation of skeletal muscle protein turnover during the progression of cancer cachexia in the Apc Min/+ mouse. *PLoS One* 6, 2011. doi: 10.1371/journal.pone.0024650.

42. **Brown JL**, **Lee DE**, **Rosa-Caldwell ME**, **Brown LA**, **Perry RA**, **Haynie WS**, **Huseman K**, **Sataranatarajan K**, **Van Remmen H**, **Washington TA**, **Wiggs MP**, **Greene NP**. Protein imbalance in the development of skeletal muscle wasting in tumour-bearing mice.

J Cachexia Sarcopenia Muscle 9: 987–1002, 2018. doi: 10.1002/jcsm.12354.

43. **Manne NDPK**, **Lima M**, **Enos RT**, **Wehner P**, **Carson JA**, **Blough E**. Altered cardiac muscle mTOR regulation during the progression of cancer cachexia in the ApcMin/+ mouse. *Int J Oncol* 42: 2134–2140, 2013. doi: 10.3892/ijo.2013.1893.

44. **Gingras AC**, **Gygi SP**, **Raught B**, **Polakiewicz RD**, **Abraham RT**, **Hoekstra MF**, **Aebersold R**, **Sonenberg N**. Regulation of 4E-BP1 phosphorylation: A novel two step mechanism. *Genes Dev* 13: 1422–1437, 1999. doi: 10.1101/gad.13.11.1422.

45. **Bohnert KR**, **Goli P**, **Roy A**, **Sharma AK**, **Xiong G**, **Gallot YS**, **Kumar A**. The Toll-Like Receptor/MyD88/XBP1 Signaling Axis Mediates Skeletal Muscle Wasting during Cancer Cachexia. *Mol Cell Biol* 39: e00184-19, 2019. doi: 10.1128/mcb.00184-19.

46. **Rausch V**, **Sala V**, **Penna F**, **Porporato PE**, **Ghigo A**. Understanding the common mechanisms of heart and skeletal muscle wasting in cancer cachexia. *Oncogenesis* 10, 2021. doi: 10.1038/s41389-020-00288-6.

47. **Bordignon C**, **Dos Santos BS**, **Rosa DD**. Impact of Cancer Cachexia on Cardiac and Skeletal Muscle: Role of Exercise Training. *Cancers (Basel)* 14: 342, 2022. doi: 10.3390/cancers14020342.

48. **Podbregar M**, **Lainscak M**, **Prelovsek O**, **Mars T**. Cytokine response of cultured skeletal muscle cells stimulated with proinflammatory factors depends on differentiation stage. *Sci World J* 2013, 2013. doi: 10.1155/2013/617170.

49. **Catalano MG**, **Fortunati N**, **Arena K**, **Costelli P**, **Aragno M**, **Danni O**, **Boccuzzi G**. Selective up-regulation of tumor necrosis factor receptor I in tumor-bearing rats with cancer-related cachexia. *Int J Oncol* 23: 429–436, 2003. doi: 10.3892/ijo.23.2.429.

50. **Cai D**, **Frantz JD**, **Tawa NE**, **Melendez PA**, **Oh BC**, **Lidov HGW**, **Hasselgren PO**,

Frontera WR, **Lee J**, **Glass DJ**, **Shoelson SE**. IKKβ/NF-κB activation causes severe muscle wasting in mice. *Cell* 119: 285–298, 2004. doi: 10.1016/j.cell.2004.09.027.

51. **Shioi T**, **Matsumori A**, **Kihara Y**, **Inoko M**, **Ono K**, **Iwanaga Y**, **Yamada T**, **Iwasaki A**, **Matsushima K**, **Sasayama S**. Increased expression of interleukin-1β and monocyte chemotactic and activating factor/monocyte chemoattractant protein-1 in the hypertrophied and failing heart with pressure overload. *Circ Res* 81: 664–671, 1997. doi: 10.1161/01.RES.81.5.664.

52. **Curtsinger JM**, **Agarwal P**, **Lins DC**, **Mescher MF**. Autocrine IFN-γ Promotes Naive CD8 T Cell Differentiation and Synergizes with IFN-α To Stimulate Strong Function. *J Immunol* 189: 659–668, 2012. doi: 10.4049/jimmunol.1102727.

53. **Castro F**, **Cardoso AP**, **Gonçalves RM**, **Serre K**, **Oliveira MJ**. Interferon-gamma at the crossroads of tumor immune surveillance or evasion. *Front Immunol* 9: 847, 2018. doi: 10.3389/fimmu.2018.00847.

CHAPTER 4. RESEARCH SUMMARY AND FUTURE DIRECTIONS

Our investigations into the translational capacity and control signaling in skeletal muscle during cancer cachexia have yielded several significant insights. Both LP07 and LLC preclinical models of LC exhibit significant muscle wasting, distinct anabolic deficits, neuromuscular impairments, and proinflammatory cytokine profiles. In the Yoshida AH-130 rat hepatoma tumor model, we found that both skeletal and cardiac muscle wasting are associated with reduced translational capacity, impaired anabolism, and increased expression of pro-inflammatory cytokines. These findings collectively advance our understanding of the molecular mechanisms underlying muscle wasting in cancer cachexia.

The first study (**Chapter 2**) aimed to determine whether muscle wasting in the LP07 and LLC preclinical models of lung cancer-induced cachexia involved similar anabolic deficits and the local expression of proinflammatory factors. Cancer cachexia is characterized by the loss of body weight, muscle, and adipose tissue, and remains a significant clinical challenge. We aimed to determine whether different lung tumor lines would involve similar mechanisms of muscle wasting or if they would exhibit tumor-specific mechanisms. Our findings showed divergent anabolic deficits and local expression of proinflammatory cytokines between the LP07 and LLC tumor models, despite both causing significant muscle loss.

On a molecular level, we found that muscle rRNA levels were significantly reduced in LP07 but not in LLC tumor-bearing mice, via a specific impairment in Pol I elongation in the LP07 model. Interestingly, the expression of Pol I subunits involved in transcription elongation was higher in LP07 tumor-bearing mice, possibly as a compensatory response to reduced rRNA production. We have observed a similar compensatory mechanism in a previous study involving

an ovarian cancer cachexia model (1). In mice xenografted with the ES-2 ovarian cancer tumor, our lab noted significant disruptions in translational capacity and rDNA transcription. Despite this, there was an increase in mRNA expression of several Pol I factors and subunits, indicating an attempt to maintain ribosome production following insult. However, it should be noted that these findings were based on qPCR data, and the corresponding protein levels of these subunits and transcription factors might not reflect the same pattern. The current research on translational capacity and rDNA transcription in cachectic muscle is limited, highlighting the need for further studies to better understand these mechanisms.

Additionally, we uncovered distinct differences in muscle intracellular signaling between the two models. While both models showed reduced phosphorylation of RPS6 and 4E-BP1, a reduction in mTOR phosphorylation was only apparent in LLC mice. This possibly suggests that alterations in additional signaling pathways, such as the Ras/Raf/ERK pathway, may contribute to the regulation of RPS6 and 4E-BP1 phosphorylation in LC. A companion study to this one was also carried out comparing the HCT116 and C26 colorectal tumor models of cachexia (2). This too found divergent outcomes in the mTORC1 signaling pathway in a manner that was tumor specific. However, it is also possible that these results were due to the use of a mTOR antibody specific to S2448 phosphorylation. Autophosphorylation of S2481 is reported to be more representative of direct mTOR catalytic activity (3), and use of a mTOR S2481 phospho-specific antibody may help further confirm the possibility of an mTOR independent reduction in 4E-BP1 and RPS6 phosphorylation.

Proinflammatory cytokine profiles also varied between the models in the expression of IL-6 and TNF-α. Both models exhibited similar mRNA levels of NLRP3, indicating a potential role of the inflammasome in local cytokine production. However, the absence of changes in IL-

1β and IL-18 mRNA suggests that these cytokines may be induced during the acute phase of muscle wasting rather than at the end stage we studied. A more thorough time-course investigation of cachexia development is needed to further elucidate this question.

In conclusion, our findings reveal that while both LP07 and LLC preclinical models of LC result in significant muscle wasting, they exhibit distinct anabolic deficits, neuromuscular impairments, intracellular signaling alterations, and proinflammatory cytokine profiles. These results underscore the importance of considering tumor-specific mechanisms in cancer cachexia research and suggest that further studies are needed to explore the temporal dynamics and contributions of different tumor types to muscle wasting in preclinical models. The biggest limitation of this study was the differing genetic backgrounds of the LLC and LP07 mouse models. It is possible that some observed differences were due to the mouse strains rather than the tumors themselves. However, most current research on these models uses the C57BL6 mouse for the LLC tumor and the BALB/c mouse for the LP07 tumor. Future studies should seek to control for this variable. Overall, our findings in study 1 suggest that the manifestation of cancer-induced muscle wasting may be tumor-type dependent rather than a universal phenomenon.

In Study 2 (**Chapter 3**), we examined the impact of tumor burden on translational capacity and efficiency in skeletal and cardiac muscle using the Yoshida AH-130 hepatoma model. This study focused on the mechanisms of striated muscle wasting. We observed that tumor cell inoculation led to skeletal and cardiac muscle wasting, anabolic deficits, increased UPR, and elevated pro-inflammatory cytokines. Consistent with findings in ovarian (1), lung (**Chapter 2**), and colon cancer models (2), the Yoshida AH-130 tumor reduced rRNA in skeletal muscle, supporting the idea that impairments to translational capacity are central to muscle wasting in cachexia.

We also found significant decreases in 4E-BP1 phosphorylation in both skeletal and cardiac muscle. Notably, previous studies on the Yoshida model reported conflicting findings in anabolic signaling pathways. Some studies found increased phosphorylation of S6K1 and 4E-BP1 in skeletal muscles (4), while others reported no changes in Akt or 4E-BP1 phosphorylation (5). Similarly, studies on cardiac muscle showed varied results regarding Akt and 4E-BP1 phosphorylation. Akt phosphorylation was reduced in the hearts of cachectic rats, while 4E-BP1 phosphorylation remained unchanged (6). In another study, neither Akt nor 4E-BP1 phosphorylation was found to be altered within the cardiac muscle of AH-130 cachectic rats (7). However, our findings of decreased 4E-BP1 phosphorylation add to the uncertainty of the role of translational signaling in straited muscle wasting in the Yoshida model. These inconsistencies are surprising as many of the studies demonstrate a similar loss in body weight, heart, and skeletal muscle mass while utilizing a similar tumor-load. Thus, future investigations into the translational signaling pathways in cachectic skeletal or cardiac muscle may want to consider the use of alternative cancer models.

We also investigated possible activation of the UPR. Our findings only partially align with previous observations (8, 9), raising questions about the conservation of UPR across different cachexia models. We found a reduction in sXBP1 in both skeletal and cardiac muscle, contrary to increases to XBP1 splicing reported in other studies (8, 9). This discrepancy suggests that a defective UPR could exacerbate muscle atrophy, as seen in other models where UPR inhibition exacerbated muscle wasting. However, the study of UPR function in cachexia is still in its infancy and more research is needed before any meaningful conclusions can be drawn.

Pro-inflammatory cytokine expression patterns also varied. IL-6 mRNA increased in both muscle and heart, though not significantly, possibly due to variability in the Yoshida model itself.

This model posed unique challenges due to the high variability in some assays, while providing a fairly homogenous outcome in others. Changes in TNF-α were also highly variable and not significantly elevated in skeletal muscle, contrasting with previous reports of elevated TNF-α in this model (10). The conflicting data across multiple studies in the Yoshida AH-130 Hepatoma rat further highlights the complications of this model's use in cachectic research. Lastly, it is possible that some of our findings were skewed by the infiltration of inflammatory cells. Cellular infiltration in the skeletal muscle of the AH-130 tumor-bearing rats has been observed previously (11) and may explain the variability present in the findings of Study 2.

Additional research on the role of double-stranded RNA-dependent protein kinase (PKR) could provide further insight into both UPR activity and the production of pro-inflammatory cytokines in skeletal muscle during cachexia. Systemic inflammation, a hallmark of cancer cachexia, leads to increased PKR activation. This activation, in turn, triggers the UPR and promotes nuclear factor kappa-light-chain-enhancer of activated B cells (NFκB)-mediated expression of pro-inflammatory cytokines (12). A prior study shows that phosphorylation of PKR is increased in the muscle of MAC16 tumor-bearing mice, and the use of a PKR inhibitor can attenuate muscle atrophy, eIF2α phosphorylation, and the nuclear translocation of NFκB (13). Therefore, future research on UPR activity and the muscle-specific production of pro-inflammatory cytokines in cancer cachexia may benefit from the study of PKR activity as well.

In summary, this study suggests that impaired anabolism, UPR, and pro-inflammatory cytokines contribute to tumor-induced skeletal and cardiac muscle wasting. While the reductions in translational capacity were clear, the divergence in translation signaling and cytokine expression in the Yoshida model. The aggressive nature of the AH-130 tumor, leading to rapid

host death, also questions its translatability to human cachexia, necessitating additional models that better reflect the human condition, whose disease progression is typically more gradual.

4.1 REFERENCES

1. **Kim H-G**, **Huot J**, **Pin F**, **Guo B**, **Bonetto A**, **Nader G**. Reduced rDNA transcription diminishes skeletal muscle ribosomal capacity and protein synthesis in cancer cachexia. *FASEB* 35: e21335, 2021. doi: 10.1096/fj.202002257R.
2. **Kim HG**, **Huot JR**, **Pin F**, **Belcher DJ**, **Bonetto A**, **Nader GA**. Metastatic or xenograft colorectal cancer models induce divergent anabolic deficits and expression of pro-inflammatory effectors of muscle wasting in a tumor-type-dependent manner. *J Appl Physiol* 133: 1273–1283, 2022. doi: 10.1152/japplphysiol.00247.2022.
3. **Soliman GA**, **Acosta-Jaquez HA**, **Dunlop EA**, **Ekim B**, **Maj NE**, **Tee AR**, **Fingar DC**. mTOR Ser-2481 autophosphorylation monitors mTORC-specific catalytic activity and clarifies rapamycin mechanism of action. *J Biol Chem* 285: 7866–7879, 2010. doi: 10.1074/jbc.M109.096222.
4. **Aversa Z**, **Bonetto A**, **Costelli P**, **Minero VG**, **Penna F**, **Baccino FM**, **Lucia S**, **Fanelli FR**, **Muscaritoli M**. β-hydroxy-β-methylbutyrate (HMB) attenuates muscle and body weight loss in experimental cancer cachexia. *Int J Oncol* 38: 713–720, 2011. doi: 10.3892/ijo.2010.885.
5. **Pötsch MS**, **Ishida J**, **Palus S**, **Tschirner A**, **von Haehling S**, **Doehner W**, **Anker SD**, **Springer J**. MT-102 prevents tissue wasting and improves survival in a rat model of severe cancer cachexia. *J Cachexia Sarcopenia Muscle* 11: 594–605, 2020. doi: 10.1002/jcsm.12537.

6. **Springer J**, **Tschirner A**, **Haghikia A**, **Von Haehling S**, **Lal H**, **Grzesiak A**, **Kaschina E**, **Palus S**, **Pötsch M**, **Von Websky K**, **Hocher B**, **Latouche C**, **Jaisser F**, **Morawietz L**, **Coats AJS**, **Beadle J**, **Argiles JM**, **Thum T**, **Földes G**, **Doehner W**, **Hilfiker-Kleiner D**, **Force T**, **Anker SD**. Prevention of liver cancer cachexia-induced cardiac wasting and heart failure. *Eur Heart J* 35: 932–941, 2014. doi: 10.1093/eurheartj/eht302.

7. **Poetsch MS**, **Palus S**, **Van Linthout S**, **von Haehling S**, **Doehner W**, **Coats AJS**, **Anker SD**, **Springer J**. The small molecule ACM-001 improves cardiac function in a rat model of severe cancer cachexia. *Eur J Heart Fail* 25: 673–686, 2023. doi: 10.1002/ejhf.2840.

8. **Bohnert KR**, **Gallot YS**, **Sato S**, **Xiong G**, **Hindi SM**, **Kumar A**. Inhibition of ER stress and unfolding protein response pathways causes skeletal muscle wasting during cancer cachexia. *FASEB J* 30: 3053–3068, 2016. doi: 10.1096/fj.201600250RR.

9. **Bohnert KR**, **Goli P**, **Roy A**, **Sharma AK**, **Xiong G**, **Gallot YS**, **Kumar A**. The Toll-Like Receptor/MyD88/XBP1 Signaling Axis Mediates Skeletal Muscle Wasting during Cancer Cachexia. *Mol Cell Biol* 39: e00184-19, 2019. doi: 10.1128/mcb.00184-19.

10. **Catalano MG**, **Fortunati N**, **Arena K**, **Costelli P**, **Aragno M**, **Danni O**, **Boccuzzi G**. Selective up-regulation of tumor necrosis factor receptor I in tumor-bearing rats with cancer-related cachexia. *Int J Oncol* 23: 429–436, 2003. doi: 10.3892/ijo.23.2.429.

11. **Salazar-Degracia A**, **Busquets S**, **Argilés JM**, **López-Soriano FJ**, **Barreiro E**. Formoterol attenuates increased oxidative stress and myosin protein loss in respiratory and limb muscles of cancer cachectic rats. *PeerJ* 5: e4109, 2017. doi: 10.7717/PEERJ.4109.

12. **Smith JA**. Regulation of cytokine production by the unfolded protein response; Implications for infection and autoimmunity. *Front Immunol* 9: 422, 2018. doi:

10.3389/fimmu.2018.00422.

13. **Eley HL**, **Russell ST**, **Tisdale MJ**. Attenuation of muscle atrophy in a murine model of cachexia by inhibition of the dsRNA-dependent protein kinase. *Br J Cancer* 96: 1216–1222, 2007. doi: 10.1038/sj.bjc.6603704.

VITA

Daniel J. Belcher

EDUCATION

2018-2024	**Ph.D., Integrative and Biomedical Physiology** Pennsylvania State University, University Park, PA
2016-2018	**M.S., Exercise Science & Health Promotion: Exercise Physiology** Florida Atlantic University, Boca Raton, FL
2007-2012	**B.A., Exercise Science** Capital University, Columbus, OH

PUBLICATIONS

1. **Belcher, D. J.**, Kim, N., Navarro, B., Möller, M., López-Soriano, F. J., Busquets, S., & Nader, G.A. (2024). Anabolic deficits and divergent unfolded protein response underlie muscle and heart growth impairments in the Yoshida hepatoma tumor model of cancer cachexia. *Physiological Reports. (Under Peer-Review)*
2. **Belcher, D. J.**, Guitart, M., Hain, B., Kim, H. G., Waning, D., Barreiro, E., & Nader, G. A. (2022). LP07 and LLC pre-clinical models of lung cancer induce divergent anabolic deficits and expression of pro-inflammatory effectors of muscle wasting. *Journal of Applied Physiology*, *133*(6), 1260-1272
3. Kim, H. G., Huot, J. R., Pin, F., **Belcher, D. J**., Bonetto, A., & Nader, G. A. (2022). Metastatic or xenograft colorectal cancer induce divergent anabolic deficits and pro-inflammatory effectors of muscle wasting in a tumor-type dependent manner. *Journal of Applied Physiology*, *133*(6), 1273-1283
4. Guo, B., Bennet, D., **Belcher, D. J.**, Kim, H. G., & Nader, G. A. (2021). Chemotherapy agents reduce protein synthesis and ribosomal capacity in myotubes independent of oxidative stress. *American Journal of Physiology-Cell Physiology*, *321*(6), C1000-C1009
5. Johnson, T. K., **Belcher, D. J.**, Sousa, C. A., Carzoli, J. P., Khamoui, A. V., Visavadiya, N. P., Whitehurst, M., & Zourdos, M. C. (2020). Low Volume Acute Multi-Joint Resistance Exercise Elicits a Circulating Brain-Derived Neurotrophic Factor Response but Not a Cathepsin B Response in Well-Trained Men. *Applied Physiology, Nutrition, and Metabolism*, *45*(12), 1332-1338
6. Carzoli, J. P., Sousa, C. A., **Belcher, D. J.**, Helms, E. R., Khamoui, A. V., Whitehurst, M., & Zourdos, M. C. (2019). The effects of eccentric phase duration on concentric outcomes in the back squat and bench press in well-trained males. *Journal of sports sciences*, *37*(23), 2676-2684
7. **Belcher, D. J.**, Sousa, C. A., Carzoli, J. P., Johnson, T. K., Helms, E., Visavadiya, N. P., Zoeller, R. F., Whitehurst, M., & Zourdos, M. C. (2019). Time Course of Recovery is Similar for the Back Squat, Bench Press, and Deadlift in Well-Trained Males. *Applied Physiology, Nutrition, and Metabolism*, *44*(10), 1033-1042
8. **Belcher, D.** (2017). Considerations for Ruck Injury Prevention in the Low Back, *NSCA Tactical Strength & Conditioning Report, Issue 46,* 12-17
9. **Belcher, D.** (2017). The Sumo Deadlift. *Strength & Conditioning Journal, 39(4)*, 97-104

SELECTED PRESENTATIONS

1. **Belcher, D. J.**, Kim, N., Nader, G. A. Determining the role of RRN3 in Skeletal Muscle: A Necessary Mediator for Hypertrophy. *2024 Huck Life Sciences Symposium. State College, PA. 2024*
2. **Belcher, D. J.**, de la Rosa Guitart, M., Hain, B., Kim, H. G., Waning, D., Barreiro, E., & Nader, G. A. (2022). The LP07 and LLC pre-clinical models of lung cancer present divergent anabolic deficits and expression of pro-inflammatory effectors of muscle wasting. The FASEB Journal, 36
3. Kim, H. G., Huot, J., Pin, F., **Belcher, D.**, Bonetto, A., & Nader, G. A. (2022). Divergent Anabolic Deficits and Pro-inflammatory Effectors of Muscle Wasting in Xenograft and Metastatic Tumor Models of Colorectal Cancer. The FASEB Journal, 36
4. **Belcher, D.**, Guo, B., Nader, G. Chemotherapeutic agents impair myotube anabolic capacity by reducing rDNA transcription and global protein synthesis. *Noll Seminar Series: Graduate Student Competition. State College, PA. 2020*
5. Guo, B., **Belcher, D.,** Nader, G. Chemotherapeutic drugs negatively affect myoblast proliferation and myotube anabolism by reducing rDNA transcription. *The FASEB Journal, 34*(S1), 1-1